

Mechanism-Based Inactivation (MBI) of Cytochrome P450 Enzymes: Structure–Activity Relationships and Discovery Strategies To Mitigate Drug–Drug Interaction Risks

Suvi T. M. Orr,[†] Sharon L. Ripp,[‡] T. Eric Ballard,[†] Jaclyn L. Henderson,[†] Dennis O. Scott,[§] R. Scott Obach,[‡] Hao Sun,[‡] and Amit S. Kalgutkar^{*,§}

[†]Worldwide Medicinal Chemistry and [‡]Pharmacokinetics, Dynamics and Metabolism, Pfizer Global Research and Development, Eastern Point Road, Groton, Connecticut 06340, United States

[§]Pharmacokinetics, Dynamics and Metabolism, Pfizer Global Research and Development, 620 Memorial Drive, Cambridge, Massachusetts 02139, United States

1. INTRODUCTION

Cytochrome P450s (CYPs) constitute a superfamily of heme-containing enzymes that catalyze the oxidative metabolism of structurally diverse molecules including drugs, chemical carcinogens, steroids, and fatty acids.¹ CYP1A2, 2C9, 2C19, 2D6, and 3A4/3A5 participate in the metabolism of ~80% of marketed drugs, and more than half of these agents are metabolized by the CYP3A family. Modulation of CYP activity via induction or inhibition by xenobiotics (including drugs) can lead to clinical drug–drug interactions (DDIs) with consequences ranging from loss of efficacy to the introduction of adverse effects, respectively, for coadministered drugs. The drug that causes changes in CYP activity is referred to as the “perpetrator” or “precipitant” of DDI, whereas the coadministered drug that is affected by the change in CYP activity is referred to as the “victim” or “object” of DDI. DDIs arising from CYP inhibition are more frequent and, in some cases, have resulted in the withdrawal of the marketed perpetrator drug (e.g., the antihypertensive agent mibefradil), especially those drugs associated with potent inhibition of the major constitutively expressed human CYP enzyme CYP3A4. Removal of a drug from the marketplace due to DDI issues is usually based on (a) the nature and frequency of the pharmacokinetic (PK) interaction leading to safety concerns, (b) availability of alternative medications without DDI liability, and (c) the pharmacologic benefits of the perpetrator drug that do not significantly outweigh the risks in the population.

CYP inhibitors can be categorized as reversible (competitive or noncompetitive), quasi-irreversible, or irreversible in nature. Reversible inhibition usually involves two or more agents competing for binding at the active site of a CYP isozyme, with one drug inhibiting the metabolism of the other agent. In contrast, drugs converted to electrophilic reactive metabolites (RMs) by CYP may interact with the CYP quasi-irreversibly or irreversibly leading to enzyme destruction. The inactivated CYP is catalytically incompetent and must be replenished by newly synthesized protein. The phenomenon is oftentimes referred to as time-dependent inhibition (TDI), mechanism-based inactivation (MBI), and/or suicide inactivation. Compared to reversible CYP inhibition, drug-induced MBI of CYPs presents a greater safety concern because of the increased propensity for PK interactions upon multiple dosing and the sustained duration of these interactions after discontinuation of the mechanism-based inactivator. Furthermore, depending on the fraction of the

mechanism-based inactivator that is metabolized by the inactivated CYP, an additional clinical consequence could involve nonstationary increases in systemic exposure of the inactivator itself after multiple doses. Finally, covalent modification of CYP enzymes by RMs can also lead to haptan formation and, in some cases, can trigger an autoimmune response in susceptible patients.

The importance of mitigating DDI risks particularly with respect to CYP TDI has been recognized by the regulatory agencies (e.g., United States Food and Drug Administration guidance documents) and by pharmaceutical companies (position papers by member companies of the Pharmaceutical Research and Manufacturers of America (PhRMA)).² Given the concern around PK interactions through TDI of CYP isoforms, *in vitro* CYP TDI is routinely assessed as part of lead optimization efforts in preclinical drug discovery. Identification of an *in vitro* CYP TDI liability, however, can raise several questions such as the following: What is the mechanism of TDI? Does it involve the formation of RMs? Is there a 1:1 correlation between CYP TDI and RM formation (as measured from RM trapping studies using nucleophiles)? What is the likelihood that a CYP time-dependent inhibitor will also cause toxicity? What are the DDI risk mitigation options when dealing with CYP inactivators in drug discovery: compound progression or termination? Several drugs exhibit *in vitro* TDI of CYP enzymes, but only a fraction of them cause clinical DDIs. Hence, when do we initiate labor-intensive medicinal chemistry efforts to design compounds devoid of CYP TDI liability? What are the best methods to precisely predict the occurrence of clinical DDIs with drug candidates that inactivate CYP enzymes? What are (if any) the qualifying considerations for clinical progression of a CYP time-dependent inactivator with projected clinical DDI risks? In an effort to address these questions and hopefully provide answers to some of them, we embarked on the present venture wherein we highlight the current state-of-the-art knowledge in this field with a special emphasis on (a) available biochemical and mechanistic approaches in drug discovery to examine TDI/MBI of CYP isozymes with new chemical entities, (b) structure–activity relationship (SAR) studies with marketed drugs associated with DDIs via CYP inactivation, (c) case studies of medicinal

Received: January 15, 2012

Published: March 12, 2012

chemistry tactics to abrogate CYP inactivation liability, (d) strategies for progression of CYP MBI-positive drug candidates, and (e) the utility of in silico methodology, including the use of physiologically based PK (PBPK) simulators, in drug discovery to predict the magnitude of clinical DDI risks anticipated with new clinical candidates.

2. METHODOLOGY TO EVALUATE CYP MBI IN DRUG DISCOVERY

2.1. Determination of Kinetic Rate Constants for CYP Inactivation.

By definition, time-dependent enzyme inhibitors are compounds that display an increasing degree of enzyme inhibition upon increased duration of preincubation with the enzyme. Mechanism-based inactivators represent a subset of time-dependent inhibitors where the inhibitory effects not only are time-dependent but also require metabolism (to a reactive intermediate) by the enzyme that is ultimately inactivated. In the case of CYP enzymes, a source of NADPH cofactor is required to generate MBI. The process leading to MBI is irreversible, and catalytic activity cannot be restored by dialysis or gel filtration. From a drug discovery standpoint, characterization of the CYP inactivation kinetics is essential for quantitative predictions of clinical DDI potential of TDI-positive drug candidates. Furthermore, quantitative comparison of inactivation kinetics can be useful for rank ordering compounds and establishing SAR for CYP TDI within a chemical series. In subsequent discussions throughout the review, we will reserve the terminology “mechanism-based inactivator” or “MBI” only in cases where the biochemical basis of time-dependent CYP inactivation (i.e., the mechanism of inactivation) has been characterized. The rest of the compounds will be simply referred to as “time-dependent inhibitors” or “TDIs”.

The important kinetic constants for assessing potential severity of CYP inactivation include the maximal inactivation rate constant (k_{inact}), inactivator concentration that yields half of the maximum inactivation rate (K_I), and the partition coefficient. In vitro experimental protocols^{3–7} to measure k_{inact} and K_I for major human CYP enzymes are labor-intensive and are generally not amenable to high-throughput screening in early drug discovery programs. Examination of TDI of CYP activity requires two sequential incubations. The first incubation contains the enzyme source (i.e., liver microsomes, hepatocytes, recombinant expression system, or purified reconstituted system), NADPH, and the putative inactivator (i.e., “inactivation incubation”).^{3–9} Periodically, aliquots from the inactivation incubation mixture are added to a second incubation containing a probe substrate of the CYP isozyme at a high concentration that approaches saturation (e.g., $10 \times K_M$, the substrate concentration that yields half of the maximum rate of catalysis). The probe substrate concentration is kept high to minimize reversible CYP inhibition by the inactivator. The secondary reaction mixture is incubated for a set period of time after which the reaction is quenched and the product of metabolism of the probe CYP substrate is measured (i.e., the “activity incubation”). In most instances, the inactivation incubation is diluted into the activity incubation.⁸ In other cases, the probe CYP substrate is added to the inactivation incubation mixture to start the activity incubation.³ To determine k_{inact} and K_I , a minimum of six inactivator concentrations and six inactivation incubation time points should be included. The percentage of activity remaining after inactivation relative to the one measured in the absence of inactivator is calculated. This percentage is plotted

versus inactivation incubation time to yield a series of first order decay curves (Figure 1A).

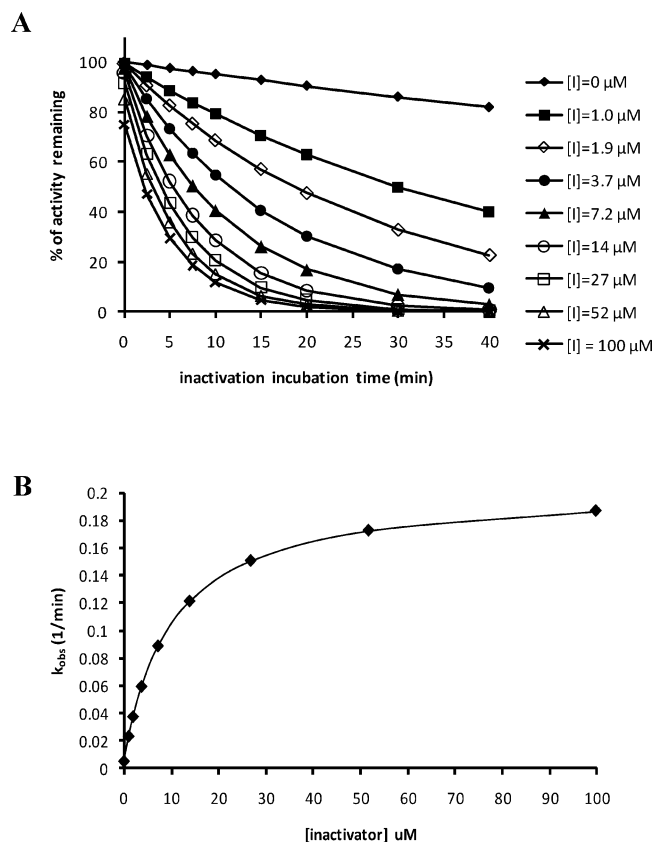


Figure 1. Depiction of a CYP TDI experiment to generate k_{inact} and K_I values: (A) measurement of loss of CYP activity over time; (B) plot of k_{obs} values versus inactivator concentration used in estimation of k_{inact} and K_I .

These curves are then fitted to the function

$$\%A = \%A_{t=0} e^{-k_{\text{obs}}t}$$

The values for k_{obs} are the first order rate constants for loss of CYP activity (A) at each inactivator concentration. These are plotted versus the inactivator concentrations used in the inactivation incubation (Figure 1B), and the data are fit to the function

$$k_{\text{obs}} = k_{\text{obs},[I]=0} + \frac{k_{\text{inact}}[I]}{K_I + [I]}$$

The term $k_{\text{obs},[I]=0}$ describes the decline in activity that is typically observed for CYP enzymes when incubated with NADPH in the absence of substrate. From this analysis, the terms K_I and k_{inact} can be estimated. From a drug discovery standpoint, large k_{inact} and small K_I values generally increase the likelihood of DDIs resulting from CYP inactivation. In preclinical drug discovery, efficiency of CYP inactivation within a given chemical series can be gauged from the k_{inact}/K_I ratio. The partition coefficient is a measure of inactivation efficiency and also can be a useful parameter to obtain for rank-ordering CYP inactivators. Mechanism-based inactivators are substrates of the enzymes they inactivate. The partition coefficient represents the ratio of the number of inactivator molecules that get metabolized relative to the number of enzyme

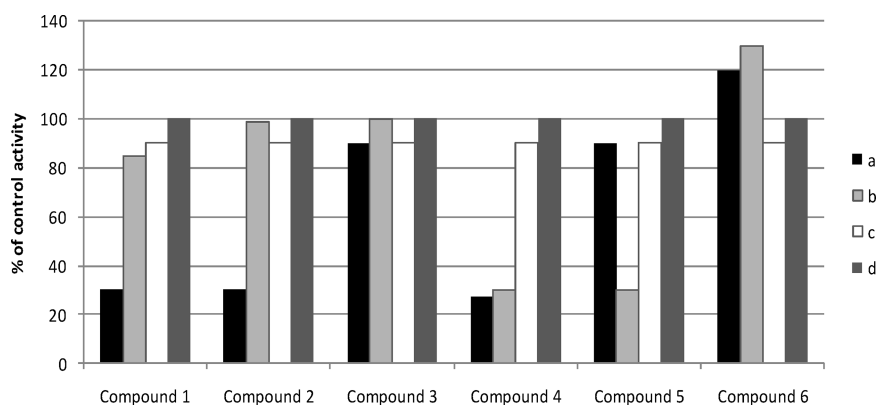


Figure 2. Six possible outcomes when testing for CYP TDI in a simplified “one concentration” approach. Compound 1 depicts TDI with some reversible inhibition component. Compound 2 is also a time-dependent inactivator but shows no detectable reversible inhibition. Compound 3 is neither a time-dependent inactivator nor a reversible inhibitor. Compound 4 is a potent reversible inhibitor. Compound 5 is a reversible inhibitor that is consumed during the preincubation. Compound 6 is an activator (i.e., it stimulates the activity of CYP). (a) The test compound is preincubated with CYP enzyme and NADPH. (b) The test compound is not preincubated with CYP enzyme. (c) CYP preincubation is in the absence of test compound and in the presence of NADPH. (d) Results from the control (no test compound and no preincubation) are shown.

molecules inactivated. As an inactivator is metabolized, it can be released from the CYP enzyme (as a metabolite) or it can covalently attach to the protein causing inactivation. A highly efficient inactivator will be more prone to the latter event and thus have a low partition ratio. The partition ratio is determined by measuring (a) the inactivation rate and converting the value to moles of enzyme inactivated per unit time and (b) the consumption of the inactivator during incubation (moles of inactivator consumed per unit time). The ratio of these two values represents the partition ratio.

2.2. “Abbreviated” Methodology for Examining CYP TDI in Drug Discovery. In order to satisfy compound throughput requirements in early drug discovery, methods for quantitative assessment of CYP TDI without the need for generating K_i and k_{inact} values have been described. The “scaled-down” methods typically are used to detect (a) time-dependent loss of CYP activity following incubation at a single compound concentration and/or (b) a shift in the IC_{50} following preincubation at multiple concentrations of the compound of interest. The simplest approach for quantitative assessment of CYP inactivation requires four experimental measurements: (a) the effect of a single concentration of the test compound on catalytic activity of CYP upon preincubation with the enzyme source and NADPH cofactor for a set duration of time, (b) the effect of the same concentration on CYP activity as in (a) but without preincubation, (c) a control incubation involving preincubation of the enzyme with NADPH for the same set time as in (a) but lacking the test compound, and (d) a control incubation of enzyme and NADPH without preincubation and in the absence of the test compound. Typical incubation times and inactivator concentrations are 30–60 min and 10–60 μM , respectively. CYP activity in (a) is compared to those in (b) and (c), with all three normalized to CYP activity in (d). Replicates of each are necessary to provide statistical power in stating that TDI is real (not an artifact). Incubation in (b) is necessary to ensure the possibility that potent reversible inhibition is not mistaken for TDI. Incubation in (c) is necessary to ensure that the spontaneous loss of activity that is frequently observed when CYP is incubated with NADPH (possibly due to generation of reactive oxygen species) is not mistaken for TDI. There are several possible outcomes for such an abbreviated protocol, and some of these are depicted in Figure 2.

An experimental design that resides between a complete K_i and k_{inact} determination and the aforementioned simple four-incubation approach is the “ IC_{50} shift” measurement. In this experiment, multiple concentrations of the test compound are preincubated with the CYP source in the presence and absence of NADPH for a preset time period (usually ~ 30 min), followed by measurement of activity using a probe CYP substrate concentration at its K_M value.^{3,5,10–12} This is a prototypical design for estimating IC_{50} values for reversible CYP inhibition except for the preincubation step. The two-step process can be accomplished either by diluting the inactivation incubations into a solution containing probe CYP substrate or by adding a concentrated substrate solution to the inactivation incubation.³ The IC_{50} values calculated in the presence and absence of NADPH cofactor are compared; a decrease in IC_{50} upon preincubation is suggestive of TDI (Figure 3). Because the

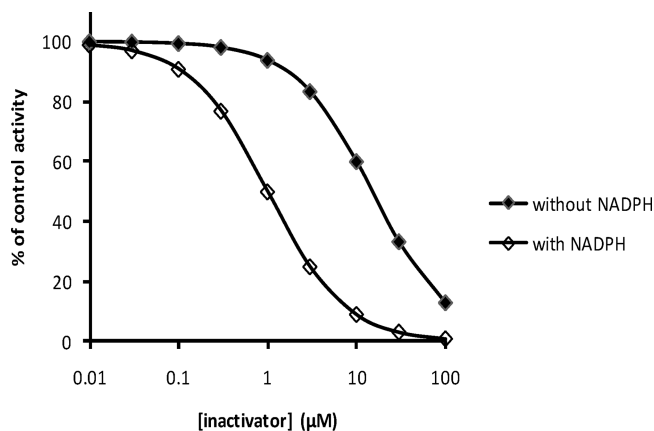


Figure 3. Graphical representation of an IC_{50} shift experiment to identify TDIs of CYP enzymes.

degree of the change in IC_{50} is dependent on the experimental design, individual laboratories must calibrate the data against well-established CYP inactivators. Among the various assays used to assess CYP TDI, the IC_{50} shift experiment is most commonly used because of its relative ease of execution in a drug discovery setting. However, such an experimental protocol is best utilized to probe SAR for CYP inactivation in hit-to-lead

optimization and not for the quantitative prediction of clinical DDIs. Additional discussion on the latter topic is provided in section 6 of this Perspective.

2.3. Mechanistic Investigation of Factors Leading to CYP TDI. CYP TDI usually proceeds through metabolic activation (also referred to as bioactivation) of a functional group to a RM. As seen in Table 1, there is a common theme

with respect to substituents (also referred to as structural alerts and/or toxicophores) associated with CYP inactivation as well as idiosyncratic drug toxicity.¹³ However, in contrast with nonspecific protein reactivity of RMs, mechanism-based inactivators of CYP enzymes are highly specific because (a) the inactivator must first bind reversibly to the enzyme and must satisfy all the constraints imposed on normal substrates of

Table 1. Illustrations of Functional Groups Associated with Mechanism-Based Inactivation of CYP Enzymes^a

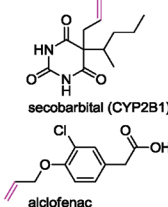
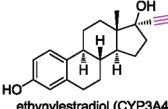
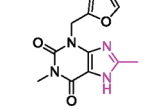
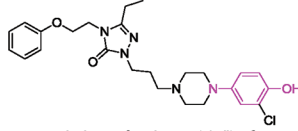
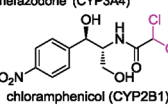
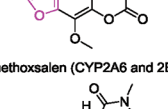
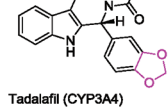
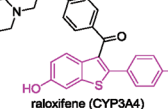
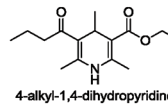
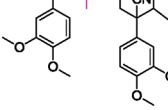
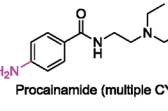
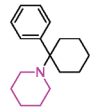
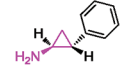
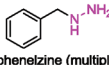
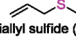
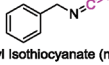
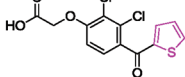
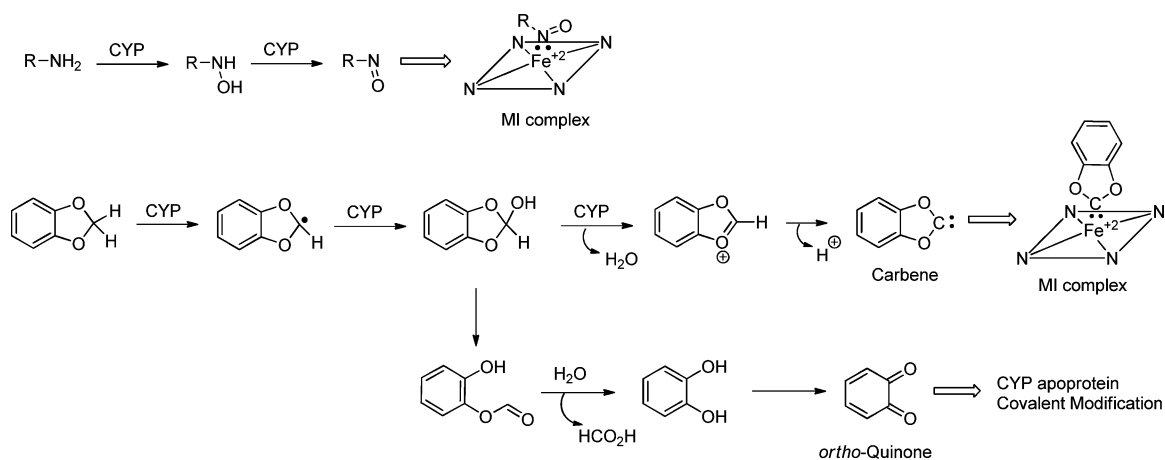
Functional Group	Classification (Reactive Intermediate)	Representative Examples - (CYP isoform inactivated)
Alkene	Heme or apoprotein alkylation (cation radical and/or epoxide)	 <p>secobarbital (CYP2B1)</p> <p>alclofenac</p>
Alkyne	Heme or apoprotein alkylation (ketene or oxirene)	 <p>ethynylestradiol (CYP3A4)</p>
2-Alkylimidazole	Apoprotein alkylation (iminemethide)	 <p>furafylline (CYP1A2)</p>
Aminophenol [§]	Apoprotein arylation (quinoneiminium)	 <p>hydroxynefazodone metabolite of nefazodone (CYP3A4)</p>
Dihaloalkane	Apoprotein acylation (acylhalide)	 <p>chloramphenicol (CYP2B1)</p>
Furan	Apoprotein arylation (epoxide)	 <p>methoxsalen (CYP2A6 and 2B1)</p>
1,3-Benzodioxole	Quasi-irreversible (carbene)	 <p>Tadalafil (CYP3A4)</p>
Phenol	Apoprotein arylation (quinone or quinonemethide)	 <p>raloxifene (CYP3A4)</p>
2-Alkyl-1,4-dihydropyridine [†]	Heme alkylation (alkyl radical)	 <p>4-alkyl-1,4-dihydropyridine</p>
Alkylamine	Quasi-irreversible (nitroso)	 <p>Verapamil (CYP3A4)</p>
Arylamine	Quasi-irreversible (nitroso)	 <p>Procalnamide (multiple CYPs)</p>

Table 1. continued

Functional Group	Classification (Reactive Intermediate)	Representative Examples - (CYP isoform inactivated)
Cyclic tertiary amine	Apoprotein alkylation (iminium ion)	 phencyclidine (multiple CYPs)
Cyclopropylamine (only aminium pathway is N-oxidation)	Heme or apoprotein alkylation (iminium ion, hydrate or aminium radical), Quasi-irreversible (nitroso)	 tranycypromine (multiple CYPs)
Hydrazine	Heme alkylation (diazene or C-based radical)	 phenelzine (multiple CYPs)
Allylsulfide	Heme alkylation (sulfone or epoxide)	 Diallyl sulfide (CYP2E1)
Isothiocyanate	Apoprotein alkylation (C-based electrophilic center or reactive sulfur)	 Benzyl isothiocyanate (multiple CYPs)
Thiophene	Apoprotein arylation (S-oxide or epoxide)	 Tienilic acid (CYP2C9/10)

^a(§) Hydroxyl installed through prior CYP metabolism. (‡) Forms amine cation radical, then aromatizes releasing the active alkyl radical species. In the case of verapamil, formation of the nitroso intermediate requires N-dealkylation of the parent molecule.

Scheme 1. Quasi-Irreversible CYP Inactivation and Formation of MI Complex by Amines and 1,3-Benzodioxoles



the enzyme, (b) it must be acceptable as a substrate and thus undergo bioactivation to a RM, and finally, (c) the resulting reactive species must irreversibly modify the enzyme and permanently remove it from the catalytic pool. Mechanism-based CYP inactivators can be categorized into four mechanistically distinct classes: (a) compounds that quasi-irreversibly bind to the prosthetic heme iron atom, (b) compounds that alkylate (or arylate) the apoprotein, (c) compounds that alkylate (or arylate) the porphyrin framework of the heme, and (d) compounds that degrade the prosthetic heme group to products that can, in some cases, themselves modify the apoprotein.¹³ This mechanistic classification is not rigid, as in the course of CYP metabolism, a compound could simultaneously partition into more than one inhibitory trajectories. Experiments that probe the mechanism underlying the time-dependence requirement for CYP inhibition usually yield critical information in designing compounds devoid of the liability, since the cause of the problem can be isolated and fixed through iterative structural modification.

2.3.1. Quasi-Irreversible Inactivation of CYP Enzymes. Quasi-irreversible inactivation occurs when the reactive species

complexes with the ferrous form of heme (product of reduction of resting state ferric enzyme by NADPH-CYP reductase) in a tight, noncovalent interaction. Such metabolite-intermediate (MI) complexes exhibit a very distinctive CYP UV-visible spectrum shift in the Soret region between 448 and 460 nm when the heme iron is in the ferrous state. MI complexes are catalytically inactive; the ferrous form of the enzyme can no longer bind to carbon monoxide, which represents a diagnostic test to assess whether CYP TDI occurs via MI complex formation. Quasi-irreversible inactivation *in vitro* via MI complex formation is reversible after dialysis. *In vivo*, however, such a complex is known to be so stable that inactivated CYP enzyme is generally unavailable for drug metabolism. As a result, DDIs due to quasi-irreversible inhibitors are more prominent after multiple dosing than those of reversible inhibitors.¹⁴ Primary amines and 1,3-benzodioxole (methylenedioxyphenyl) derivatives are the most common quasi-irreversible CYP inactivators. Primary amines are oxidized to nitroso metabolites (via the intermediate hydroxylamine metabolites), which can form a MI complex with the ferrous form of the heme iron atom (Scheme 1).¹⁵ Although a primary amine substituent is required, secondary and tertiary

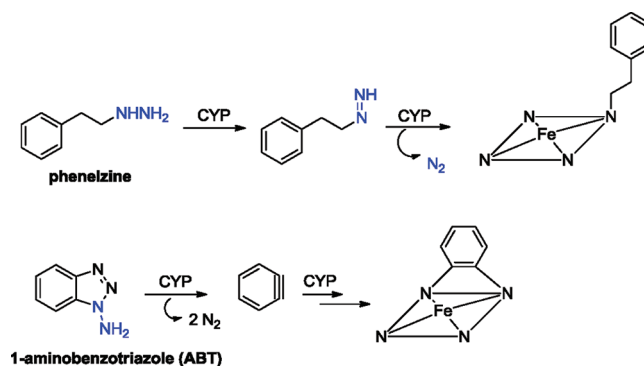
amines can serve as suitable precursors for MI complexation provided they are N-dealkylated to primary amines. Nitroso-heme complexes can be dissipated *in vitro* upon treating the inactivated CYP with potassium ferricyanide, which oxidizes the iron to the ferric state and liberates the active carbon monoxide-binding CYP enzyme.¹⁶ The ferrous to ferric transition weakens the complex, indicating that the reactive species, like carbon monoxide, only strongly coordinates to the ferrous iron. MI complexes from aromatic amines differ from those of alkylamines in that they can be dissipated by the addition of sodium dithionite. The crystal structure of a complex between a nitroso compound and a model iron porphyrin shows, as expected, that the nitrogen rather than the oxygen atom of the nitroso group is bound to the iron. MI complex formation with 1,3-benzodioxole derivatives occurs through a carbene intermediate, formed via hydrogen atom abstraction from the methylene carbon or by elimination of water from a hydroxymethylene intermediate (Scheme 1).¹⁷ The hydroxymethylene intermediate can also undergo demethylenation, yielding a catechol intermediate and formic acid. Oxidation of the catechol metabolite to the electrophilic *o*-quinone can also result in CYP inactivation through covalent modification of an active site residue(s) in CYP.¹⁸ Similar to amines, the 1,3-benzodioxole-CYP MI complex is characterized by a different absorption spectrum with maxima at 427 and 455 nm.¹⁷ It is noteworthy to point out that potassium ferricyanide does not disrupt the carbene-heme complex of 1,3-benzodioxoles. SAR studies on a series of 4-alkoxy-1,3-benzodioxole analogues reveal that the size and lipophilicity of the alkoxy group is an important determinant of the complex stability; alkyl chains of one to three carbon atoms yield unstable complexes, whereas those with longer alkyl chains are stable.¹⁹

2.3.2. Covalent Modification of Heme Prosthetic Group and/or Apoprotein in CYP Enzymes. TDI of CYP activity can also arise through covalent adduction of the RM to the heme prosthetic group and/or to an active site amino acid residue in the apoprotein. While the pyrrole nitrogens that make up the heme porphyrin ring are not very nucleophilic (especially in comparison to many cellular components), the generation of extremely reactive species (e.g., free radicals, ketenes) in proximity to the heme prosthetic group can lead to facile alkylation of the porphyrin ring. Changes in the integrity of the porphyrin ring system can be examined by UV/visible spectroscopy, liquid chromatography tandem mass spectrometry (LC-MS/MS), and carbon monoxide binding studies. Inactivated apoprotein retains its ability to bind carbon monoxide, which provides a convenient method to distinguish protein adducts from heme modifiers. Analysis of modified heme was pioneered by Ortiz de Montellano and co-workers, and this technique has been used to map the orientation of the heme within the CYP active site.²⁰ Alkenes, alkynes, hydrazines, and cyclopropylamines are common functional groups associated with heme alkylation. The CYP-catalyzed oxidation of terminal olefins is often associated with N-alkylation of the prosthetic heme as well as apoprotein modifications leading to enzyme inactivation. Studies with 5-allyl barbiturates such as secobarbital (see Table 1) demonstrated that the oxidative metabolism on the olefin results in the comparable loss of CYP activity and heme content and accumulation of “green pigments” identified as abnormal loss of porphyrins.²¹ In the case of secobarbital, the reactive species derived from olefin oxidation is partitioned between heme N-alkylation and apoprotein modification.²¹ It has been speculated that a secobarbital-derived cation radical

intermediate formed upon olefin oxidation by CYP covalently adducts to the heme prosthetic group or a aminoacid residue in proximity, prior to collapsing to the stable epoxide metabolite observed in the microsomal incubations and *in vivo*. The finding that amobarbital (a saturated analogue of secobarbital) is not a CYP inactivator is consistent with the proposed mechanism of CYP inactivation involving bioactivation of the olefinic double bond to a reactive intermediate. In contrast with the mechanistic observations on secobarbital and related sedatives, investigations into the mechanism of CYP inactivation by the allylic phenol derivative and anti-inflammatory agent alclofenac (see Table 1) revealed that the synthetic standard of the epoxide metabolite of alclofenac detected in human and mouse urine demonstrated TDI of CYP activity in a NADPH-independent fashion.²² This observation suggests that the electrophilic epoxide covalently modifies CYP directly and does not require further metabolic processing to a reactive species.

CYP inactivation by the hydrazine derivative phenelzine (Table 1) results in the generation of the *N*-(2-phenylethyl)-protoporphyrin IX heme adduct, which presumably arises through covalent interaction of the heme with the 2-phenethyl radical species (Scheme 2).²³ The chemical oxidation of

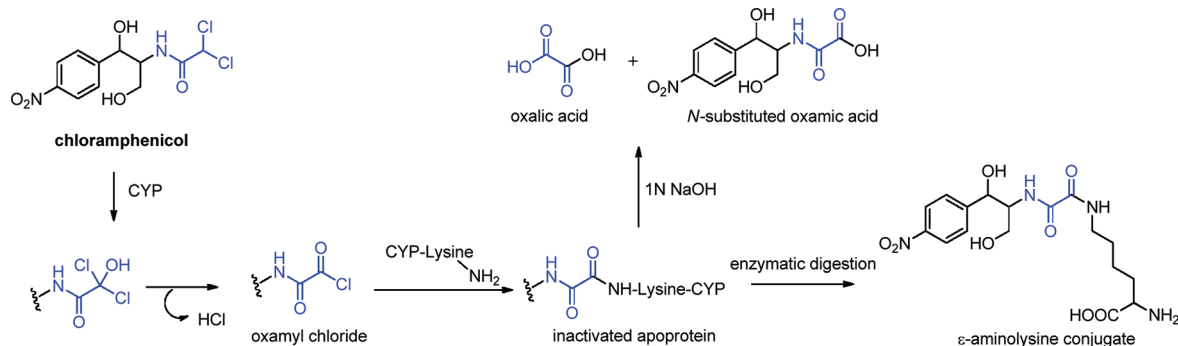
Scheme 2. Heme Alkylation and Arylation by Hydrazine Derivatives



1-aminobenzotriazole (ABT), which is often used to probe the role of CYP enzymes in drug metabolism, yields benzyne, an exceedingly reactive species, and two molecules of dinitrogen (Scheme 2). The observation that benzyne is bound across two of the nitrogen atoms of the prosthetic heme isolated from inactivated CYP enzymes suggests that the enzyme-catalyzed oxidation of ABT follows the same reaction pathway.²⁴ It is unclear whether ABT oxidation to benzyne proceeds via hydroxylation of the exocyclic nitrogen or electron abstraction to afford a radical or a radical cation, but a notable similarity exists between the inactivation mechanism proposed for ABT and related 1,1-disubstituted hydrazines.

Besides heme modification, the RM can also selectively react with CYP apoprotein. Apoprotein modification will result in alteration of the CYP enzymatic activity or, more likely, the complete inactivation of CYP. Inactivated CYP apoprotein can be denatured and subjected to high resolution LC-MS/MS analysis to identify the specific region of the polypeptide modification, which amino acid(s) has been specifically adducted, and the structure of the adduct.²⁵ The protein can be further subjected to partial digestion with specific enzymes, such as trypsin, to yield peptides that can be analyzed by LC-MS/MS. Comparison of the mass spectral data from control and treated CYPs can pinpoint the site of modification, the specific

Scheme 3. CYP Apoprotein Acylation by the Broad-Spectrum Antibiotic Chloramphenicol



amino acid(s) modified, and the nature of the RM formed in the course of metabolism. Dihaloalkanes, furans, phenols, and thiophenes are common functional groups responsible for apoprotein modification.¹³ The broad spectrum antibacterial agent chloramphenicol (Scheme 3) was among the first CYP inactivators shown to act by irreversible apoprotein modification.²⁶ Proteolytic digestion of enzyme inactivated by [¹⁴C]-chloramphenicol revealed a single ¹⁴C-modified amino acid. The release of lysine and chloramphenicol fragments (oxalic acid and a N-substituted oxamic acid) upon alkaline hydrolysis of the modified amino acid and the observation that the difluoromethyl derivative does not inactivate CYP suggest that chloramphenicol is oxidatively dechlorinated to the reactive acylating agent oxamyl chloride that either acylates a critical lysine residue or is hydrolyzed to the stable oxamic acid derivative depicted in Scheme 3.²⁷

Modified CYP apoprotein can be potentially immunogenic.²⁸ As with any covalently modified protein, it is postulated that an immune response to the modified CYP enzyme can generate CYP-specific antibodies. The antihypertensive drug dihydralazine (Figure 4) is associated with immunoallergic hepatitis

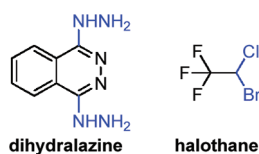


Figure 4. Immunogenic drugs dihydralazine and halothane.

typically characterized by the appearance of anti-CYP1A2 autoantibodies in the sera of susceptible patients.²⁹ The finding is consistent with the *in vitro* observations on CYP1A2 covalent modification by a RM of dihydralazine, which leads to the formation of a neoantigen that triggers an immune response characterized by autoantibodies against CYP1A2.³⁰ Likewise, the inhaled anesthetic halothane (Figure 4) is associated with a rare but severe form of hepatitis characterized by the presence of serum antibodies that react with CYP2E1.³¹ The clinical observation is consistent with the major role of human CYP2E1 in the oxidative dehalogenation of halothane to a reactive trifluoroacetyl chloride species, which acylates the CYP isoform, resulting in enzyme inactivation.³²

From a mechanistic standpoint, understanding the biotransformation pathways for TDI-positives can yield critical insight into the mechanism(s) of apoprotein inactivation. The RM generated in the course of oxidative metabolism can partition between enzyme inactivation and/or release from the active site to ultimately form a stable metabolite, which can be

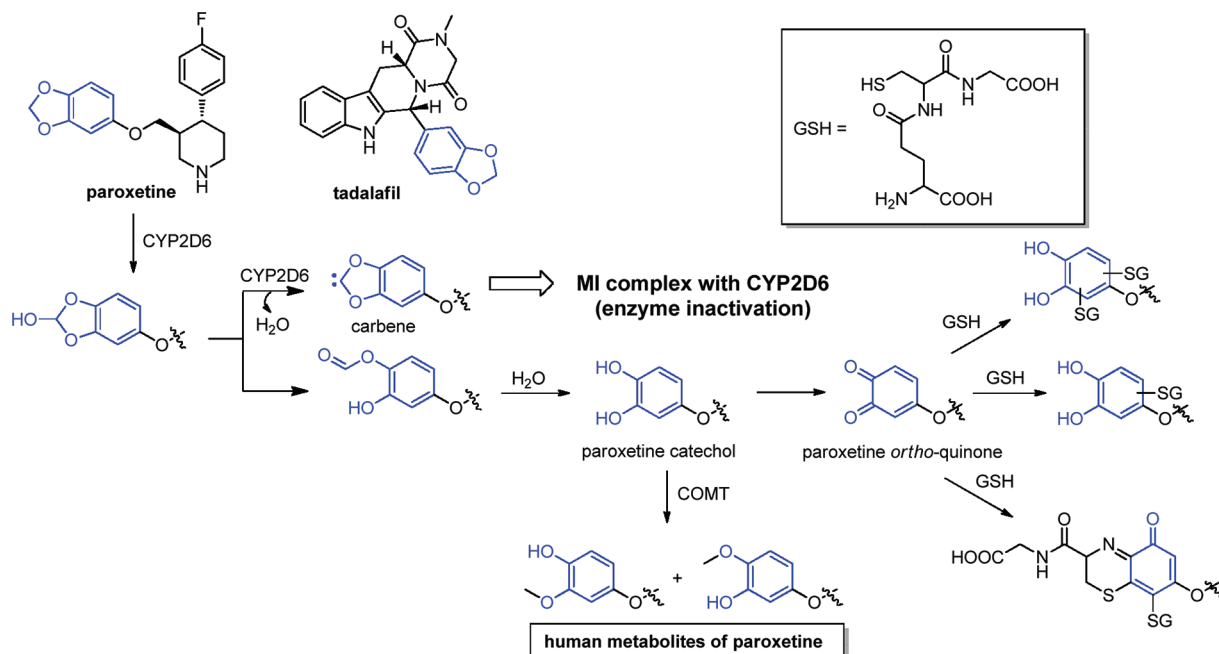
detected in the course of metabolite identification studies. For instance, the reactive ketene generated from the metabolic activation of an alkyne can be hydrolyzed to the stable acetic acid metabolite amenable to characterization. Likewise, in incubations containing exogenous nucleophiles (e.g., reduced glutathione (GSH), semicarbazide, methoxylamine, cyanide), the characterization of stable conjugates of RMs that diffuse out of the CYP active site provides circumstantial evidence for their formation and potential involvement in the activation process. Elucidation of the structures of these stable RM conjugates provides an insight into the metabolism process that leads to CYP inactivation.

2.3.3. Covalent Modification of CYP by Heme Fragments. During the catalytic oxidation of some substrates (e.g., carbon tetrachloride), some CYP enzymes are inactivated via a process in which fragments of the heme are irreversibly bound to apoprotein.³³ The features that predispose CYPs to cross-linking between a heme fragment(s) and the apoprotein remain unclear. Studies with carbon tetrachloride suggest that generation of free radical species is important but not sufficient, since not all CYP enzymes that form radical species undergo MBI via heme fragmentation.³⁴

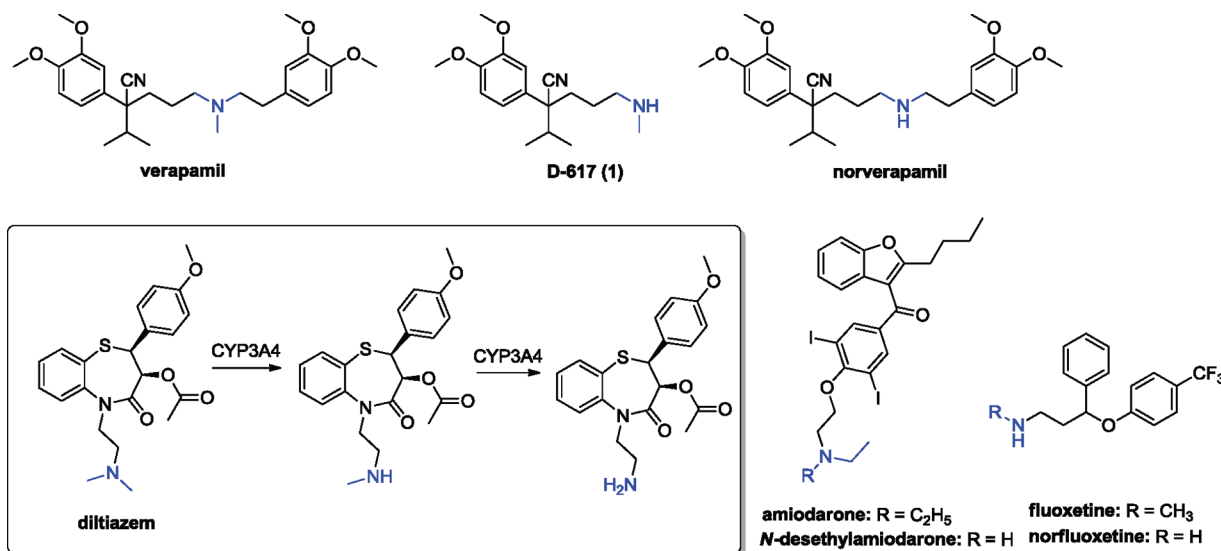
3. REPRESENTATIVE EXAMPLES OF MARKETED DRUGS ASSOCIATED WITH MBI OF CYP ENZYMES

3.1. Quasi-Irreversible Inactivation by Drugs. Paroxetine and tadalafil (Scheme 4) are two noteworthy examples of drugs that inactivate CYP2D6 and CYP3A4, respectively, via MI complex formation through a carbene intermediate.^{12,35} The major metabolic pathway of paroxetine in humans also involves CYP2D6-mediated 1,3-benzodioxole ring scission to a catechol intermediate, which is converted to the corresponding guaiacol isomers via the action of catechol-*O*-methyltransferase (COMT).³⁶ GSH conjugates resulting from Michael addition of the thiol nucleophile to electrophilic *o*-quinone species also have been characterized in human liver microsomes (HLM) incubations of paroxetine.³⁶ Because CYP2D6 is responsible for paroxetine metabolism, MBI of CYP2D6 activity by paroxetine is associated with nonstationary PK in CYP2D6 extensive metabolizers.³⁷ In other words, paroxetine inactivates its own clearance mechanism, which results in reduced clearance and high accumulation with repeated administration. Likewise, DDIs with coadministered drugs whose clearance is mediated by CYP2D6 have been demonstrated. Examples of characterized clinical DDIs with paroxetine include interactions with desipramine,³⁸ metoprolol,³⁹ risperidone,⁴⁰ and atomoxetine,⁴¹ where the clearance of the affected drugs is impaired by 5- to 8-fold. The fold increases in the area under the plasma concentration

Scheme 4. Structures of Paroxetine and Tadalafil and Proposed Mechanism of CYP2D6 Inactivation by Paroxetine



Scheme 5. Amine-Based Drugs That Form MI Complex with CYP Enzymes Resulting in MBI



versus time curve (AUC) of the victim drug(s) appear to be in reasonable agreement with the values obtained upon scaling of the *in vitro* kinetic constants for CYP2D6 MBI by paroxetine.⁴² In contrast with the observations on paroxetine, the clinical PK of midazolam and lovastatin, probe substrates of CYP3A4, are unaffected by up to 14 days of tadalafil administration, despite the CYP3A4 liability.³⁵ The reason(s) for the *in vitro*–*in vivo* discrepancy with tadalafil remains unclear. Besides MBI, tadalafil also induces CYP3A4 activity *in vitro*,³⁵ and it is possible that simultaneous induction and inactivation of CYP3A4 could counterbalance the DDI resulting from the CYP inactivation component.

There are several literature examples on structurally diverse aliphatic amine-based drugs that form MI complexes with CYP enzymes. The mechanism of inactivation is thought to involve metabolism of the amine substituent to a nitrosoalkane intermediate, although this has not been firmly established in some

cases. In almost all instances, the amine motif is also crucial for primary pharmacology. An interesting SAR feature that emerges from mechanistic studies on CYP MBI by amines is the lack of a direct correlation between N-dealkylation by a CYP enzyme and inactivation of that same CYP enzyme via MI complex formation. For example, N-demethylation of fluoxetine to norfluoxetine is catalyzed by CYP2D6, but the process is not accompanied by MBI of the isozyme. At present, it is not known why some CYP enzymes are capable of oxidizing the parent alkylamine drug to inhibitory metabolites but are incapable of forming an MI complex.

Verapamil is a calcium channel blocker that is N-dealkylated by CYP3A4 into two major metabolites N-desalkylverapamil D-617 (1) and norverapamil (Scheme 5).⁴³ Both parent drug and metabolites form MI complexes with CYP3A4, resulting in the MBI of the enzyme. On the basis of the k_{inact} to K_i ratio, the efficiency of inactivation is norverapamil > verapamil > 1.

The observations of nonstationary PK, due to autoinactivation, and clinical DDIs, due to CYP3A4 MBI, are consistent with the role of CYP3A4 in verapamil metabolism.⁴⁴ Thus, in healthy volunteers, the oral AUCs of drugs metabolized by CYP3A4 such as midazolam, cyclosporin A, simvastatin, and buspirone increase 2- to 6-fold after multiple doses of verapamil.

Long-term treatment with the calcium channel blocker diltiazem (Scheme 5) also leads to DDIs resulting in lowered clearance of CYP3A4 substrates.⁴⁵ Diltiazem is extensively metabolized in humans via multiple pathways including N-demethylation, O-demethylation, and cleavage of the ester linkage.⁴⁶ N-Desmethyl diltiazem is the major metabolite of diltiazem in humans that undergoes further N-demethylation to yield a primary amine metabolite. In HLM, the products of sequential N-demethylation competitively inhibit CYP3A4 activity with K_i values of 2.0 and 0.1 μM .⁴⁶ In addition, TDI of CYP3A4 activity has also been reported in HLM for both diltiazem and the N-demethylated secondary amine metabolite.^{47,48} Jones et al.⁴⁷ demonstrated that TDI of CYP3A4 activity by diltiazem occurs primarily via MI complex formation in a NADPH-dependent fashion. Increased TDI of CYP3A4 is also associated with loss of parent drug and simultaneous accumulation of the N-demethylated metabolites, with the secondary amine metabolite being significantly more potent as a CYP3A4 inactivator than the parent drug.⁴⁸ The structure of the species that is responsible for TDI via MI complex formation is not known but can be assumed to be a nitroso intermediate. It has been suggested that the N-demethylated metabolites produced via CYP3A4-catalyzed metabolism of diltiazem may accumulate during chronic therapy and lead to inhibition of the enzyme *in vivo*.

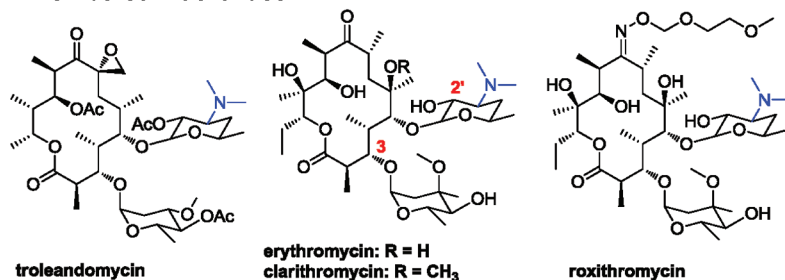
The tertiary amine derivative amiodarone (Scheme 5) is a class III antiarrhythmic agent, which is widely used in conjunction with other drugs. While few drugs, if any, have been shown to affect amiodarone PK, amiodarone itself has significant effects on the PK and PD of coadministered drugs that are metabolized by CYP1A2, CYP2C9, CYP2D6, and CYP3A4.⁴⁹ MI complex formation with rodent CYP enzymes is consistent with the metabolism of the tertiary amine group in amiodarone to the nitrosoalkane intermediate.⁵⁰ In humans, amiodarone is metabolized by CYP3A4 (with additional involvement from CYP2C8 and CYP2D6) to *N*-desethylamiodarone, which appears to inactivate CYP isozymes distinct from those inactivated by the parent drug. The *in vitro* inactivation profiling of CYPs in human hepatic tissue has not been fully resolved with amiodarone. In one instance, amiodarone (but not *N*-desethylamiodarone) was shown to exhibit CYP3A4 TDI, whereas in a recent report, CYP3A4 TDI was demonstrated with both the parent drug and metabolite.^{51,52} *N*-Desethylamiodarone, but not amiodarone, is consistently reported as a mechanism-based inactivator of CYP2D6, which highlights the importance of studying metabolites separately as inactivators of CYP enzymes.^{51,52} Amiodarone also inactivates CYP2C8 and CYP2C9;^{52,53} however, spectral studies have not detected MI complex formation or heme loss with CYP2C8.⁵³ CYP2C9 has similar time- and concentration-dependent inactivation by both amiodarone and *N*-desethylamiodarone. It is likely that *N*-desethylamiodarone formation is essential for CYP2C9 inactivation, as a correlation has been found between the warfarin dose and plasma concentrations of *N*-desethylamiodarone but not with amiodarone concentration.⁵⁴

Similar to amiodarone, the selective serotonin reuptake inhibitor fluoxetine (Scheme 5) is a substrate and inhibitor of

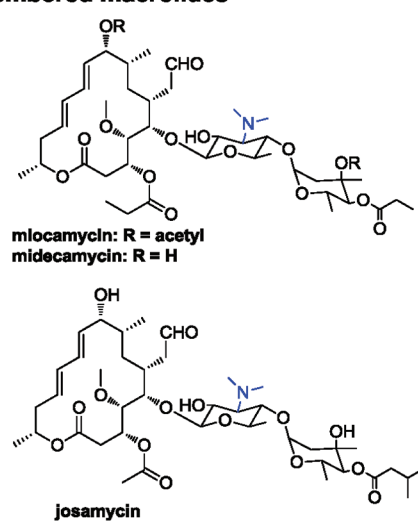
multiple CYP enzymes. The principal route of fluoxetine metabolism is via N-demethylation to norfluoxetine, which is catalyzed mainly by CYP2D6 along with some contributions from other isoforms, including CYP3A4 and CYP2C9.⁵⁵ Both fluoxetine and norfluoxetine reversibly inhibit multiple CYP enzymes including CYP2D6, CYP2C19, and CYP3A4, with norfluoxetine displaying greater potency relative to the parent drug.⁵⁶ In addition to reversible inhibition, TDI of CYP3A4 and CYP2C19 activity has also been demonstrated with fluoxetine in HLM and human hepatocytes.⁹ Recently, Stresser et al.⁵⁷ reported that norfluoxetine also exhibits TDI of CYP2C19 activity in HLM, suggesting that conversion of fluoxetine to norfluoxetine represents a metabolic pathway leading to TDI. Interestingly, CYP2D6 and CYP2C9 both form norfluoxetine efficiently but are not inactivated in the presence of fluoxetine. More so, fluoxetine demonstrates TDI of CYP2C19 activity but is a very poor substrate.⁵¹ It is possible that norfluoxetine formed by CYP2D6 and CYP2C9 is released and then inactivates other enzymes such as CYP3A4 and CYP2C19. The mechanism of TDI by fluoxetine/norfluoxetine in human hepatic tissue is unclear but most likely represents MI complex formation with a nitrosoalkane intermediate based on evidence presented using rat microsomal protein.⁵⁸ Overall, the case studies with tertiary amines illustrate the critical role that N-dealkylated metabolites play in CYP inactivation; therefore, from a drug discovery perspective, quantitative accounting for all N-dealkylated metabolites and individual assessment of parent drug and metabolites for MBI of all major human CYP isoforms are important for quantitative understanding and predictions of *in vivo* CYP inactivation. With the exception of certain macrolide drugs (e.g., erythromycin), PK profiling of most alkylamine drugs reveals the presence of N-dealkylated metabolites in circulation, often at plasma concentrations significantly higher than that of the parent drug.

Several members of the macrolide class of antibacterial agents, which contain a tertiary amine group, are also known to form MI complexes with CYP3A4 following sequential metabolism to the nitrosoalkane intermediate.⁵⁹ In humans, numerous PK interactions with CYP3A4 substrates upon coadministration with macrolides have been noted.⁶⁰ On the basis of their affinity for CYP3A4 and their propensity to cause DDIs, macrolides may be classified into three different categories (Figure 5). The first category (e.g., troleandomycin, erythromycin, clarithromycin) comprises macrolides that are particularly prone toward MI complexation with CYP3A4 via the intermediate nitrosoalkanes.^{59,61} The second group (e.g., josamycin, flurithromycin, roxithromycin, midecamycin, and miocamycin) forms MI complexes with CYP3A4 to a lesser extent and rarely causes DDIs.^{62,63} The last group (e.g., spiramycin, rokitamycin, dirithromycin, and azithromycin) does not inactivate CYP3A4 and does not cause DDIs.⁶⁴ SAR studies have shown that a high log *P* and a nonhindered readily accessible *N,N*-dimethylamino group appear to be important properties for MI complex formation with macrolides. For example, introduction of bulky functional groups in position 3 in erythromycin dramatically decreases MI complex formation with rat CYP3A enzymes, whereas introducing substituents simultaneously at the 3 and 2' positions (adjacent to the *N,N*-dimethylamino group) virtually blocked CYP3A inactivation via MI complex formation.⁶⁵ An additional trend that emerges from these SAR analyses is that 14-membered macrolides (e.g., troleandomycin, erythromycin, and clarithromycin) are more prone to MI complex formation than are 15- or 16-membered macrolides (e.g.,

14-Membered macrolides



16-Membered macrolides



15-Membered macrolide

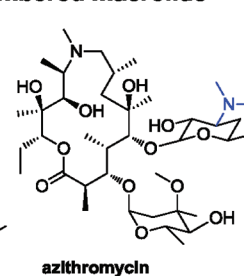


Figure 5. SAR analysis for MI complexation of macrolides with CYP3A4.

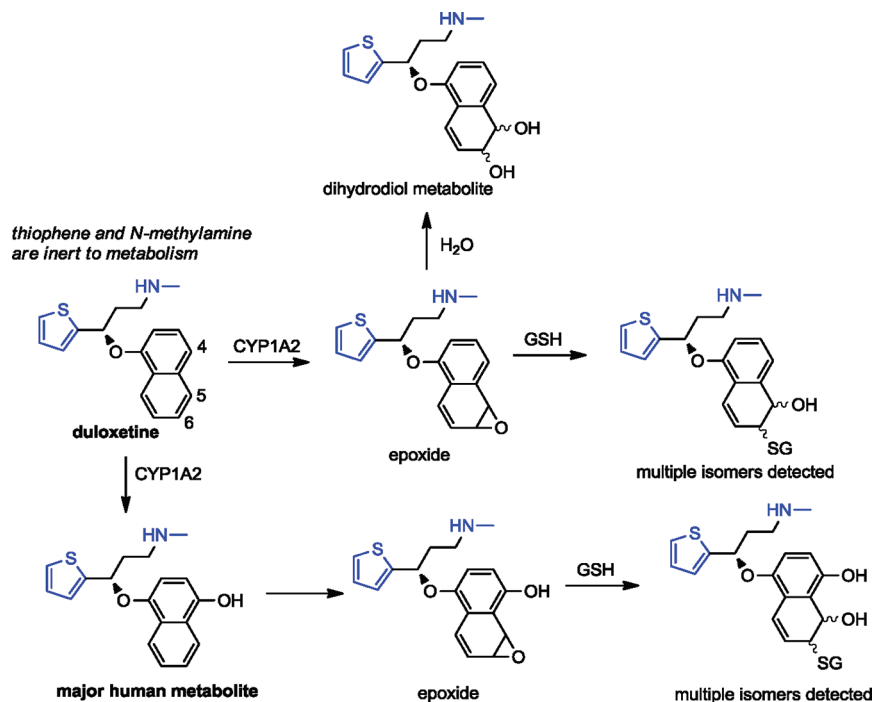
micomycin, midecamycin, spiramycin, and josamycin). The structure of CYP3A4–erythromycin cocrystal has been solved, and electron density corresponding to the macrolide ring could be identified close to the heme group in one of the molecules in the asymmetric unit.⁶⁶ Furthermore, the protein undergoes dramatic conformational changes upon erythromycin binding with an increase in the active site volume by >80%.⁶⁶ As such, the extreme flexibility revealed upon binding of inhibitor to enzyme also challenges any prospective attempt to apply computational design tools without the support of relevant experimental data.

From an SAR standpoint, the antidepressant duloxetine (Scheme 6) provides an interesting perspective. Paris et al. reported that duloxetine causes reversible inhibition as well as TDI of multiple CYP enzymes including CYP1A2, 2B6, 2C19, and 3A4 in an IC₅₀ shift assay format in HLM.⁶⁷ However, attempts to estimate kinetic constants for CYP TDI by duloxetine utilizing a sequential incubation protocol failed to detect the time-dependent component.⁶⁸ Certainly, clinical data support the latter findings wherein duloxetine is more prone to PK interactions as a victim drug rather than a perpetrator.⁶⁹ Structurally, duloxetine contains an *N*-methyl group and a thiophene ring, which can inactivate CYP enzymes via MI complex formation (amine → nitrosoalkane) and/or apoprotein covalent modification through RM (thiophene → thiophene *S*-oxide, thiophene epoxide, sulfenic acid, etc.) generation. However, both amine and the thiophene substituents are inert to oxidative metabolism by CYP enzymes in humans. Instead, duloxetine biotransformation in humans proceeds through CYP1A2-catalyzed hydroxylations of the naphthyl ring at the

4-, 5-, or 6-position, yielding reactive epoxide intermediates that have been trapped with GSH in HLM.⁷⁰ Despite the RM liability, duloxetine does not appear to be associated with TDI of CYP1A2 activity. The duloxetine example highlights key points to take into account when assessing CYP TDI in drug discovery: (a) not all RM-positive compounds will lead to MBI of CYP isoforms that catalyze their formation and (b) the presence of a prototypic structural alert(s) in a molecule does not necessarily translate into a CYP MBI-positive compound. The hypothesis must be tested experimentally through the conduct of a CYP TDI experiment.

As a class, HIV protease inhibitors are frequently associated with PK interactions when coadministered with other acquired immune deficiency syndrome-related therapeutic agents, such as hypolipidemics, macrolide antibiotics, calcium channel blockers, and hormones.⁷¹ All the currently available HIV protease inhibitors are metabolized mainly by CYP3A4 and are potent competitive inhibitors of the isozyme.⁷¹ Protease inhibitors such as ritonavir, nelfinavir, amprenavir, lopinavir, and saquinavir (Figure 6) are also associated with potent TDI of CYP3A4 activity in HLM (ritonavir, $k_{\text{inact}} = 0.4 \text{ min}^{-1}$, $K_{\text{I}} = 0.17 \text{ }\mu\text{M}$; nelfinavir, $k_{\text{inact}} = 0.22 \text{ min}^{-1}$, $K_{\text{I}} = 1.0 \text{ }\mu\text{M}$; amprenavir, $k_{\text{inact}} = 0.59 \text{ min}^{-1}$, $K_{\text{I}} = 0.37 \text{ }\mu\text{M}$; lopinavir, $k_{\text{inact}} = 0.11 \text{ min}^{-1}$, $K_{\text{I}} = 1.0 \text{ }\mu\text{M}$; saquinavir, $k_{\text{inact}} = 0.26 \text{ min}^{-1}$, $K_{\text{I}} = 0.65 \text{ }\mu\text{M}$).^{72,73} Indinavir appears to be the only protease inhibitor devoid of CYP3A4 TDI, although the drug is a potent competitive inhibitor of the isozyme.⁷² Within the chemical class, ritonavir is the most potent (lowest K_{I}) and most efficient inactivator (highest $k_{\text{inact}}/K_{\text{I}}$). In fact, ritonavir is one of the most potent mechanism-based inactivators of CYP3A4 ever

Scheme 6. Oxidative Bioactivation of Duloxetine by CYP1A2 Does Not Lead to MBI of the Isozyme



characterized among drug substances. On the basis of spectral determinations, MI complex formation with the ferrous heme iron atom in CYP3A4 has been observed for some protease inhibitors, although structural details on the metabolite(s) involved in MI complex formation remain unresolved for most compounds. With the exception of amprenavir and ritonavir, which contain structural motifs (aniline in amprenavir and thiazole rings in ritonavir) capable of metabolism-dependent CYP interactions, other protease inhibitors do not contain prototypical functional groups associated with MI complex formation.^{72,73} In the case of nelfinavir, the catechol metabolite generated via oxidation of the cresol moiety by CYP3A4 was considered unlikely to be responsible for CYP inactivation, as the addition of COMT cofactor *S*-adenosyl methionine did not protect against CYP3A4 inactivation in HLM.⁷³ Furthermore, separate preincubation of the catechol metabolite in NADPH-supplemented HLM did lead to MBI of CYP3A4 activity.⁷³ Lack of MI complex formation with lopinavir and saquinavir, coupled with the protective effect of GSH and reactive oxygen scavengers against inactivation, suggests an inactivation mechanism involving the formation of RMs and/or reactive oxygen species. With ritonavir, SAR studies reveal that CYP3A4 MBI requires the presence of both the 5-thiazolyl and 2-(1-methylethyl)thiazolyl groups.⁷⁴ Consistent with the SAR observations, Ma et al.⁷⁵ recently demonstrated the CYP3A4-mediated ring scission of ritonavir's thiazole rings, which results in the formation of the corresponding stable glyoxal derivatives as metabolites (Figure 6). On the basis of these experimental observations, it is possible that the initial oxidation step involving epoxidation of the thiazole rings in ritonavir (prerequisite for thiazole ring scission by CYP enzymes) by CYP3A4 also results in covalent modification of the heme or apoprotein. Given its potent inhibitory effects on CYP3A4, ritonavir is used as a booster of other protease inhibitors.⁷¹ The use of low-dose ritonavir with a second HIV protease inhibitor allows the achievement of a PK benefit that leads to increased

systemic exposure, creating a higher genetic barrier to resistance. Boosting of protease inhibitors has become common practice and is recommended in treatment guidelines with most protease inhibitors. Like ritonavir, the thiazole analogue cobicistat (Figure 6) is a mechanism-based inactivator of CYP3A4 and is currently in phase III trials to boost systemic exposure of protease inhibitors (notably the HIV integrase inhibitor elvitegravir). In contrast with ritonavir, cobicistat has no anti-HIV activity of its own.⁷⁶

3.2. Covalent Modification of Heme and/or Apoprotein by Drugs. The nontricyclic antidepressant nefazodone (Scheme 7) is a substrate and potent inhibitor (reversible and time-dependent) of CYP3A4 in HLM (IC_{50} values for competitive and TDI of 1.5 and 0.015 μ M, respectively, estimated from the IC_{50} shift assay format).^{77,78} Consistent with the *in vitro* observations, nefazodone is associated with nonstationary PK upon dose escalation⁷⁹ and increases maximal plasma concentrations (C_{max}) and AUC of diverse CYP3A4 substrates upon coadministration in humans,^{79,80} some of which are life-threatening (e.g., cases of rhabdomyolysis associated with simvastatin and nefazodone use).⁸¹ In addition to the CYP3A4 TDI, nefazodone use has been associated with numerous cases of idiosyncratic hepatotoxicity, many of which required liver transplantation and/or resulted in fatalities.⁸² Nefazodone use has been banned in many countries in the European Union and Canada, and the generic version carries a black box warning (BBW) label in the United States. Both of nefazodone's liabilities including CYP3A4 TDI and hepatotoxicity have been linked to its metabolism to RMs capable of covalently modifying CYP3A4 and other critical proteins in hepatic tissue.⁸³ The mechanism of RM formation involves metabolism of *p*-hydroxynefazodone, a circulating metabolite of nefazodone in humans, to reactive quinonoid species (quinoneiminium and *p*-benzoquinone derivatives), which can be trapped as GSH conjugates in HLM incubations (Scheme 7).^{77,78}

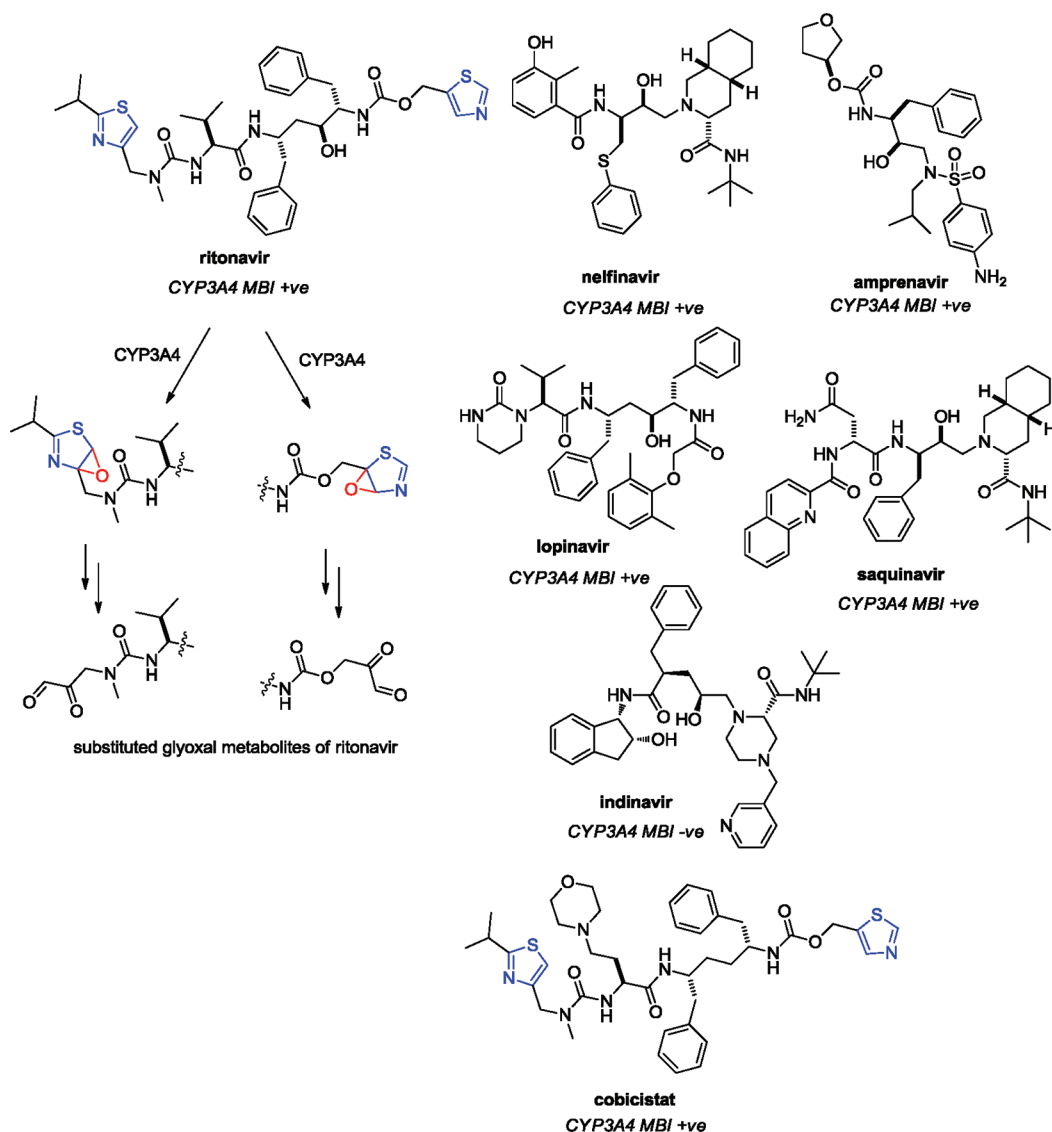
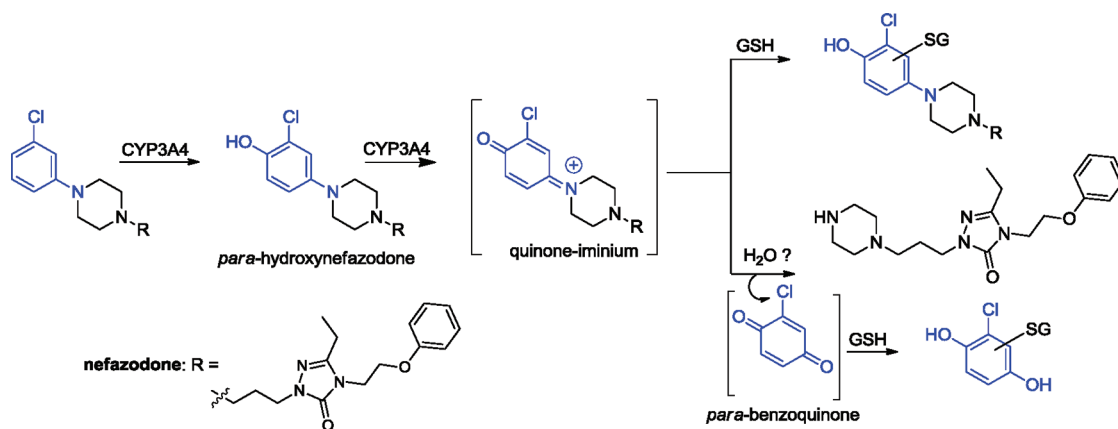


Figure 6. HIV protease inhibitors that cause TDI of CYP3A4.

Scheme 7. Proposed Mechanism of CYP3A4 Inactivation by the Tricyclic Antidepressant Nefazodone



From a SAR standpoint, structurally related antidepressants trazodone, aripiprazole, and buspirone exhibit little to no CYP3A4 TDI in vitro (Figure 7).⁸⁴ Side-by-side analysis of nefazodone and aripiprazole in the IC₅₀ shift assay indicates that aripiprazole is devoid of CYP3A4 TDI seen with nefazodone.⁷⁸ The diminished

and/or lack of CYP3A4 inactivation with these agents is consistent with the absence of PK interactions with CYP3A4 substrates. Like nefazodone, trazodone also contains the 3-chlorophenylpiperazine ring, which is oxidatively metabolized by CYP3A4 to *p*-hydroxytrazodone, a major urinary

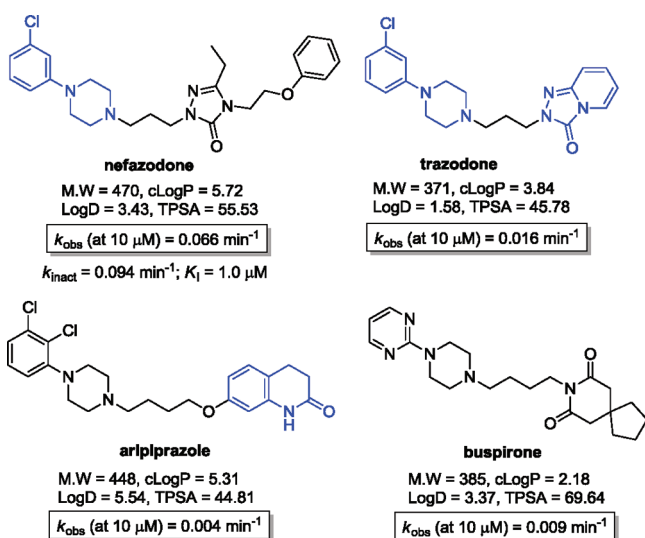
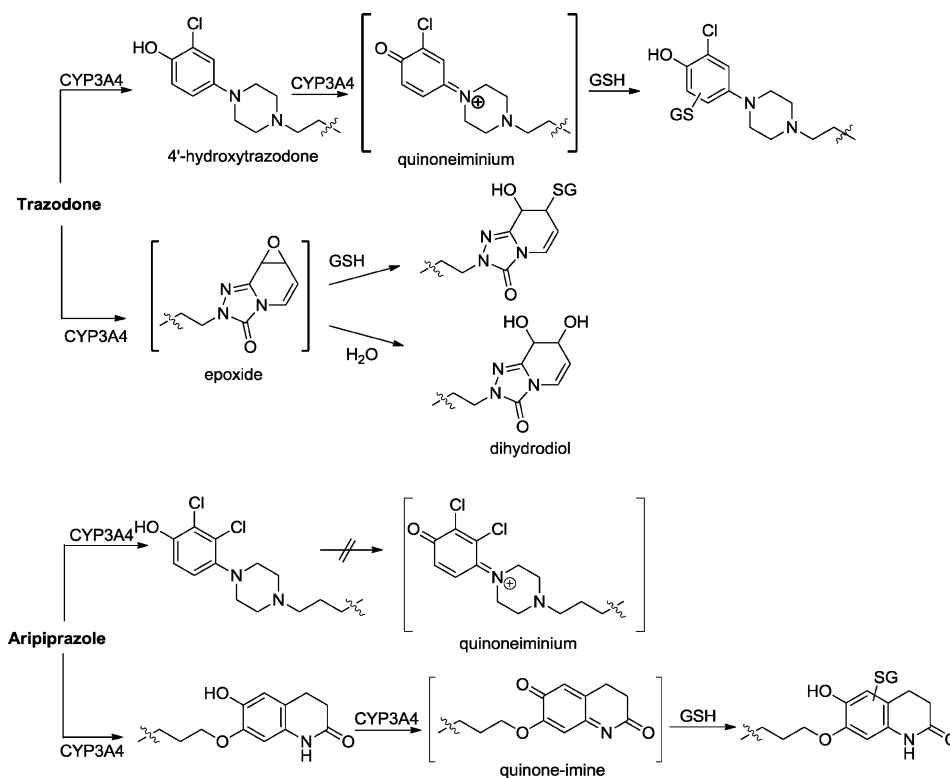


Figure 7. Chemical structures, physicochemical properties, and CYP3A4 TDI data for nontricyclic antidepressants. Structural elements in blue represent the region susceptible to RM formation by CYP3A4. TPSA refers to topological polar surface area. Initial observed inactivation rate (k_{obs}) at a single inactivator concentration of 10 μM is as reported in ref 84.

metabolite in humans. A reactive quinoneiminium species obtained from the two-electron oxidation of the *p*-hydroxytrazodone metabolite has been trapped with GSH in HLM (Scheme 8).⁸⁵ In addition, the detection of a dihydrodiol metabolite of trazodone in human urine is suggestive of a second bioactivation sequence involving the formation of an electrophilic epoxide on the triazolopyridinone moiety present in the drug. Indeed, HLM and recombinant CYP3A4 incubations of trazodone

in the presence of GSH have led to the detection of stable dihydrodiol and a GSH conjugate derived from epoxide ring-opening.⁸⁵ While the bioactivation pattern of trazodone bears resemblance to nefazodone, the degree of CYP3A4 inactivation by trazodone is significantly weaker.⁸⁴ The reason(s) for this disconnect is unclear. One possibility is that trazodone is less susceptible to CYP3A4-catalyzed metabolism/bioactivation than nefazodone because of its lower lipophilicity. With aripiprazole, CYP3A4-mediated aromatic hydroxylation on the 2,3-dichlorophenylpiperazine ring leads to the *p*-hydroxyaripiprazole circulating metabolite, which can also form a quinoneiminium species similar to nefazodone. However, failure to detect GSH adducts derived from conjugation with the *p*-hydroxyaripiprazole metabolite in HLM suggests that the secondary oxidation does not occur.⁷⁸ In contrast, sequential metabolism of the pendent acetanilide motif in aripiprazole by CYP3A4 does lead to a reactive quinoneimine intermediate in HLM. Despite this liability, aripiprazole does not inactivate CYP3A4 nor is it associated with life-threatening hepatotoxicity.^{78,84} Aripiprazole is more lipophilic than nefazodone (Figure 7) and is more tightly bound to microsome and plasma protein, a phenomenon that may reduce the overall rate of metabolism because of a significant reduction in free fraction available for metabolism. The markedly improved safety profile of aripiprazole (versus nefazodone) can be potentially explained by the vast improvement in human PK (aripiprazole, oral bioavailability of 87%; clearance of 0.8 $\text{mL min}^{-1} \text{kg}^{-1}$, half-life of 75 h; nefazodone, oral bioavailability of 20%, clearance of 7.5 $\text{mL min}^{-1} \text{kg}^{-1}$, half-life of 1 h) via a reduction in propensity for CYP3A4-mediated metabolism/bioactivation, phenomena that ultimately translate to a significantly lower efficacious daily dose (10–15 mg) compared with nefazodone (200–600 mg). Finally, buspirone possesses a pyrimidinylpiperazine motif in lieu of the 3-chlorophenylpiperazine scaffold in nefazodone.

Scheme 8. Metabolism of Nontricyclic Antidepressants Trazodone and Aripiprazole by CYP3A4 to RMs



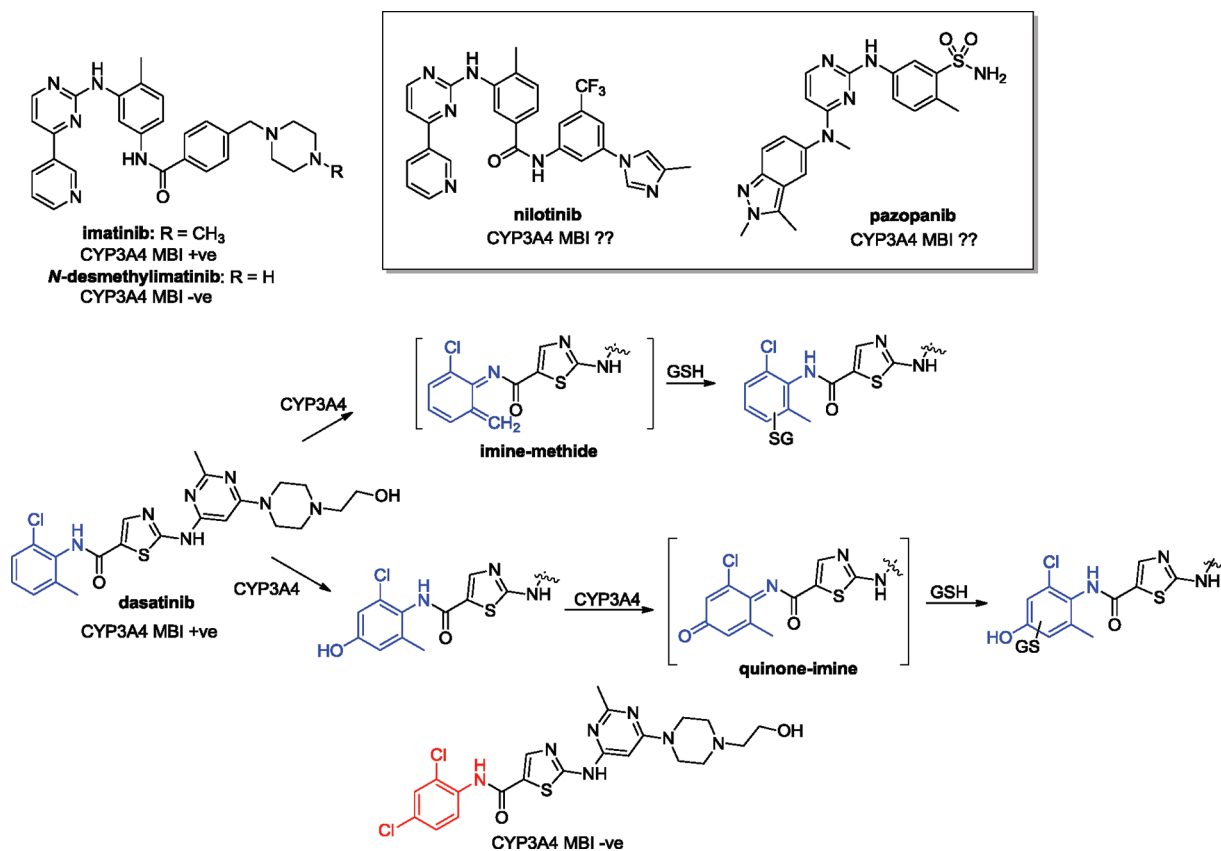
While *p*-hydroxybuspirone represents a major circulating metabolite in human, lack of CYP3A4 TDI and/or detection of GSH conjugates in HLM incubations of buspirone suggests that *p*-hydroxybuspirone does not succumb to RM formation in a manner similar to that observed with *p*-hydroxynefazodone.⁷⁷ Absence of RM formation with buspirone is consistent with *ab initio* calculations, which suggest that a weaker resonance stabilization of the oxidation products and the greater acidity make *p*-hydroxybuspirone less favorable for the two-electron oxidation process.⁷⁷

Certain multitargeted tyrosine kinase (TK) inhibitors (e.g., imatinib, dasatinib, erlotinib, lapatinib, etc.), which are frequently used in the treatment of cancer, also cause PK interactions with CYP3A4 substrates.⁸⁶ Because TK inhibitors are usually prescribed for prolonged periods in patients with comorbidities, the risks of DDIs tend to significantly increase with comedication in this patient population. Imatinib (Scheme 9) was the first rationally designed TK inhibitor, which revolutionized the treatment of chronic myelogenous leukemia, advanced gastrointestinal stromal tumors, and other hematological diseases. Inhibitory effects of imatinib against CYP3A4 have been investigated in a clinical DDI study with simvastatin, wherein imatinib (400 mg daily) decreased simvastatin clearance by 70%, suggesting a strong CYP3A4 inhibitory effect *in vivo*.⁸⁷ Imatinib (400–600 mg daily) also reduces CYP3A4 activity in patients by 10–70%, as reflected in the erythromycin breath test.⁸⁸ The clinical observations are consistent with TDI ($k_{\text{inact}} = 0.07 \text{ min}^{-1}$; $K_I = 14.3 \text{ }\mu\text{M}$) of CYP3A4-catalyzed midazolam 1'-hydroxylation *in vitro*.⁸⁹ The active *N*-desmethylimatinib metabolite (i.e., CGP74588) is not a

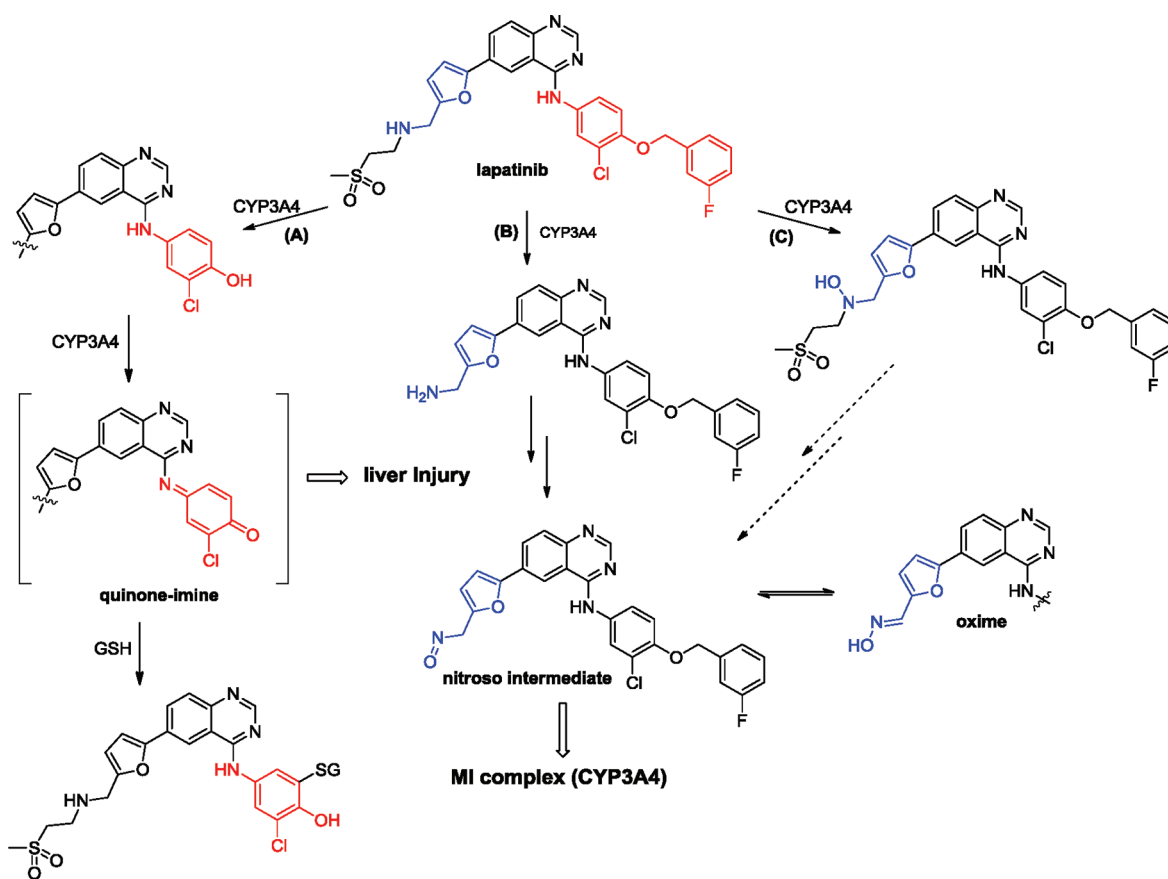
time-dependent inactivator of CYP3A4.⁸⁹ The precise mechanism of CYP3A4 inactivation by imatinib remains unclear. It is possible that RMs (e.g., imine methide) derived from the bioactivation of the alkyraniline/acetanilide motif are responsible for enzyme modification. Certainly hydroxylation of the benzylic methyl group is a known metabolic fate of imatinib in humans. From a SAR standpoint, nilotinib is structurally related to imatinib and is a second-generation TK inhibitor approved for the treatment of chronic myelogenous leukemia resistant to, or intolerant of, prior treatment that included imatinib. PK interactions with substrates of CYP3A4, CYP2C8/2C9, and CYP2D6 have been attributed to nilotinib's competitive inhibitory effects against the respective CYP isozymes.⁹⁰ The propensity of nilotinib to cause TDI of CYPs is presently unknown; the chemical structure of nilotinib preserves the aminopyrimidine and amide pharmacophores of imatinib but incorporates substituents alternative to the basic *N*-methyl-piperazine ring in imatinib, thereby leading to greater lipophilicity. Like imatinib, nilotinib is cleared in humans via oxidative metabolism by CYP3A4, but information on the biotransformation pathways is not available.⁹⁰ Likewise, pazopanib is the newest TK inhibitor approved for the treatment of advanced or metastatic renal cell carcinoma. Pazopanib is associated with severe and fatal hepatotoxicity resulting in a BBW label. Pazopanib is primarily cleared in humans via metabolism by CYP3A4; however, details on its biotransformation pathways and/or ability to cause CYP3A4 TDI have not been published.

Dasatinib (Scheme 9) has been approved for the treatment of imatinib-resistant acute myeloid leukemia. Increases in

Scheme 9. Pyrimidine-Based Tyrosine Kinase Inhibitors Imatinib and Dasatinib as Time- and Concentration-Dependent Inactivators of CYP3A4



Scheme 10. Proposed Mechanism of CYP3A4 Inactivation and Idiosyncratic Hepatotoxicity Associated with the Tyrosine Kinase Inhibitor Lapatinib



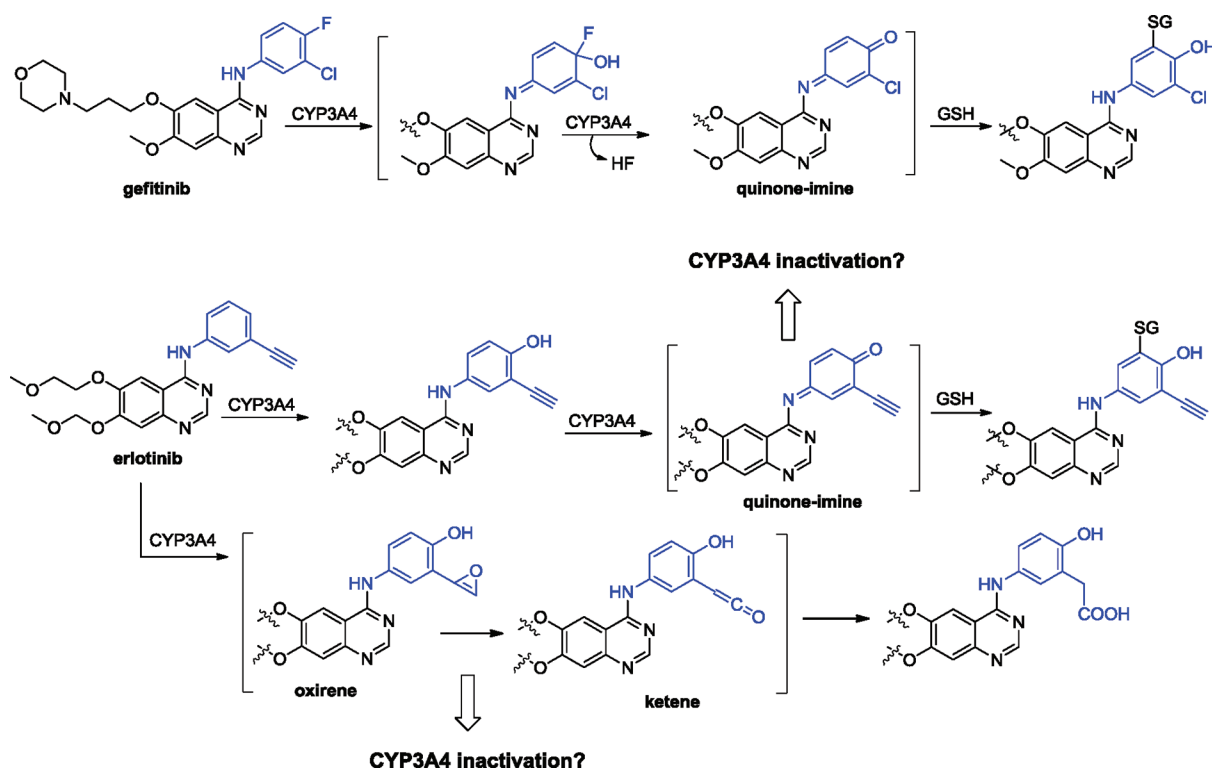
simvastatin C_{\max} and AUC upon coadministration of dasatinib suggest CYP3A4 inhibitory effects similar to those of imatinib.⁸⁶ Li et al.⁹¹ established TDI of CYP3A4 activity ($k_{\text{inact}} = 0.034 \text{ min}^{-1}$ and $K_I = 6.3 \text{ } \mu\text{M}$) by dasatinib in HLM. The mechanism is thought to involve CYP3A4-mediated *p*-hydroxylation of the 2-chloro-6-methylphenyl ring (the major metabolite of dasatinib in humans) followed by further oxidation to the reactive quinoneimine. Formation of a reactive imine methide is also detected but appears to be a minor bioactivation pathway. Characterization of stable GSH adducts of these RMs in HLM incubations of dasatinib provides evidence for the proposed bioactivation pathway. From a SAR standpoint, modifications on the piperazine or methylpyrimidine rings of dasatinib do not abolish CYP3A4 TDI, but consistent with the inactivation mechanism, simultaneously removing the methyl group and blocking the para-position of the chloromethylphenyl ring with a chlorine atom eliminate CYP3A4 inactivation.⁹¹

TDI of CYP3A4 has also been reported with the TK inhibitor lapatinib (Scheme 10),⁹² which is used in the treatment of advanced metastatic breast cancer. Lapatinib also carries a BBW for idiosyncratic hepatotoxicity including rare cases of liver-related fatalities that can occur several days to a month after initiation of treatment. In vitro lapatinib is extensively metabolized by CYP3A4 and, to a lesser extent, CYP2C8 to yield products of O- and N-dealkylation.⁹² O-Dealkylation of lapatinib in humans generates a *p*-hydroxyaniline derivative that is oxidized by CYP3A4 to a reactive quinoneimine intermediate amenable to trapping by GSH (Scheme 10, pathway A).⁹² It has

been proposed that lapatinib bioactivation to the quinoneimine metabolite could trigger downstream reactions leading to liver injury.⁹² In contrast, the mechanism of CYP3A4 inactivation by lapatinib ($k_{\text{inact}} = 0.02 \text{ min}^{-1}$ and $K_I = 1.7 \text{ } \mu\text{M}$) is thought to occur via quasi-irreversible MI complex formation (and not via adduction of the reactive quinoneimine metabolite to apoprotein or heme).⁹³ An increase in the signature Soret absorbance at $\sim 455 \text{ nm}$ and restoration of enzymatic activity with potassium ferricyanide support this hypothesis. In addition, products of amine oxidation that include the lapatinib hydroxylamine and the oxime form of N-dealkylated lapatinib have been characterized, suggesting that a nitroso intermediate(s) derived from these metabolites is involved in MI complex formation (Scheme 10, pathways B and C).⁹³ Because lapatinib is a CYP3A4 substrate, MBI of CYP3A4 translates into nonstationary increases in systemic exposure of the drug upon repeated dosing in humans.⁹²

The observations on lapatinib bioactivation parallel that for other structurally related TK inhibitors such as gefitinib and erlotinib, which form reactive quinonoid intermediates (Scheme 11) and where hepatotoxicity is a side effect of treatment.^{94,95} Gefitinib is a *p*-fluoroaniline derivative that undergoes a CYP3A4-mediated oxidative defluorination to the corresponding quinoneimine species.⁹⁴ In the case of erlotinib, the *p*-hydroxyaniline metabolite generated via a CYP3A4-mediated oxidation of its 3-ethynylaniline motif is oxidized further to the quinoneimine.⁹⁵ Evidence for formation of reactive quinonoid intermediates has been obtained by virtue of GSH trapping studies.^{94,95} Interestingly, metabolism of erlotinib

Scheme 11. Bioactivation of the TK Inhibitors Gefitinib and Erlotinib by CYP3A4 That Leads to MBI with Erlotinib (but Not Gefitinib)



(but not gefitinib) is accompanied by TDI of CYP3A4 ($k_{\text{inact}} = 0.035\text{--}0.09\text{ min}^{-1}$; $K_I = 6.3\text{--}22\text{ }\mu\text{M}$).⁹⁵ Furthermore, CYP3A4 inactivation by erlotinib is consistent with a reported case of rhabdomyolysis arising from an interaction between erlotinib and the CYP3A4 substrate simvastatin.⁹⁶ SAR studies suggest that CYP3A4 TDI is not dependent upon oxidation of the alkyne group to a reactive oxirene or ketene species, since replacement of the alkyne with a cyano functionality does not abolish CYP3A4 inactivation.⁹⁵ However, the role of the alkyne in CYP3A4 inactivation cannot be entirely dismissed given that oxidation of this functionality to the corresponding arylacetic acid is a known metabolic fate of erlotinib in humans (see Scheme 11)⁹⁵ and is catalyzed by several human CYPs (e.g., CYP2D6 and CYP1A1/1A2) in addition to CYP3A4. It is possible that oxidation of the alkyne may act as a second route of CYP3A4 inactivation.

Time-dependent inactivation of CYP3A4 (in addition to competitive inhibitory effects on CYP3A4, CYP2D6, and CYP2C19) has also been demonstrated with sorafenib (Figure 8),⁸⁴ which

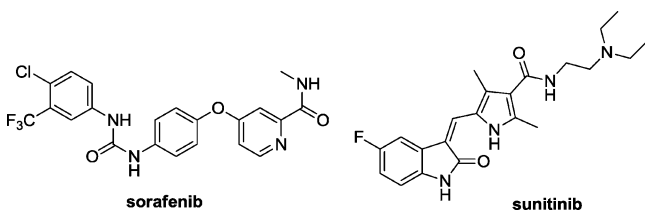


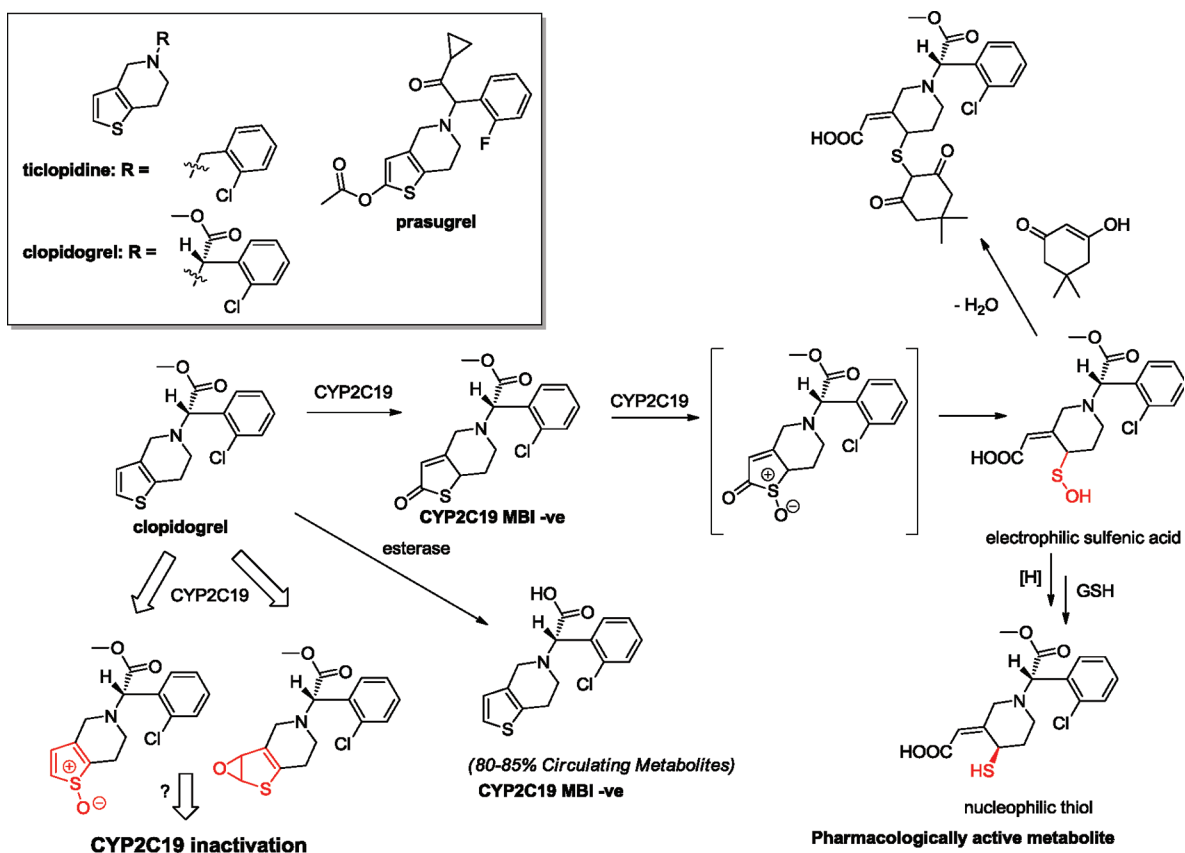
Figure 8. Structures of tyrosine kinase inhibitors sorafenib (CYP3A4 TDI +ve) and sunitinib (CYP3A4 TDI -ve).

has been approved for the treatment of hepatocellular carcinoma. In patients, sorafenib at 400 mg twice daily alters the systemic exposures of probe CYP3A4, CYP2D6, and/or

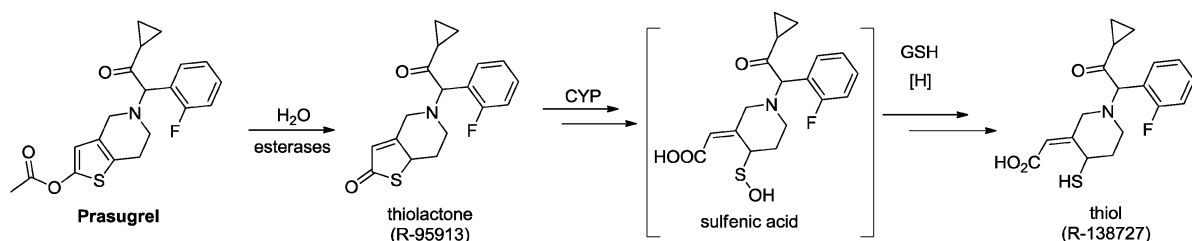
CYP2C19 substrates. However, differences in PK are sufficiently small that a clinically significant *in vivo* inhibition of these CYP isoenzymes is deemed unlikely.⁹⁷ Lack of clinical DDIs despite potent *in vitro* inhibitory effects on CYP3A4 can be explained on the basis of mass balance studies, which indicate that most of the sorafenib dose ($\sim 65\%$) in humans is subject to fecal excretion (in the unchanged form) and phase II glucuronidation by UGT1A9, with minimal contribution ($\sim 5\%$) from CYP3A4.⁹⁸ The mechanism of CYP3A4 TDI by sorafenib remains unknown; sorafenib *N*-oxide, which is formed by CYP3A4, is the main circulating metabolite in humans and has *in vitro* potency similar to that of sorafenib.⁹⁹ Sunitinib (Figure 8) is a multitargeted receptor TK inhibitor that is used in the treatment of renal cell carcinoma as well as gastrointestinal stromal tumor. Available evidence suggests that sunitinib is metabolized mainly by CYP3A4 but does not cause TDI of CYP3A4 activity, a phenomenon that is consistent with lack of DDIs with CYP3A4 substrates in the clinic.^{84,86}

Tetrahydrothienopyridines ticlopidine, clopidogrel, and prasugrel (Scheme 12) are prodrugs, which require biotransformation into “active” reactive metabolites for antithrombotic activity. Metabolites of ticlopidine and clopidogrel are produced via a CYP-catalyzed oxidation (principally mediated by CYP2C19) involving initial conversion to the corresponding thiolactone metabolites followed by *S*-oxidation and subsequent ring scission to the free thiol derivatives, which form a covalent disulfide linkage with a cysteinyl residue on the P2Y₁₂ receptor in platelets.¹⁰⁰ Recently, Dansette et al.¹⁰¹ studied the pathway associated with the thiolactone ring scission in tetrahydrothienopyridines and identified the intermediate sulfenic acid species via trapping studies in HLM using dimedone as a nucleophile (Scheme 12).¹⁰¹ Subsequent reduction of the sulfenic acid intermediate by GSH could lead to the pharmacologically active

Scheme 12. Postulated Mechanism of CYP2C19 Inactivation by Tetrahydrothienopyridine Antithrombotic Drugs Clopidogrel and Ticlopidine



Scheme 13. Metabolism of Prasugrel Leading to Its Pharmacologically Active Metabolite

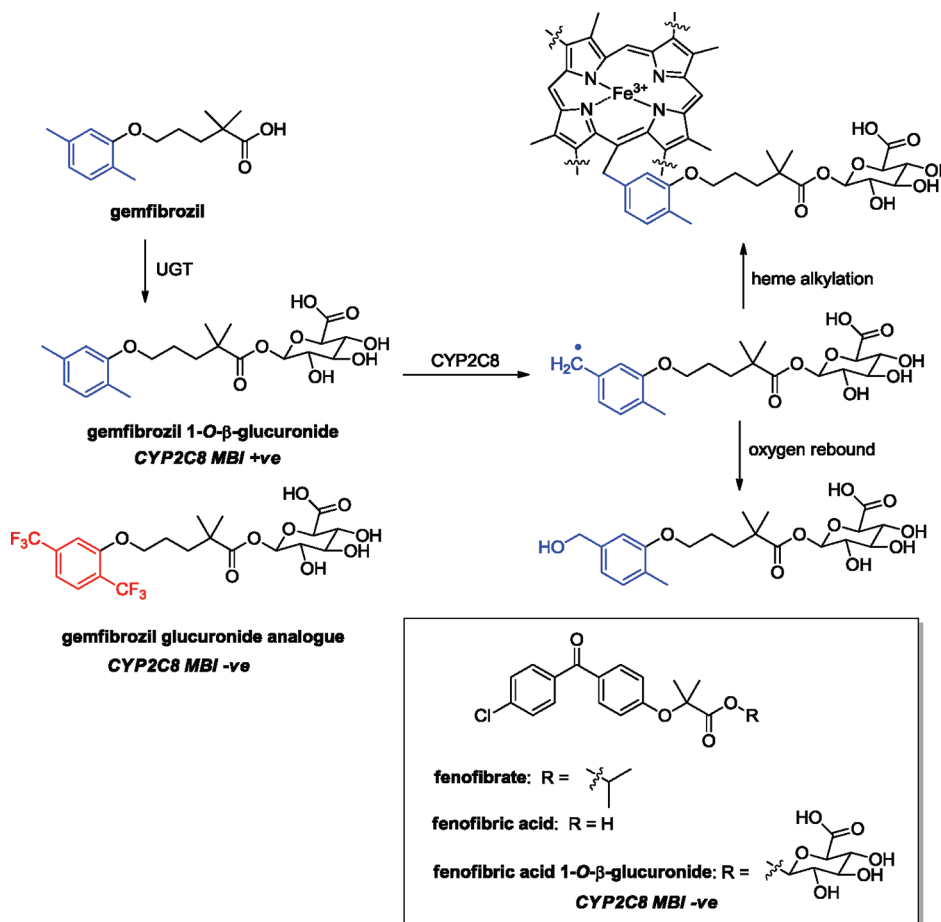


thiol derivatives (see Scheme 12). In vitro metabolic processing of ticlopidine and clopidogrel into RMs also leads to TDI of CYP2C19 activity (ticlopidine, $k_{\text{inact}} = 0.07 \text{ min}^{-1}$, $K_I = 3.3 \mu\text{M}$; clopidogrel, $k_{\text{inact}} = 0.055 \text{ min}^{-1}$, $K_I = 14.3 \mu\text{M}$).^{102,103} Since inactivation is only discerned with the parent prodrugs and not with the respective thiolactone metabolites, it is likely that thiophene ring oxidation to the thiolactone metabolites generates reactive species (e.g., thiophene S-oxide and/or thiophene epoxide) that inactivate CYP2C19.¹⁰² Recent reports have shown that the clinical pharmacological effect of clopidogrel is affected by the polymorphically expressed CYP2C19 genotype.¹⁰⁴ Furthermore, Kurihara et al.¹⁰⁵ reported that CYP2C19 is one of the CYP enzymes responsible for the oxidation of clopidogrel and its thiolactone in vitro. Collectively, these observations suggest that the oxidative metabolism of clopidogrel by CYP2C19 to yield the active metabolite and the inactivation of CYP2C19 occur simultaneously.

From a DDI perspective, it is interesting to note that most (>70%) of the clopidogrel daily dose in humans is rapidly hydrolyzed by human carboxylesterases to the inactive carboxylic

acid metabolite, which does not cause TDI of CYP2C19 activity.¹⁰⁶ Furthermore, both clopidogrel and ticlopidine cause CYP2C19 inactivation but only ticlopidine is associated with a 5.0- to 6.2-fold increase in the AUC of the probe CYP2C19 substrate omeprazole in extensive metabolizers.¹⁰³ Lack of DDIs via CYP2C19 inactivation by clopidogrel appears to be in reasonable agreement with the predicted fold increase in AUC of ~ 1.0 with CYP2C19 substrates, presumably due to the extremely low unbound circulating concentrations.¹⁰³ In contrast with the observations on ticlopidine and clopidogrel metabolism, prasugrel does not inactivate CYP2C19. The thiolactone metabolite (R-138727) of prasugrel is produced via an esterase-mediated hydrolysis (as opposed to the action of CYP enzymes) followed by CYP oxidation to afford the thiol metabolite R-95913 (Scheme 13).¹⁰⁷ The process of ester bond cleavage is so facile that the parent drug is not detected in vivo. Consistent with this overall behavior, prasugrel does not cause TDI of CYP2C19 and is not expected to cause DDIs in vivo.¹⁰³

In addition to CYP2C19 inactivation, clopidogrel, ticlopidine, and their respective thiolactone metabolites also lead to

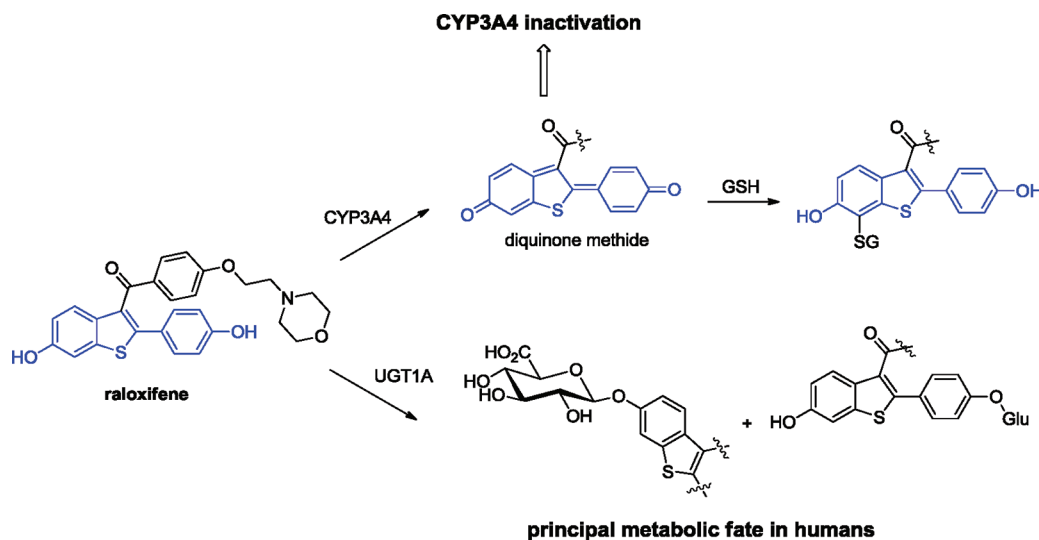
Scheme 14. MBI of CYP2C8 by the Gemfibrozil-1-*O*- β -glucuronide Metabolite of Gemfibrozil

MBI of CYP2B6 activity *in vitro*.¹⁰⁸ In particular, clopidogrel is highly potent and selective for CYP2B6 inactivation in HLM, with K_I and k_{inact} of 0.5 μM and 0.35 min^{-1} , respectively.¹⁰⁹ These findings make clopidogrel the most potent mechanism-based inhibitor known for CYP2B6. Mass spectral analysis of CYP2B6 that had been inactivated by either clopidogrel or the thiolactone metabolite showed an increase in the mass of the protein by ~ 350 Da, which is consistent with the addition of the thiol metabolite of clopidogrel to CYP2B6.¹¹⁰ Peptide mapping of tryptic digests of the inactivated CYP2B6 suggests Cys475 as the site of covalent modification possibly via disulfide bond formation. Consistent with this observation, mutation of Cys475 to a serine residue eliminated the formation of the protein adduct and prevented the C475S variant from MBI by the thiolactone metabolite of clopidogrel. Interestingly, this mutation does not prevent the C475S variant from being inactivated by clopidogrel. Furthermore, inactivation of both wild-type CYP2B6 and C475S by clopidogrel, but not by the thiolactone metabolite, leads to the loss of the heme, which accounts for most of the loss of the catalytic activity. Collectively, these results suggest that clopidogrel inactivates CYP2B6 primarily through destruction of the heme, whereas the thiolactone metabolite of clopidogrel inactivates CYP2B6 through covalent modification of Cys475. Recent clinical studies have demonstrated that ticlopidine and clopidogrel are potent inhibitors of CYP2B6 in humans as judged by the increase in systemic exposure to bupropion, an antidepressant drug and specific substrate for CYP2B6, by 85 and 60%, respectively, and a decrease in the systemic exposure of the metabolite hydroxybupropion by 84 and 52%, respectively.¹¹¹

Against this backdrop, the thiolactone metabolite of prasugrel is 10- to 22-fold less potent, respectively, as a time-dependent inactivator of CYP2B6 than ticlopidine and clopidogrel.¹⁰⁸ Consistent with this *in vitro* finding, prasugrel was found to be a weak inhibitor of CYP2B6 activity in humans, with the exposure of bupropion increased by 18% and that of hydroxybupropion decreased by 23%.¹¹²

The CYP inactivation mechanism of gemfibrozil (Scheme 14) is perhaps one of the most interesting ones, since it involves a phase II metabolite of the parent drug. Gemfibrozil belongs to a class of drugs known as fibrates, which are used in the treatment of dyslipidemia. Although *in vitro* studies in HLM demonstrate that gemfibrozil is a more potent reversible inhibitor of CYP2C9 ($\text{IC}_{50} = 9.6 \mu\text{M}$) than CYP2C8 ($\text{IC}_{50} = 95 \mu\text{M}$) activity,^{113,114} results from *in vivo* DDI studies reveal opposing trends. Gemfibrozil increases the systemic exposure of CYP2C8 substrates such as cerivastatin, repaglinide, rosiglitazone, and pioglitazone but has no effect on the PK of the CYP2C9 substrate warfarin.^{115–117} This discrepancy has been explained by demonstrating that the major metabolite of gemfibrozil, i.e., gemfibrozil-1-*O*- β -glucuronide, is a more potent inhibitor of CYP2C8 *in vitro*, relative to gemfibrozil (IC_{50} of 4.1 and 28 μM , respectively, for gemfibrozil glucuronide and the parent drug).¹¹⁸ In subsequent studies, Ogilvie et al.¹¹⁹ demonstrated that preincubation of the glucuronide metabolite with NADPH-supplemented HLM further lowered the IC_{50} from 24 to 1.8 μM for inhibition of CYP2C8 activity, which is consistent with TDI. Associated k_{inact} and K_I for TDI of CYP2C8 activity in HLM by gemfibrozil glucuronide were 0.21 min^{-1} and 20–52 μM ,

Scheme 15. Explanation for the Lack of Clinical DDIs with Raloxifene Despite in Vitro MBI of CYP3A4



respectively. The TDI of CYP2C8 was not observed with gemfibrozil, and neither the substrate nor the metabolite demonstrated TDI of CYP2C9. Furthermore, the NADPH dependence ruled out the possibility that CYP2C8 was inactivated via direct covalent adduction with the acyl glucuronide metabolite, which is electrophilic in nature. Consistent with the in vitro observations on CYP2C8 TDI, Tornio et al.¹²⁰ reported that volunteers who ingested 0.25 mg of repaglinide up to 12 h following a 600 mg dose of gemfibrozil demonstrated sustained (and significant) increase in repaglinide plasma concentrations compared to that observed in volunteers who ingested repaglinide and gemfibrozil simultaneously. At 12 h postadministration of gemfibrozil, plasma concentrations of gemfibrozil and its glucuronide were only 5–10% of their peak values. It was argued that the long-lasting DDI was likely due to CYP2C8 MBI by the gemfibrozil glucuronide metabolite. As such, the inhibitory effect in humans is rapid and occurs 1 h after gemfibrozil administration.¹²¹ The mechanism of CYP2C8 inactivation was initially thought to involve covalent adduction of the apoprotein by a quinone methide species generated from the aromatic hydroxylation of the 2',5'-dimethylphenoxy group in gemfibrozil glucuronide.¹¹⁹ However, LC-MS/MS analysis of inactivated CYP2C8 following reaction with gemfibrozil glucuronide and NADPH did not reveal such an adduct to the apoprotein but instead provided evidence for the direct covalent adduction of a benzylic carbon on the 2',5'-dimethylphenoxy group to the heme prosthetic group of the CYP.¹²² The regioselectivity of substrate addition to the heme group was not confirmed experimentally, but computational modeling experiments indicated that the γ -meso position was the most likely site of modification. The metabolite profile, which consisted of two benzyl alcohol metabolites and a 4'-hydroxygemfibrozil glucuronide metabolite, indicated that CYP-mediated oxidation of the glucuronide metabolite was localized to the 2',5'-dimethylphenoxy group. Overall, the results are consistent with an inactivation mechanism wherein gemfibrozil glucuronide is oxidized to a benzyl radical intermediate, which evades oxygen rebound, and adds to the γ -meso position of heme (Scheme 14). The proposed mechanism is also consistent with SAR studies, wherein replacement of the aromatic methyl groups in gemfibrozil glucuronide with trifluoromethyl functionalities abolishes MBI of CYP2C8.¹²³ An additional SAR perspective

stems from the fact that commonly prescribed fibrates, in particular fenofibrate, (Scheme 14), have not been associated with TDI of CYP2C8, although the drug is prone to glucuronidation following hydrolytic cleavage of its ester linkage to the active component, fenofibric acid. Likewise, acylglucuronide derivatives of structurally diverse drugs (e.g., nonsteroidal anti-inflammatory agents, statins) are devoid of CYP2C8 inactivation.¹²³ Finally, it is noteworthy to comment on the possibility that DDIs with gemfibrozil could also arise via non-CYP mechanisms, involving inhibition of (i) organic anion transporting polypeptide 2 by the parent drug and its glucuronide¹¹⁸ and (ii) uridine glucuronosyl transferase (UGT) mediated glucuronidation of victim drugs.¹²⁴ For instance, the most pronounced gemfibrozil interactions have been observed with repaglinide and cerivastatin, which are only partially metabolized by CYP2C8. Finally, the ability of gemfibrozil to induce CYP2C8 (in addition to inhibitory effects) may further complicate the ability to retrospectively predict the magnitude of clinical DDIs.¹²⁵

Raloxifene (Scheme 15) is a selective estrogen receptor modulator that is used in the treatment of osteoporosis in postmenopausal women. Raloxifene is a well-characterized mechanism-based inactivator of CYP3A4 activity (k_{inact} and K_I of 0.16 min^{-1} and $9.9 \mu\text{M}$, respectively) in HLM.^{126–129} In vitro, raloxifene is metabolized by CYP3A4 to produce several electrophilic species including a diquinone methide intermediate that can be trapped with GSH.¹²⁶ The process is also accompanied by microsomal covalent binding and irreversible inactivation of CYP3A4.^{126–129} Mass spectral analyses indicate that a single equivalent of raloxifene is bound to the intact CYP apoprotein.¹²⁷ Furthermore, analysis of peptides following digestion with proteinase K revealed covalent binding to Cys239 presumably via the diquinone methide intermediate.^{127,128} The findings are consistent with the observation that iodoacetamide or *N*-(1-pyrene)iodoacetamide (cysteine-specific alkylating agents) prevents CYP3A4 TDI by raloxifene. Analysis of the structure of raloxifene metabolites along with CYP3A4 active site docking studies using a computational model defined by X-ray crystal structure data suggests that the binding occurs on the pendent phenyl group.¹²⁸ Interestingly, CYP3A5, which lacks the Cys239 residue (corresponding residue is Ser239), is resistant to MBI by raloxifene, a finding that is associated with a significant increase in GSH conjugates of raloxifene compared

with that for CYP3A4. Contrary to the findings of Baer et al.,¹²⁷ a second group of investigators identified the nucleophilic OH group of Tyr75 in CYP3A4 as the site of adduction to raloxifene diquinone methide.¹²⁸ Despite the *in vitro* observations on CYP3A4 MBI, raloxifene is not associated with significant DDIs with CYP3A4 substrates (raloxifene package insert). A probable reason for the discrepancy is that the principal clearance mechanism of raloxifene in humans is via phenolic glucuronidation that is mediated by intestinal UGT 1A enzymes (Scheme 15).¹³⁰ Thus, the likelihood of raloxifene bioactivation leading to CYP3A4 MBI *in vivo* is in question when compared with the efficiency of the glucuronidation in the small intestine.

This section cannot be complete without a final and perhaps the most important account of life-threatening DDIs arising via CYP3A4 MBI with mibefradil (Figure 9), a nondihydropyridine

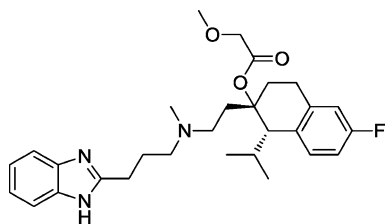


Figure 9. Structure of nondihydropyridine calcium antagonist mibefradil, a potent mechanism-based inactivator of CYP3A4.

calcium channel blocker approved for the treatment of hypertension. Within months of approval in the United States in 1997, there were several reports of significant PK interactions between mibefradil and drugs primarily metabolized by CYP3A4. In one instance, a single dose of the dihydropyridine nifedipine was consumed 24 h after the last dose of mibefradil. The ensuing hypotension and bradycardia were refractory to all available therapy, and the patient died within 24 h of ingesting the dihydropyridine.¹³¹ Plasma concentrations of drugs such as simvastatin, tacrolimus, cyclosporine, and digoxin also exhibited a marked increase when coadministered with mibefradil.¹³² Mibefradil was voluntarily withdrawn from the market within the first year of its release because of the heightened potential for rhabdomyolysis, renal failure, or bradycardia upon coadministration with other drugs.¹³³ Soon after withdrawal from the market, mibefradil was characterized as a potent reversible (IC_{50} of 0.3–2.0 μM) and time-dependent ($k_{\text{inact}} = 0.4 \text{ min}^{-1}$; $K_I = 2.3 \mu\text{M}$) inhibitor of CYP3A4 activity *in vitro*.¹³⁴ The mechanism of TDI has been the subject of much debate; mibefradil is cleared primarily through hepatic metabolism via N-dealkylation of the tertiary amine motif, hydroxylation on the benzimidazole moiety, and hydrolytic cleavage of the ester side chain.¹³⁵ MI complex formation between the N-dealkylated metabolite and the heme prosthetic group in CYP3A4 has been ruled out given the lack of a concomitant increase in Soret absorbance at 455 nm.¹³⁶ Likewise, failure to detect adducts in NADPH-supplemented CYP3A4 incubations of mibefradil and nucleophiles (e.g., GSH, cyanide, amines) negates the possibility of RM formation (e.g., quinoneimine generation via oxidation of the hydroxybenzimidazole metabolite).¹³⁶ Foti et al.¹³⁶ recently demonstrated that the NADPH- and time-dependent inactivation of CYP3A4 activity by mibefradil correlated well with the time-dependent loss of carbon monoxide binding, which, coupled with the lack of stable heme and/or apoprotein adducts, suggests heme destruction/fragmentation as the putative mechanism of

inactivation in a manner similar to that of carbon tetrachloride.^{56,57} The mibefradil case illustrates the degree of complexity in probing mechanisms of CYP inactivation and also provides an important perspective in maintaining appropriate vigilance and awareness of DDIs, particularly for recently released medications.

4. MEDICINAL CHEMISTRY TACTICS TOWARD MINIMIZING/ELIMINATING CYP MBI IN DRUG DISCOVERY

Insights into the mechanism(s) underlying time-dependent CYP inhibition are a practical starting point for the rational design of compounds to circumvent CYP inactivation. However, eliminating CYP inactivation in lead chemical matter is not a trivial exercise; designing compounds to design out undesired CYP inhibitory effects could introduce a detrimental effect on primary pharmacology (e.g., changes in agonist/antagonist behavior and/or subtype selectivity for target receptor or enzyme) and otherwise attractive pharmacokinetic attributes. Chemical intervention strategies to abolish CYP inactivation liability must be an iterative process, the success of which will be heavily dependent on a close working relationship between medicinal chemists, pharmacologists, and drug metabolism scientists, as evident from the examples in this section.

Several publications have demonstrated tactics to minimize and/or eliminate CYP TDI without affecting primary pharmacology and/or disposition characteristics. Solutions range from modulation of lipophilicity resulting in diminished rates of metabolism (and bioactivation to RMs) to virtually eliminating the potential for RM formation via functional group manipulations. Alterations in physicochemical properties within MBI-positive compounds will diminish rates of enzyme inactivation but may not completely eliminate the liability. An illustration of such an approach is evident in the work of Magee et al.,¹³⁷ wherein both the high metabolic turnover and CYP3A4 TDI associated with the third generation macrolide (ketolide) antibiotic telithromycin are improved by modulation of physicochemical properties (Figure 10). As described in section 3, CYP3A4 inactivation by macrolides such as telithromycin

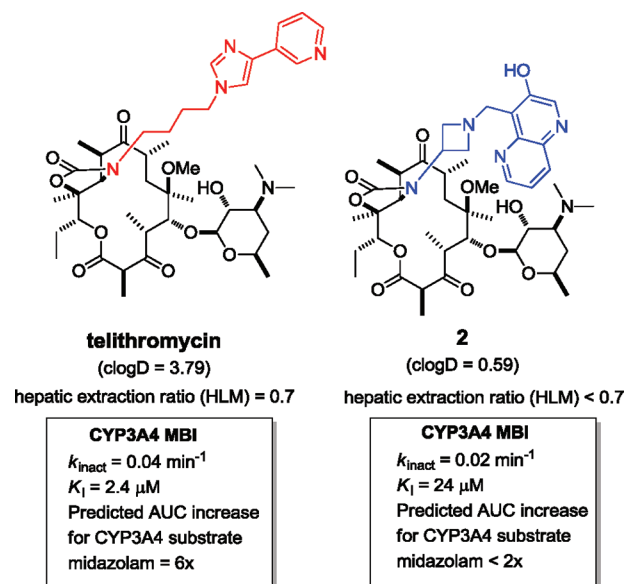


Figure 10. Reduction in lipophilicity as a tactic to attenuate CYP MBI liability with ketolide antibiotics.

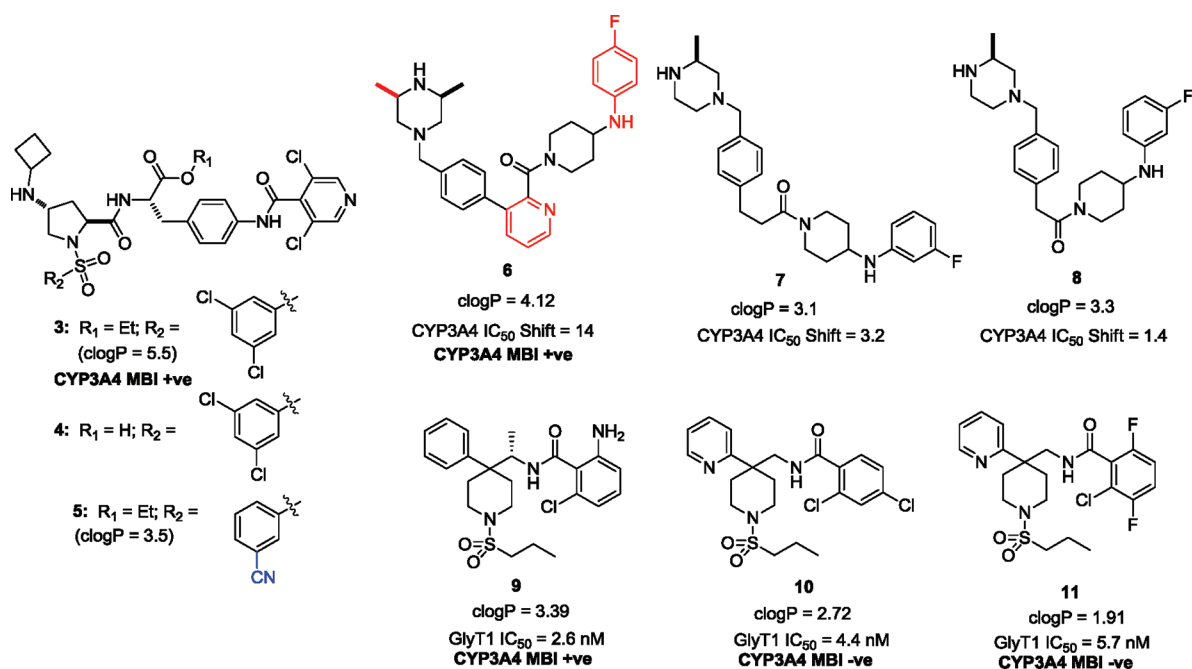


Figure 11. Additional illustrations of physicochemical property manipulations to attenuate MBI of CYP enzymes.

results from sequential metabolism of the *N,N*-dimethyl group to the corresponding nitroso intermediate that forms an MI complex with the ferrous form of the heme iron atom. Because this functional group is required for the antibacterial activity, replacement or modifications thereof are not tolerated. Thus, cyclization of the tether connecting the aryl-alkyl group to the macrocyclic ring system in telithromycin and strategic placement of a nitrogen into the conformationally constrained tether were utilized as a means to introduce polarity into the telithromycin scaffold as illustrated with compound 2, which was a weak CYP3A4 inactivator relative to telithromycin.¹³⁷ As such, the key analogues described in this work generally matched the in vitro potency of telithromycin against the common susceptible- and macrolide-resistant strains.

Another example of the successful utilization of this tactic is evident from SAR studies on a series of proline-based antagonists of the very late antigen-4 receptor (Figure 11).¹³⁸ The ethyl ester derivative of the lead compound 3 displayed potent CYP3A4 TDI with a k_{inact} and K_i of 0.05 min^{-1} and $0.4 \mu\text{M}$, respectively. Metabolism studies with the parent carboxylic acid 4 in HLM also revealed covalent binding to microsomal protein in a NADPH-dependent fashion, consistent with RM formation. Replacement of the 3,5-dichlorophenyl group of 3 with a 3-cyanophenyl group (compound 5) resulted in a net reduction of the clogP from 5.5 to 3.5, a feature that appeared to be consistent with a somewhat reduced propensity for CYP3A4 inactivation ($k_{\text{inact}} = 0.04 \text{ min}^{-1}$ and $K_i = 1.7 \mu\text{M}$) and covalent binding to HLM. Information pertaining to the metabolic pathways leading to CYP inactivation by 3 is unclear. As such, the picomolar whole blood activity and slow dissociation rates against the receptor displayed by 5 were shown to be sufficient to overcome the poor animal PK, and sustained activity as measured by receptor occupancy was achieved in preclinical species after oral dosing.

Reduction of CYP3A4 inactivation by introducing polarity was also successfully applied by Westaway and co-workers in their work leading to the discovery of the first small molecule agonist of the motilin receptor (see Figure 11).¹³⁹ The lead

compound 6 revealed TDI of CYP3A4 activity (~14-fold decrease in IC₅₀ upon preincubation for 30 min; IC₅₀ at 0–5 min of $20 \mu\text{M}$; IC₅₀ at 25–30 min of $1.4 \mu\text{M}$) in a manner consistent with enzyme inactivation. On the basis of the hypothesis that the CYP interaction is driven by size and lipophilicity, analogues of 6 were designed with reduced molecular weight and clogP. Thus, replacement of the pyridyl and dimethylpiperazine rings of 6 with a two-carbon linker and (2*S*)-methylpiperazine ring, respectively, led to compounds with reduced agonist potency; however, these changes in combination with a terminal 3-fluoro substituent afforded 7, which demonstrated an improved CYP3A4 inhibition profile (<3.2-fold decrease in CYP3A4 IC₅₀ in a 30 min preincubation; IC₅₀ at 0–5 min of $10 \mu\text{M}$; IC₅₀ at 25–30 min of $3.1 \mu\text{M}$) compared to 6 while retaining motilin potency. Further reduction in the linker size afforded 8, which demonstrated a notable improvement in agonist potency and preclinical PK (relative to 6) and drastically attenuated CYP inactivation (<2-fold decrease in CYP3A4 IC₅₀ in a 30 min preincubation; IC₅₀ at 0–5 min of $26 \mu\text{M}$; IC₅₀ at 25–30 min of $18 \mu\text{M}$).

Another example of utilizing lipophilicity modulation to reduce TDI of CYP enzymes is evident with the 4,4-disubstituted piperidine series as glycine transporter 1 (GlyT1) inhibitors for potential treatment of schizophrenia.¹⁴⁰ Replacing the C-4 phenyl group in the lead piperidine derivative 9, a time-dependent CYP inactivator, with the 2-pyridyl group and removing the metabolically labile chiral methyl and aniline NH₂ groups led to a net reduction in clogP by 0.6 log units and abrogated CYP inactivation potential in the resulting compound 10 (Figure 11). An additional 0.8 log unit reduction in lipophilicity was achieved by replacing one of the aromatic chlorine atoms with two fluorine atoms leading to 11, which was virtually devoid of CYP TDI liabilities. Compound 11 also displayed improvements in aqueous solubility and exhibited GlyT1 potency comparable to that of 9.

Elimination of CYP TDI caused by covalent modification of the heme prosthetic group and/or apoprotein by RMs can be achieved by replacing the structural motif prone to RM

Scheme 16. Elimination of CYP TDI Liability in the Potassium Ion Channel Opener 12 by Blocking Putative Site(s) of Bioactivation

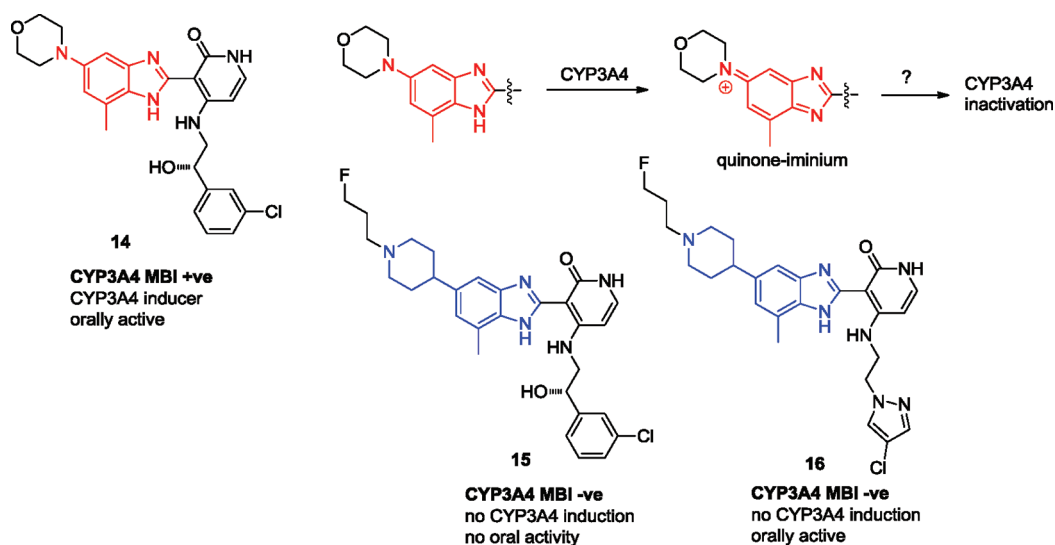
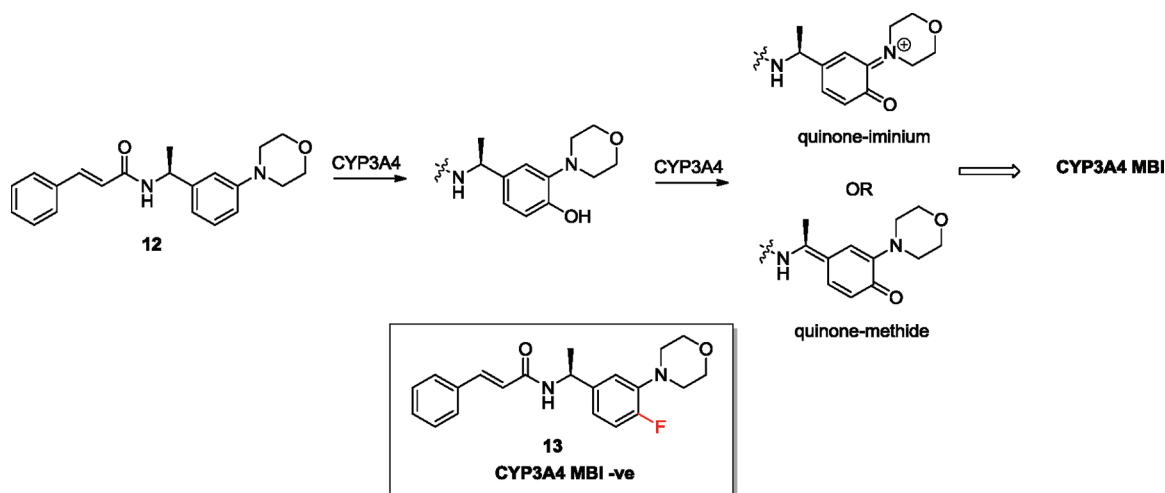


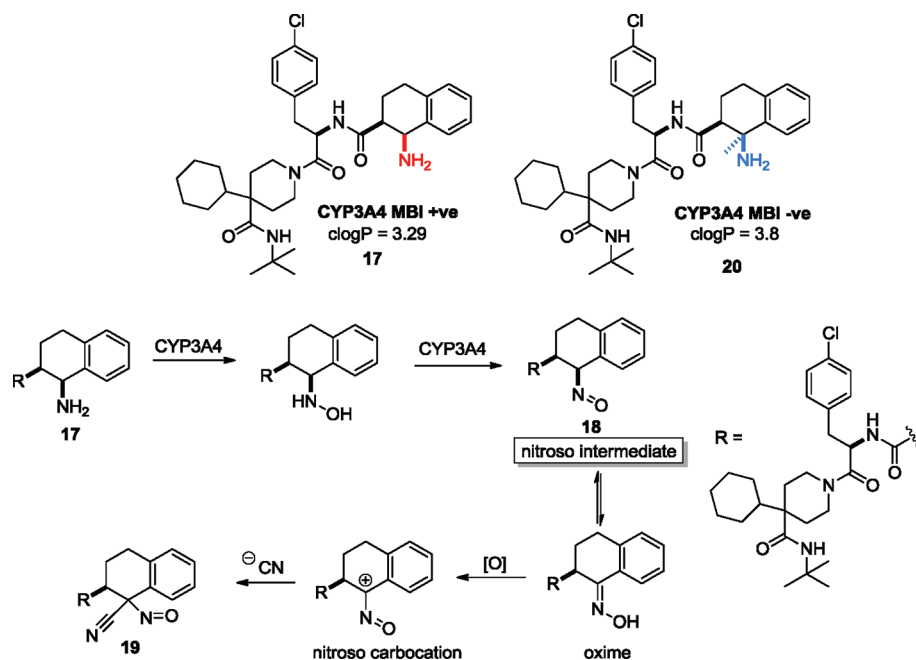
Figure 12. Simultaneously abolishing CYP3A4 inactivation and induction liabilities in the insulin-like growth factor-1 receptor kinase inhibitor 14.

formation with a metabolically latent functional group or via strategic placement of a complementary substituent(s) to block the site of initial metabolism that precludes RM formation. The potassium ion channel opener 12 provides an excellent example of successful utilization of an approach to abrogate RM formation and CYP inactivation (Scheme 16). Replacement of one of the hydrogen atoms ortho to the morpholine ring in 12 with a fluorine atom (compound 13) eliminated TDI liability against CYP3A4.¹⁴¹ The lack of CYP3A4 inactivation by 13 appears to be consistent with a bioactivation pathway involving initial aromatic hydroxylation ortho to the morpholine ring (or para to the benzylamine methine) in 12. Further two-electron oxidation of the hydroxylated metabolite by CYP3A4 would lead to the reactive quinoneiminium or quinone methide species capable of protein conjugation. The potential formation of either RM was prevented by introduction of the fluorine atom. Compound 13 was shown to be devoid of CYP inactivation while retaining the pharmacologic and PK attributes of the prototype compound 12.

The second example deals with the orally active insulin-like growth factor-1 receptor kinase inhibitor BMS-536924 (14)

(Figure 12), whose preclinical development was suspended because of its liability involving simultaneous inactivation and induction of CYP3A4 activity.¹⁴² To reduce/eliminate CYP induction and inactivation while retaining oral pharmacology, morpholine and phenethylamine replacements of 14 were investigated. The lead optimization process was greatly facilitated by cocrystallization of the insulin-like growth factor-1 receptor with several analogues of 14, which suggested that the morpholine group in 14 is solvent exposed and therefore could be open to SAR exploration to eliminate CYP liabilities without affecting potency. Appending various substituted morpholines did not impact CYP3A4 inactivation and/or induction. Likewise, replacing the morpholine ring with appropriate bioisosteres such as piperazines and 4-amino-piperidines and attenuating the basicity of the distal nitrogen did not yield an optimal compound that balanced CYP3A4 inactivation, CYP3A4 induction, and oral PK. However, a significant improvement in CYP3A4 profile was observed when a C-4 connected piperidine was appended on the benzimidazole core in place of morpholine (compound 15, Figure 12). From a CYP inhibition standpoint, removal of the nitrogen

Scheme 17. Strategy To Eliminate CYP3A4 MBI Liability in the Selective Melanocortin 4 Receptor Agonist 17



atom that connected the heterocycle to the benzimidazole core and replacing it with a carbon appeared to have diminished the affinity for CYP3A4. Alternatively, the SAR observation suggests that the mechanism of CYP3A4 inactivation could potentially involve bioactivation of the dianiline-like motif in **14** to an electrophilic quinoneiminium intermediate. Overall, improvements in preclinical disposition properties and cellular potency were also observed by reducing the basicity of the piperidine nitrogen and installing the chloropyrazole side chain in place of the phenethylamine side chain as illustrated with compound **16**.

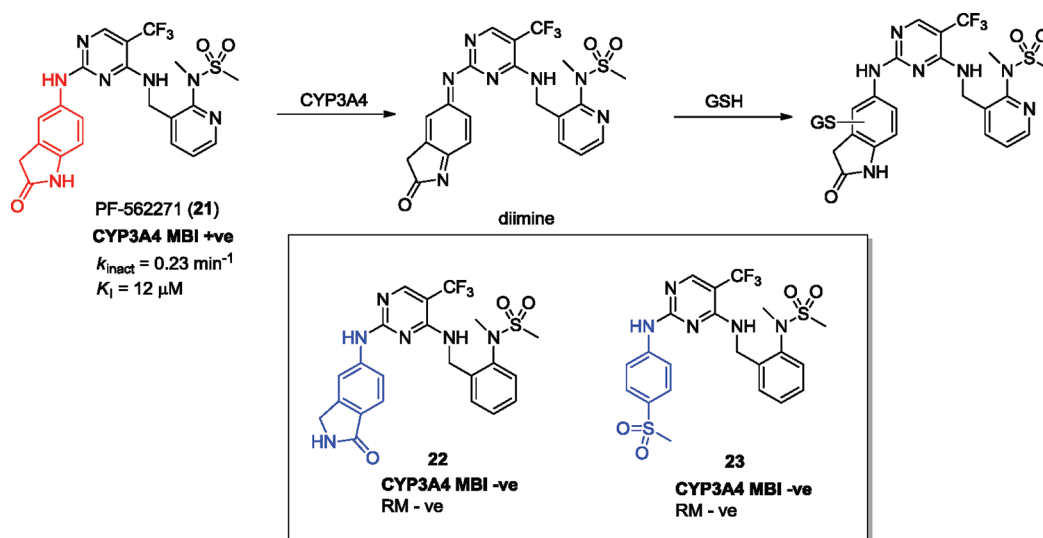
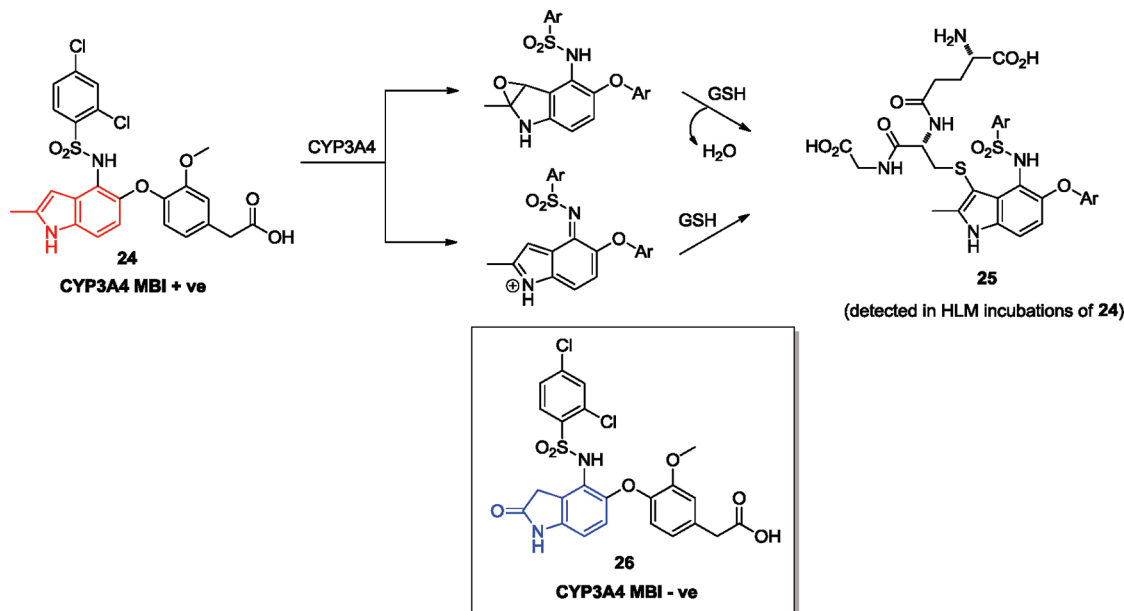
In the course of SAR studies on a series of 1-amino-1,2,3,4-tetrahydronaphthalene-2-carboxylic acid derivatives as selective agonists for the human melanocortin-4 receptor and potential antiobesity agents, the lead compound **17** (Scheme 17) demonstrated potent TDI of CYP3A4 ($k_{\text{inact}} = 0.08 \text{ min}^{-1}$, unbound $K_{\text{I}} = 23 \text{ nM}$).¹⁴³ Upon concomitant administration with CYP3A4 substrates in the clinic, increases in the AUC for the victim drugs were expected to range from 4- to 10-fold as a result of the TDI. The projected degree of clinical DDI was considered to be unacceptable for an antiobesity indication, and as a result, compound **17** was eliminated from consideration as a development candidate. Studies were undertaken to understand the mechanism underlying **17**-mediated CYP3A4 TDI to guide medicinal chemistry efforts. Incubations of **17** with recombinant CYP3A4 revealed the formation of a UV peak at 450 nm in a NADPH-dependent fashion; the UV absorbance increased with time and was reduced to near baseline following addition of potassium ferricyanide to the incubations. These observations indicated that an MI complex was formed between the heme and a RM of **17**. The RM was proposed to be the nitroso intermediate **18**, which is obtained from a two-electron oxidation of the initially formed hydroxylamine metabolite (Scheme 17). Characterization of a geminal cyanonitroso adduct **19** in incubations of **17** in NADPH-supplemented and potassium cyanide supplemented HLM was consistent with the proposed bioactivation pathway wherein the nitroso intermediate would exist in a tautomeric equilibrium with the

corresponding oxime derivative, which could be oxidized to an electrophilic nitroso carbocation and trapped by a cyanide ion.¹⁴³ On the basis of the insights gained from metabolism studies, it was envisioned that introducing an alkyl group α to the basic amine motif would shield this functionality from oxidation through steric hindrance, thereby reducing the probability of MI complex formation and CYP3A4 TDI. Indeed analogue **20** was synthesized and shown to be devoid of CYP3A4 TDI while retaining the potent and selective melanocortin-4 receptor agonism observed with **17**.

PF-562271 (**21**) (Scheme 18) is a dual inhibitor of the focal adhesion kinase and proline-rich tyrosine kinase 2 with potential utility in the treatment of ovarian cancer and osteoporosis.^{144,145} In vitro metabolism studies in HLM revealed that **21** is a CYP3A4 substrate and a time-dependent inactivator ($k_{\text{inact}} = 0.23 \text{ min}^{-1}$; $K_{\text{I}} = 12 \text{ }\mu\text{M}$), suggesting that **21** could inhibit its own clearance mechanism. The mechanism of CYP3A4 inactivation was shown to occur via a two-electron oxidation of the dianiline motif to a reactive diimine species, which was trapped with GSH (Scheme 18).¹⁴⁵ Furthermore, compound **21** demonstrated supraproportional increases in C_{max} and AUC upon repeated dosing in clinical trials, a phenomenon that was consistent with self-inactivation of its clearance mechanism. Likewise, **21** also caused >3-fold increase in the AUC of the probe CYP3A4 substrate midazolam in a clinical DDI study. Insights into the mechanism of CYP3A4 inactivation allowed a rational medicinal chemistry strategy to reduce/eliminate the MBI liability.¹⁴⁵ Thus, simply exchanging the 5-aminoindole nitrogen and carbonyl groups in **21** afforded compounds (e.g., **22** and **23**) that were virtually devoid of CYP3A4 TDI while maintaining kinase potency. In general, disruption of the electron-rich dianiline structure present in **21** also mitigated the formation of reactive diimine metabolites in the SAR studies.¹⁴⁵

The chemoattractant receptor inhibitor **24** (Scheme 19), a candidate for the treatment of asthma, also displayed potent CYP3A4 TDI.¹⁴⁶ In HLM, **24** demonstrated time-, concentration-, and NADPH-dependent inhibition of CYP3A4 activity with k_{inact} and K_{I} of 0.16 min^{-1} and $18 \text{ }\mu\text{M}$, respectively.

Scheme 18. Strategies To Eliminate CYP3A4 TDI by Virtue of Eliminating Reactive Diimine Formation with Oxindole-Based Focal Adhesion Kinase Inhibitors

Scheme 19. Bioactivation of a 2-Methylindole Derivative **24** to CYP3A4-Reactive Species

Clinical DDI predictions suggested a 4.3- to 7.5-fold increase in midazolam exposure at anticipated therapeutic concentrations of **24**. While incubation of **24** with NADPH-supplemented recombinant CYP3A4 did not lead to MI complex formation, studies with [^{35}S]**24** in HLM revealed that inactivation was accompanied by an NADPH-dependent increase in covalent binding to a 55–60 kDa microsomal protein, consistent with irreversible binding to CYP3A4 apoprotein by a RM of **24**. A GSH adduct **25** was also identified in HLM incubations and was unambiguously determined via NMR to be derived from addition of GSH to C-3 of the 2-methylindole moiety. On the basis of the structure of **25**, it was suggested that a 2,3-epoxy-2-methylindole and/or a diimine is the potential reactive species responsible for covalent adduction to CYP3A4. Replacement of the 2-methylindole motif in **24** with an oxindole group (compound **26**) prevented RM formation and abolished TDI of CYP3A4.

The degree of complexity associated with efforts to abrogate CYP3A4 TDI while maintaining potency and PK attributes is illustrated with a series of potent renin inhibitors (Figure 13).^{147,148} Lead compounds **27** and **28** and several related analogues were identified as time-dependent inhibitors of CYP3A4 (e.g., compound **27**, 110 fold shift in CYP3A4 IC_{50} over a 30 min incubation period, $k_{\text{inact}} = 0.094 \text{ min}^{-1}$, $K_1 = 3.2 \text{ } \mu\text{M}$). Trapping studies in HLM using exogenous nucleophiles (e.g., GSH, cyanide, and semicarbazide) did not prevent CYP3A4 TDI, and were not fruitful in providing insights into the RM responsible for CYP inactivation. Likewise, attempts to monitor stable metabolites derived from downstream metabolism of RM(s) were unsuccessful. O-Demethylation of **27** was observed, as well as amide hydrolysis, to reveal a cyclopropylamine metabolite that could potentially covalently bind to the heme or apoprotein after oxidation. However, replacement of the cyclopropyl group with cyclobutyl and/or

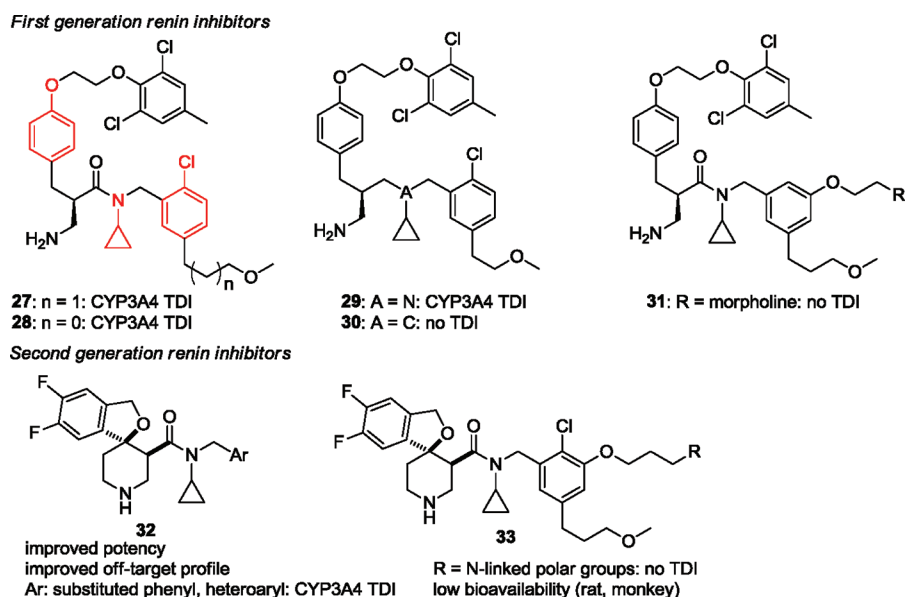


Figure 13. Attempts to eliminate CYP3A4 TDI by removal of metabolic soft spots and/or addition of polarity as illustrated with some renin inhibitors.

cyclopropylmethyl led to loss of renin inhibitory potency and did not abolish CYP3A4 TDI. Replacement of the amide carbonyl with a methylene (compound 29) or replacement of cyclopropylamine nitrogen with carbon (compound 30) significantly attenuated CYP3A4 TDI (only 6-fold shift in the CYP3A4 IC_{50} for 29 and no TDI discerned with 30) but at the cost of renin potency. Interestingly, removal of the chlorine atom from the bottom phenyl ring and attachment of a morpholine group provided compound 31, a potent renin inhibitor that was devoid of CYP3A4 TDI. However, the modification also led to significant HLM instability relative to lead compound 27. CYP3A4 TDI liability also persisted in the more potent spirocyclic variants (e.g., compound 32). On the assumption that TDI was derived from bioactivation of the right-hand aromatic region, several analogues were prepared to block metabolic soft spots but without success. Lowering the overall lipophilicity by installation of polarity to the right-hand phenyl ring provided compounds (e.g., general structure 33) that were devoid of CYP3A4 TDI liability. Unfortunately these compounds failed to provide satisfactory bioavailability in animal PK studies, and the series was dropped from further development.

The final and perhaps the most intriguing example is deuteration of CYP MBI-positive drugs as a strategy to attenuate RM formation and thus diminish the enzyme inactivation process.¹⁴⁹ In vitro metabolism studies with the doubly deuterated paroxetine analogue CTP-347 (34) (Figure 14) demonstrated

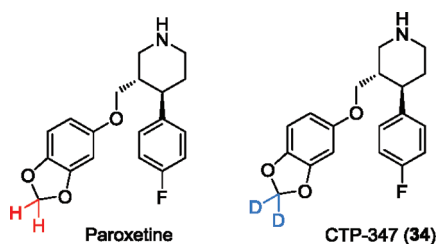


Figure 14. Attenuating CYP MBI liability through deuterium incorporation at the metabolically labile site.

little to no CYP2D6 MBI, apparently because of a dramatic reduction in the formation of the reactive carbene intermediate.¹⁴⁹ Compound 34 is currently in clinical trials for the treatment of hot flashes in menopausal women, and it has also been studied in a 96-patient single- and multiple-ascending dose clinical trial. The multiple-dose subjects initially received a single dose of dextromethorphan (a probe CYP2D6 substrate), followed by 14 days of treatment with 34, then another single dose of dextromethorphan. Subjects receiving 34 at 20–40 mg QD retained substantially greater ability to metabolize dextromethorphan compared to treatment with paroxetine administered at 20 mg QD (~15–20% inhibition of CYP2D6-catalyzed dextromethorphan metabolism to dextrorphan vs ~55–60% inhibition of CYP2D6 activity with paroxetine). As such, this DDI study represents the first clinical demonstration that deuteration can be utilized to ameliorate CYP MBI-mediated DDI liabilities in humans.

5. IN SILICO PREDICTORS OF CYP TDI POTENTIAL

Visual examination of prototypic functional groups known to be associated with CYP MBI (e.g., structural alerts) in new chemical entities usually serves as a preliminary indicator of CYP inactivation potential. However, not all structural alert-positives will lead to mechanism-based inactivation of CYP isoforms. Depending on the physicochemical attributes (molecular weight, lipophilicity, etc.), compounds may be subject to elimination via nonmetabolic routes (e.g., biliary and/or renal excretion) and may have no interaction (substrate and/or inhibitor) with CYP enzymes. For instance, the phosphodiesterase 4 inhibitor CP-671,305 (35) contains the 1,3-benzodioxole functional group (Figure 15) but does not cause TDI of the major human CYP enzymes.¹⁵⁰ Compound 35 is resistant to metabolism in animals and humans and is primarily cleared via renal and biliary excretion (in the unchanged form) via active transport.¹⁵⁰ Likewise, functionalities capable of alkylating CYPs (e.g., aminothiazole) and/or forming an MI complex (e.g., secondary basic amine) are also present in pramipexole (Figure 15), a non-ergoline dopamine agonist used to treat early stage Parkinson's disease and restless leg syndrome. However, pramipexole is subject to extensive renal excretion in humans (mediated by

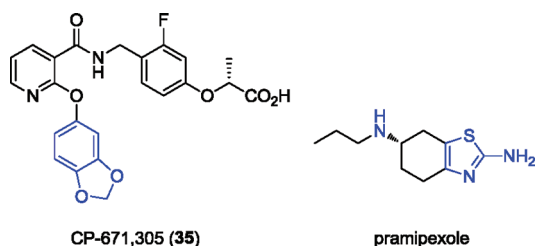


Figure 15. Examples of structural alert-positive compounds that are not associated with CYP MBI.

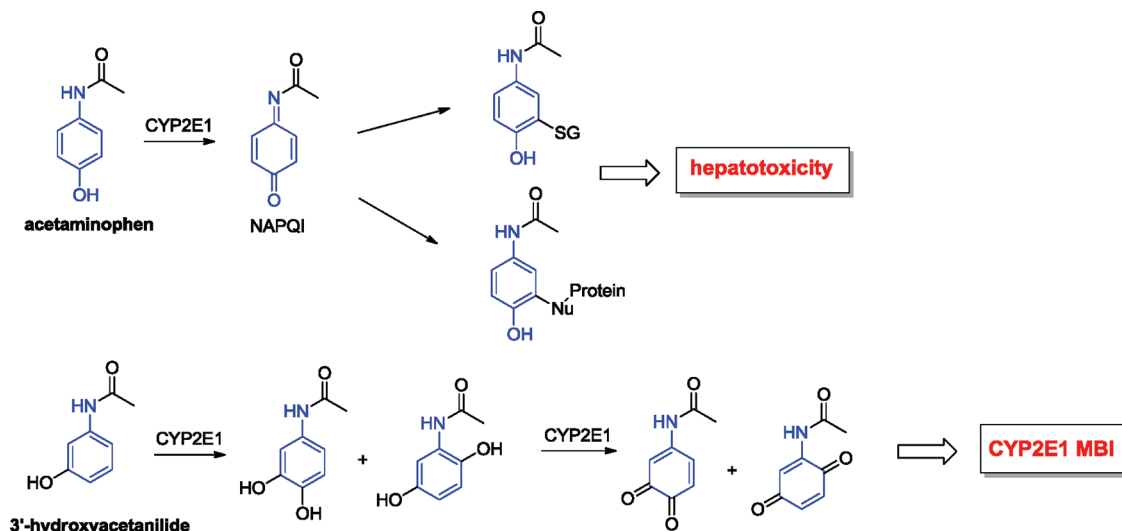
transport proteins) and is devoid of CYP-mediated metabolism/bioactivation leading to enzyme inactivation.¹⁵¹

In theory, MBI can be caused by any molecule that is bioactivated to a RM by a CYP. However, in reality, not all RM-positive compounds will covalently modify CYPs (as was discussed earlier with the antidepressant duloxetine in section 3.2). In many such cases, the RM will escape from the active site into solution prior to the inactivation step. Upon release from the CYP active site, the RMs do, however, have the potential to react nonspecifically with other proteins and/or DNA. Such an outcome has potential toxicological implications especially for drugs with high daily doses. The RM can be detoxified (via reaction with GSH) or covalently adduct to cellular proteins, resulting in immune-mediated idiosyncratic toxicity. In extreme cases (depending on the level of RM generated), depletion of endogenous GSH pools can also lead to saturation of the detoxication pathway, resulting in toxicity. This is further exemplified with the hepatotoxin and anti-inflammatory agent acetaminophen, which is metabolized to an electrophilic quinoneimine NAPQI by CYP2E1 (Scheme 20). CYP2E1, however, is not inactivated by acetaminophen during this process. Instead, NAPQI reacts with GSH and cellular proteins, causing hepatotoxicity.¹⁵² In contrast, 3-hydroxyacetanilide, the nonhepatotoxic regioisomer of acetaminophen, is metabolized by CYP2E1 to the corresponding 3,4-dihydroxy- and 3,6-dihydroxyacetanilide metabolites, which undergo further oxidation by CYP2E1 to the reactive 1,4- and 1,2-benzoquinone species (Scheme 20). In this particular circumstance, the bioactivation process is accompanied by irreversible inactivation of CYP2E1.¹⁵³

Besides the visual identification of structural alerts previously associated with CYP MBI, *in silico* computational methods, including data-based statistical models and CYP crystal structure-based quantum and molecular mechanics, have also been applied to assess TDI potential. Zientek et al.¹⁵⁴ described a CYP3A4 TDI model based on retrospective analysis of physicochemical descriptors and experimental data acquired using an automated and abbreviated TDI assay (two concentrations of test compounds at two time points). A Laplacian-corrected Bayesian classification model (a yes/no filter) categorized the compounds into two classes: positives with $\geq 25\%$ change in at least one tested concentration over time (or $\geq 15\%$ change when $\leq 70\%$ activity is left after preincubation for at least one tested concentration) and the rest as negative. This *in silico* Bayesian classifier was built on a training set containing approximately 2000 compounds, which seemed to be predictive for the same training set compounds with a cross-validation receiver operator curve value of 0.85. To validate its real predictive power, the model was then applied to predict an independent external data set of 27 TDI-positive compounds from the literature. However, only 11 compounds were predicted with positive Bayesian scores and the rest with zero or negative scores. It was suggested that the poor prediction performance on the selected testing set was caused by limited structural diversity in the training set; i.e., the compounds, which failed in the prediction, are relatively dissimilar (< 0.8 structural similarity) to the training set compounds. It is possible that the model can be improved in performance when more structurally diverse compounds are included in the training set. The model did clearly identify several 3-methyleneindazoles and -pyrazoles as positive TDI components, which correlates with CYP inactivation discerned with 3-methylindole analogues such as zafirlukast, a well-prescribed leukotriene receptor antagonist,¹⁵⁵ and SPD-304 (37), a small-molecule tumor necrosis factor- α inhibitor.¹⁵⁶

Unlike data-based models, structure-based models can provide information pertaining to the molecular basis of CYP inactivation (e.g., identification of critical active site interactions leading to MBI), which can be useful in iterative design of compounds without TDI liability. Thus, by use of molecular mechanics, alkynes such as 4-*tert*-butylphenylacetylene (BPA), which are well-established as CYP inactivators, were predicted to covalently

Scheme 20. Differences in CYP2E1 MBI by Acetaminophen and Its Regioisomer 3'-Hydroxyacetanilide



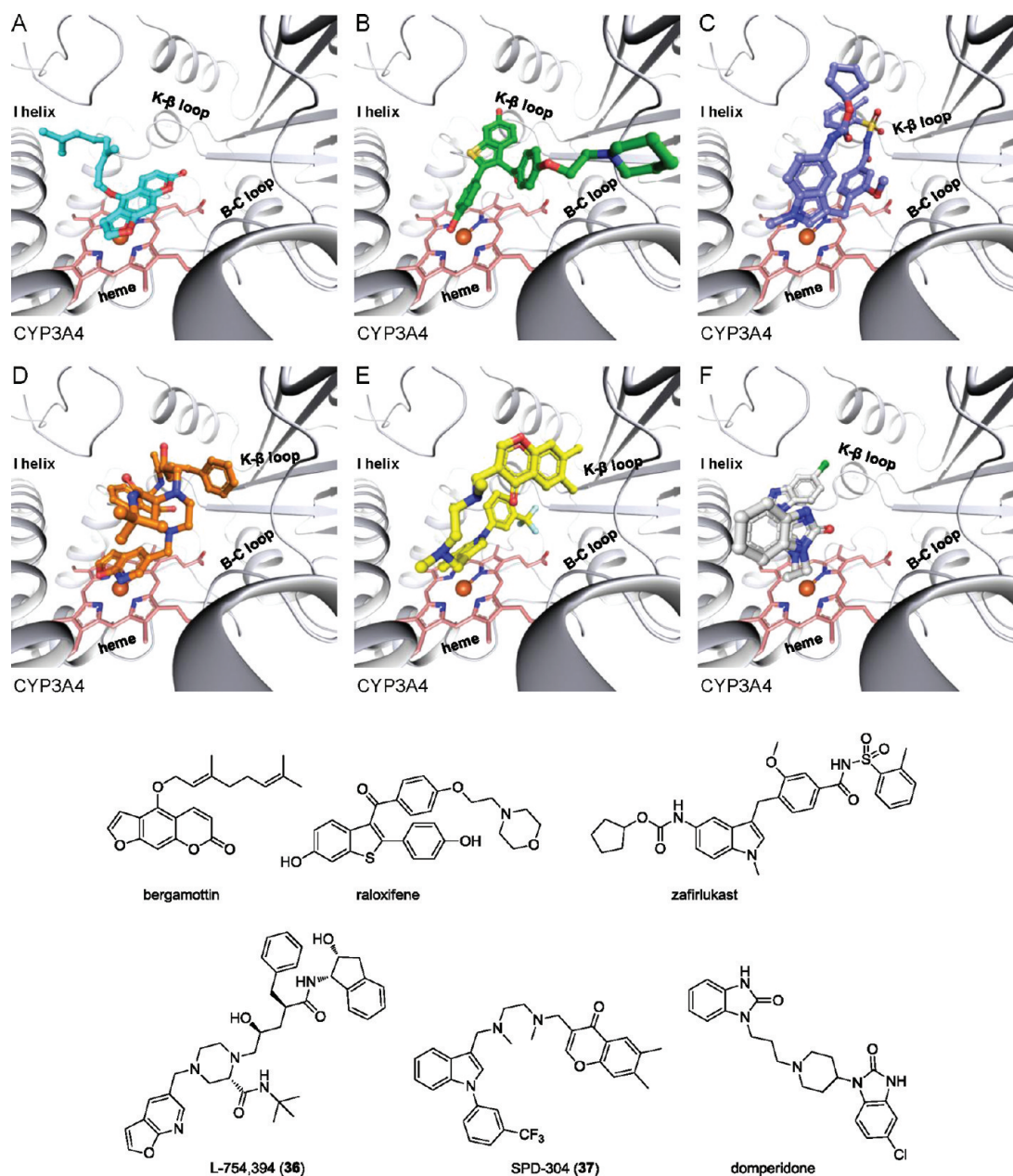


Figure 16. Postulated binding poses of CYP3A4 MBI: (A) bergamottin, (B) raloxifene, (C) zafirlukast, (D) 36, (E) 37, and (F) domperidone that can lead to RM formation.

modify a threonine 302 residue in helix I of CYP2B1, 2B4, and 2B6 isoforms, resulting in enzyme inactivation. The predictions were supported by the structural identification of the covalently bound adduct and further confirmed by the direct cocrystallization of BPA with CYP2B4.^{157,158} In general, the success of structure-based prediction using molecular and quantum mechanics approaches rests on the assumption that the reactive species generated in the course of metabolism will react with nucleophilic residues such as lysine, serine, threonine, tyrosine, or cysteine side chains within the active site, a phenomenon that is difficult to predict. Figure 16 illustrates the heterogeneity in the lowest energy binding poses for diverse CYP3A4 inactivators including furan derivatives L-754,394 (**36**) (an HIV protease inhibitor)¹⁵⁹ and bergamottin (grapefruit juice component),¹⁶⁰ zafirlukast,¹⁵⁵ raloxifene,^{126–128} compound **37**,¹⁵⁶ and domperidone, a dopamine receptor antagonist.¹⁶¹ As such, all computational

models including structure-based methods described to date are mostly retrospective in nature, since they incorporate prior mechanistic information on CYP inactivation. Without some prior information, it is virtually impossible to prospectively predict the ability of new compounds to cause CYP TDI.

6. PREDICTION OF CLINICAL DDI IN DRUG DISCOVERY USING IN VITRO CYP TDI DATA

6.1. Managing CYP TDI Issues in Drug Discovery. Most pharmaceutical companies assess CYP TDI/MBI potential with abbreviated versions of CYP inactivation screens (e.g., IC_{50} shift assay) in place to enable the assessment and/or elimination of the risk prior to candidate selection. While such an approach is useful for early detection of potent inactivators and for rank ordering compounds at the lead optimization stage, precise prediction of in vivo DDI risks from abbreviated CYP TDI

assays is difficult. Several attempts have been made to establish quantitative relationships between the magnitude of the IC_{50} shift and clinical DDI risks based on anticipated human pharmacokinetics.^{5,162} For instance, Sekiguchi et al.¹¹ investigated the use of IC_{50} shift data for 46 marketed drugs as CYP3A4 inhibitors, 26 of which were determined to be TDI positive based on an IC_{50} shift cutoff of 1.3-fold. Using the IC_{50} data along with the observed clinical DDI data, the authors established a relationship between the magnitudes of observed IC_{50} shift, the ratio of unbound inactivator concentration at steady state to competitive IC_{50} , and subsequent DDI risk. A second approach that can be used in a discovery setting is to estimate DDI using the composite parameter k_{inact}/K_I . As shown in Figure 17, given the ratio of k_{inact}/K_I and an estimate

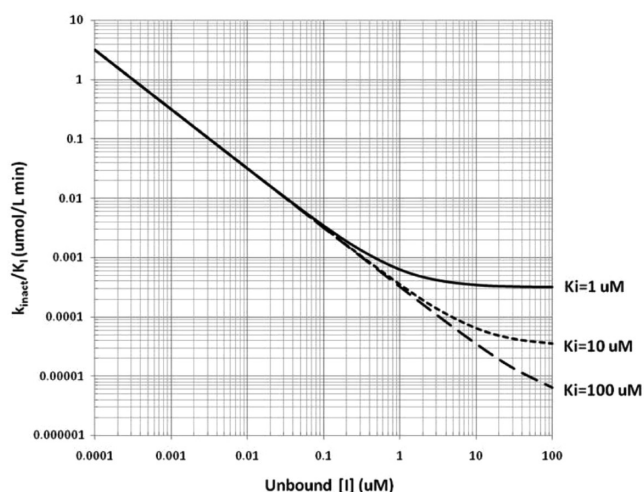


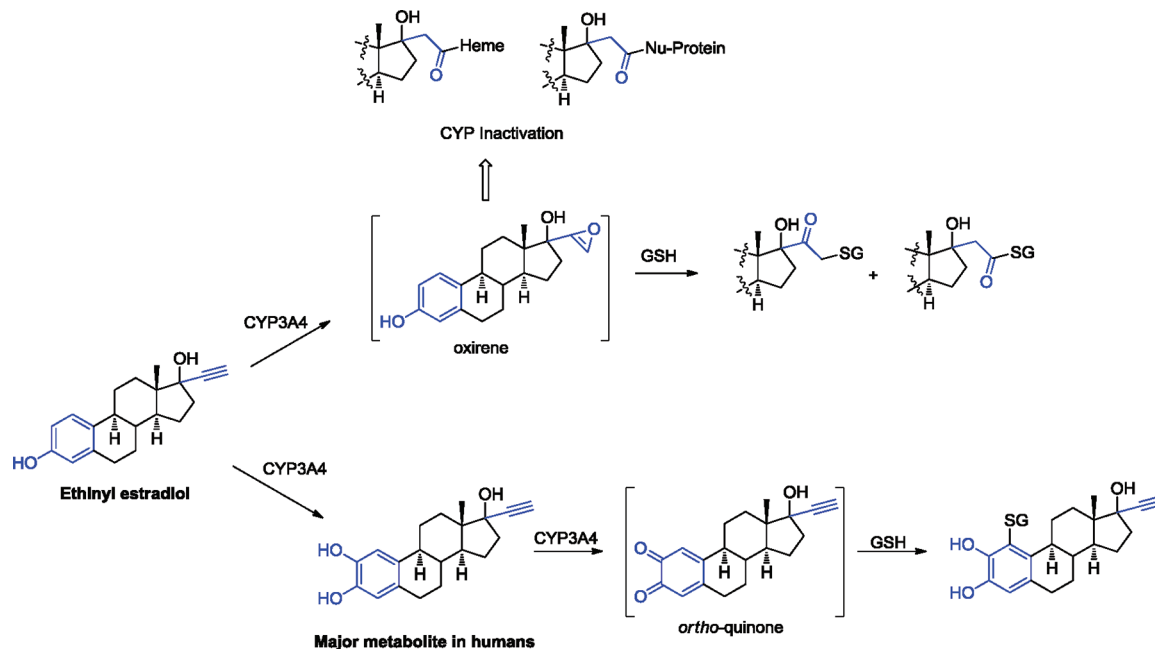
Figure 17. Relationship between the k_{inact}/K_I ratio relative to unbound plasma concentration $[I]$. Lines represent parameters that would be expected to result in a 2-fold interaction.

of the unbound plasma concentration of the inactivator $[I]$, DDI risk assessments can be made relative to an expected

2-fold interaction as shown by the lines at K_I values of 1.0, 10, and 100 μM . In this example, compounds that fall below the line would have low risk for DDI. Recently Zimmerlin et al.⁸⁴ reported a good correlation between CYP3A4 TDI data acquired from IC_{50} shift and k_{inact}/K_I assays and the one obtained from k_{obs} measurement at a single inactivator concentration of 10 μM using 400 marketed drugs and 4000 proprietary compounds as benchmarks. On the basis of comparison to clinical DDI data for marketed drugs, the authors established a lower limit of $k_{obs} = 0.020 \text{ min}^{-1}$ for the assay, with compounds falling above this threshold flagged as TDI positive. In contrast to the IC_{50} shift approach, this method allows for assessments of TDI risk to be obtained in early discovery such that once the risk is identified, structural modifications can be made in an attempt to mitigate the risk prior to compound selection.

From a medicinal chemistry perspective, an optimal approach to deal with CYP TDI would be to deploy the strategies outlined in section 4 to design compounds devoid of the liability. Such an approach serves a dual purpose of abolishing CYP inactivation liability and eliminating the potential for formation of protein-reactive metabolites that may cause idiosyncratic toxicity. It is important to note that prior to embarking on a laborious exercise to dial out CYP inactivation and/or RM formation, insights into the anticipated human PK and the daily dosing regimen for the MBI- and RM-positive compound are essential. For instance, the estrogenic contraceptive ethinyl estradiol is metabolized by CYP3A4 at the C-17 α terminal alkyne motif to a reactive oxirene species, which alkylates the heme group and/or protein resulting in the MBI of the isozyme (Scheme 21).^{163–165} In addition to acetylene bioactivation, Park et al.¹⁶⁶ have demonstrated the oxidation of the phenol ring in ethinyl estradiol to an electrophilic *o*-quinone species (via the intermediate catechol metabolite) in HLM, a process that eventually leads to microsomal covalent binding.¹⁶⁷ Lack of DDI with CYP3A4 substrates and/or idiosyncratic toxicity is most likely due to the very low dose (0.035 mg) used in birth control. Additional qualifying considerations to mitigate

Scheme 21. Metabolism of Ethinyl Estradiol into CYP3A4- and Protein-Reactive Metabolites



the risk of idiosyncratic toxicity due to RM formation have been the subject of various publications.^{168,169}

6.2. Prediction of Clinical DDI for MBI-Positive Compounds in Drug Discovery. In the course of iterative SAR efforts, molecules may emerge with significant improvements in pharmacologic potency, PK, and diminished rates of CYP inactivation relative to a prototype (e.g., compound 2 relative to telithromycin in Figure 10). However, there may be instances where compound attributes needed for pharmacological activity will be inseparable from the properties that cause CYP TDI (e.g., presence of the thiophene ring in clopidogrel and the *N,N*-dimethyl substituents in macrolide antibiotics, which are associated with pharmacologic action and CYP inactivation). Likewise, some medicinally important functional groups that are classified as structural alerts (e.g., aniline) can be quite challenging to mimic by isosteric replacement. The aniline motif is widely used in kinase inhibitor design as evident with TK inhibitors (e.g., lapatinib, sunitinib, and erlotinib), which are associated with CYP3A4 MBI and idiosyncratic hepatotoxicity. CYP MBI via RM formation will continue to emerge in kinase programs, which rely on the aniline group.¹⁴⁵ In such scenarios, drug discovery/development scientists might choose to go forward with a compound that has some degree of CYP TDI liability, especially if there is reason to believe that the combination of in vivo exposure needed for efficacy relative to potency of CYP inactivation will not result in a clinically relevant DDI.

There have been numerous publications related to strategies for using in vitro CYP TDI data for prediction of clinical DDI, with approaches ranging from very simple (three input parameters) to more complex (four or more input parameters).^{2,9,43,170} All in vitro and in vivo prediction approaches have in common three basic inputs: a measure of potency of inhibition (e.g., K_I), a measure of rate of inactivation (e.g., k_{inact}), and a measure of in vivo drug concentration (e.g., $[I]$). Approaches to predicting DDIs can be categorized into two general types, static and dynamic. Static approaches assume that the concentration of inhibitor does not change over time, while dynamic approaches incorporate changes in inhibitor concentration with time and may also incorporate other system dynamics.

6.2.1. Static Models. One of the earliest attempts at practical application of in vitro data for clinical DDI prediction was published by Mayhew et al. in 2000.⁹ The well-stirred model was adapted for extrapolation of in vitro intrinsic clearance (CL_{int}) to in vivo AUC, in addition to terms describing the effect of the CYP inactivator (K_I and k_{inact}) on the degradation rate of the enzyme. This relatively simple model requires one constant (k_{deg} , the degradation rate constant for the CYP isoform of interest) and three variable input parameters (in vitro K_I , k_{inact} , and $[I]$) as shown in eq 1 (the static model for prediction of change in AUC of a probe substrate in the presence of a time-dependent inhibitor):

$$\frac{AUC'}{AUC} = \frac{CL_{int}}{CL'_{int}} = \frac{[E]_{ss}}{[E]'_{ss}} = \frac{1}{\frac{k_{deg}}{k_{deg} + \frac{[I] \times k_{inact}}{[I] + K_I}}} \quad (1)$$

where AUC and AUC' represent the area under the curve of object drug in the absence and presence of inactivator, respectively, CL_{int} and CL'_{int} represent intrinsic clearance of the object drug in the absence and presence of inactivator, respectively, and $[E]_{ss}$ and $[E]'_{ss}$ represent the concentration of

clearing enzyme in the absence and presence of inactivator, respectively. Mayhew et al. validated the model by precisely predicting clinical DDIs for fluoxetine, clarithromycin, and *N*-desmethyl diltiazem coadministered with CYP3A4 substrates.⁹ The model was also applied to assess the risk of clinically relevant DDI for a series of ketolide compounds, using telithromycin (Figure 10) as a positive control.¹³⁷ Using eq 1, a k_{inact} of 0.04 min^{-1} , a K_I of $2.4 \text{ } \mu\text{M}$, a $[I]$ of $0.17 \text{ } \mu\text{M}$ (average unbound plasma concentration for telithromycin at steady state), and k_{deg} of 0.0005 min^{-1} led to a predicted 6.2-fold increase in AUC for a CYP3A substrate in the presence of telithromycin. This prediction is in good agreement with the observed ~ 6.0 -fold increase in midazolam AUC observed in clinical DDI study with telithromycin and midazolam and hence lends validity to the use of eq 1 for DDI prediction of the newer ketolides.¹³⁷ The basic model described by eq 1 is still commonly applied to DDI predictions, although numerous refinements and adaptations have been added to improve the accuracy of the DDI predictions. For example, a term describing the fraction of the object drug that is metabolized by the inactivated CYP ($f_{m,CYP}$) is commonly incorporated in the model to account for object drugs with additional clearance pathways.⁴³ For example, midazolam is cleared almost exclusively by CYP3A4 metabolism ($f_{m,CYP3A4} \approx 0.94$), whereas alprazolam is cleared predominantly by CYP3A4 metabolism ($f_{m,CYP3A4} \approx 0.80$) but has an additional renal excretion component (fraction cleared renally is ~ 0.20).¹⁷⁰ Therefore, a CYP3A4 inactivator would be expected to produce DDI of greater magnitude with midazolam than with alprazolam, which is in agreement with clinical DDI observations.¹⁷⁰ Incorporation of $f_{m,CYP}$ was applied in the DDI risk assessment in the melanocortin 4 receptor example described previously (Scheme 17). In this latter example, the predicted increase in AUC of a CYP3A4 substrate ($f_{m,CYP} = 1$) in the presence of 17 was 4- to 10-fold. This predicted interaction precluded further preclinical development of this compound.¹⁴³ In addition to $f_{m,CYP}$, the static model has been further refined by incorporating a term describing potential interactions at the level of the intestine for orally administered drugs. The term F_g is used to describe the fraction of drug that escapes gut extraction in the absence of a CYP inactivator. Since CYP3A4 is expressed in the human intestine, a compound that is metabolized to a significant extent in the intestine would have a low F_g ; hence, a model that takes into account the effect of intestinal CYP3A4 inhibition for an orally administered CYP3A4 inactivator and object drug would theoretically produce a more accurate prediction. Therefore, eq 1 can be adapted to incorporate $f_{m,CYP}$ and F_g as shown in eq 2 (static model for predicting effect of time-dependent inhibitor on AUC of probe substrate, with incorporation of $f_{m,CYP}$ and F_g parameters),

$$\frac{AUC'}{AUC} = \frac{1}{\left(\frac{f_{m,CYP}}{1 + \frac{k_{inact} \times [I]}{k_{deg} \times (K_I + [I])}} \right) + (1 - f_{m,CYP})} \times \frac{1}{F_g + \left((1 - F_g) \times \frac{1}{1 + \frac{k_{inact} \times [I]_g}{k_{deg,gut} \times (K_I + [I]_g)}} \right)} \quad (2)$$

and described in detail in several recent publications.^{2,43,170} Note that for the first bracketed term in eq 2, the [I] used would be the estimated hepatic concentration of inhibitor, for which the unbound maximal plasma concentration is used as a surrogate. For the second bracketed term in eq 2, the [I] used would be the gut concentration of inhibitor, which can be estimated based on dose and fraction absorbed, as described previously.⁶

The model depicted in eq 2 has been applied toward DDI risk assessment for the FAK inhibitors described previously in section 4 (compound **21**, Scheme 18). The model was used to describe the increase in AUC of a coadministered CYP3A4 substrate (midazolam) and also used to describe the accumulation of **21** upon repeat dose administration, due to autoinactivation. The model predicted a 3.4- to 12-fold accumulation, if both hepatic and gut terms were included, and a 2.1- to 7.4-fold accumulation if only the hepatic term was included. The prediction using the hepatic term only was in line with the observed drug accumulation of 1.9- to 5.7-fold.¹⁷¹ The ability to validate the model using experimental data from the lead candidate **21** increased confidence in the use of this model for DDI risk assessment for backup FAK inhibitors. The approaches described above can be applied to predict DDI for compounds that are time-dependent inactivators of CYPs. However, it is entirely possible that a compound inhibits CYP in a reversible and irreversible fashion. For example, ritonavir is both a competitive and a time-dependent inhibitor of CYP3A4 activity. Consequently, equations used to predict DDI may be adapted to include both the time-dependent component (e.g., eqs 1 and 2) and a reversible inhibition component, typically represented by eq 3 (static model for predicting effect of reversible inhibitor on AUC of probe substrate),

$$\frac{AUC'}{AUC} = 1 + \frac{[I]}{K_i} \quad (3)$$

where AUC, AUC', and [I] are as described above, and in this case K_i represents the inhibition constant for reversible inhibition.¹⁷²

In addition to CYP inhibition, compounds can also cause CYP induction, which increases the amount of enzyme expressed. It is not uncommon for CYP inhibitors to simultaneously induce CYP expression. This typically occurs via compound binding to the pregnane X receptor or constitutive androstane receptor resulting in increased CYP gene transcription. Enzyme induction is thought to be a protective mechanism whereby the nuclear receptors act as “xenosensors” to detect foreign chemicals and increase the capacity of the body’s drug metabolizing enzymes. Hence, it is not surprising that there is overlap between the substrate specificity of CYPs and the ligand selectivity of xenosensing nuclear receptors. The equations used to predict DDI may also be adapted to include a term to account for enzyme induction, represented by eq 4 (static model for predicting effect of enzyme induction on AUC of a probe substrate),

$$\frac{AUC'}{AUC} = \frac{1}{1 + \frac{E_{\max} \times [I]}{EC_{50} + [I]}} \quad (4)$$

where AUC, AUC', and [I] are as described previously, E_{\max} represents the maximum fold induction determined in an in vitro induction assay, and EC_{50} represents the concentration of inducer producing half-maximal induction in vitro. More details regarding

prediction of induction can be found in a recent review on this topic.¹⁷³

In an effort to allow for multiple CYP interaction mechanisms in the DDI prediction, a combined DDI prediction model has been proposed by Fahmi and co-workers.¹⁷⁴ This combined or “net effect” model incorporates terms for TDI (represented by eq 1), reversible inhibition (represented by eq 3), and induction (represented by eq 4), as well as $f_{m,CYP}$ and intestinal interaction terms as shown in eq 5 (net effect model for DDI prediction,¹⁷⁴ with terms for TDI, reversible inhibition, and induction represented by eqs 1, 3, and 4, respectively).

$$\frac{AUC'}{AUC} = [(eq\ 1 \times eq\ 3 \times eq\ 4) \times f_{m,CYP} + (1 - f_{m,CYP})] \times [(eq\ 1 \times eq\ 3 \times eq\ 4) \times (1 - F_g) + F_g] \quad (5)$$

In the net effect model, the first term describes the impact of TDI, reversible inhibition, and/or induction at the level of the liver while the second multiplier is used to represent interaction at the level of the intestine. Hence for the first bracketed term in eq 5, the [I] used would be the estimated hepatic concentration of inhibitor, for which the unbound maximal plasma concentration is used as a surrogate. For the second bracketed term in eq 5, the [I] used would be the gut concentration of inhibitor, which can be estimated based on dose and fraction absorbed, as described previously.¹⁷⁴

6.2.2. Dynamic Models. It is important to note that the static models described above address the extent of DDI under equilibrium, steady-state conditions, using a representative member of the human population by applying an average of the systemic blood concentrations at steady state (represented by [I] in the above equations). With the increased availability of PBPK modeling software, which may also include population based capabilities, more investigators are applying dynamic approaches to the prediction of DDI. These dynamic approaches allow one to link the time course of predicted precipitant and object liver and intestine exposure to the known CYP3A4 interaction mechanism. Several PBPK prediction software platforms are available, including but not limited to PK-Sim, GastroPlus, Cloe Predict, and Simcyp. These software platforms were developed to enable modeling and simulation of human PK and tissue distribution and, in the case of Simcyp, the capability to simulate the PK and ADME variability across a population (for a recent review on application of PBPK models in drug discovery and development, see Jones et al.¹⁷⁵). Several of the software platforms also include a framework for integration of CYP metabolism and inhibition data, thereby enabling DDI prediction. For example, researchers from FDA recently published utilization of Simcyp to develop a PBPK model for telithromycin. The model incorporated parameters describing time-dependent inhibition of CYP3A4 in order to accurately describe telithromycin PK nonlinearity and DDI with midazolam.¹⁷⁶ Relative to the predictive models discussed previously, predictions with Simcyp require more comprehensive input data such as physiochemical properties, absorption, distribution, and elimination information and hence are most often applied to predictions for later stage compounds. For example, Simcyp was utilized in the planning and design of DDI trials for the recently approved anaplastic lymphoma kinase inhibitor crizotinib, which showed time-dependent inactivation of CYP3A4 in vitro (Pfizer, unpublished results).

6.2.3. Prediction Uncertainty. Although the more complex DDI models such as the net effect model and PBPK models

should theoretically produce a more accurate prediction of DDI than simpler models, in practice this is not always the case. The impacts of reversible and time-dependent inhibition and induction on overall AUC change are multiplicative, but so are the errors associated with each of these estimates. In addition, there is error associated with each of the variables that make up the TDI, reversible inhibition, and induction terms. For example, K_i , K_j , and k_{inact} values can vary from laboratory to laboratory, depending on how the inhibition experiment is conducted (e.g., microsomal protein concentration, probe substrate concentration, incubation time, etc). Furthermore, the k_{deg} for CYP3A4 cannot be measured directly, and several different approaches toward determining this value indirectly have been applied.¹⁷⁷ Hence, the value of k_{deg} used in DDI calculations can vary.

The value of $[I]$, inhibitor concentration *in vivo*, is another variable that cannot be directly measured, and there are several approaches for estimating the appropriate $[I]$ for liver and for intestine. For example, the C_{max} concentration, corrected for plasma protein binding, is commonly used as an estimation of $[I]$ in the liver. Intestinal $[I]$ may be estimated based on dose, rate of absorption, and fraction absorbed. Unbound hepatic inlet concentration or total plasma concentrations are also sometimes used as estimates for $[I]$. There is no consensus on the correct estimate of $[I]$ *in vivo*, and typically models are validated against a set of compounds with known DDI in order to assess which measures of $[I]$ work best for a given prediction method.

Another source of uncertainty in DDI prediction is the role of competing metabolic pathways for the perpetrator drug. For example, as described in section 3.2, raloxifene is a strong CYP3A4 inactivator *in vitro* and using standard prediction methods would be predicted to cause DDI with CYP3A4 substrates *in vivo*. However, if one factors in competing metabolic pathways, in this case intestinal glucuronidation, a more accurate prediction is achieved.¹⁷⁸

Finally the value for F_g , the fraction of object drug that escapes gut extraction, can have a large impact on DDI predictions for object drugs undergoing significant gut metabolism. However, F_g is determined indirectly and is difficult to estimate accurately. The impact of F_g on DDI prediction is exemplified in a recent publication focused on prediction of AUC change for simvastatin in the presence of imatinib.⁸⁹ A version of the static eq 5 was used for the prediction, and since simvastatin undergoes significant gut metabolism, the F_g term was incorporated. However, published estimates of F_g for simvastatin vary from 0.14 to 0.66, yielding a range of DDI predictions of approximately 5-fold, depending on whether the low or high end estimate of F_g was used. This example illustrates the difficulty in accurately estimating one of the parameters used in making prospective DDI predictions. Given the number of additional parameters that need to be measured/estimated, it is not surprising that over- or underpredictions are common.

6.2.4. Which TDI Prediction Approaches Work Best? In practice, there is variable success with the predictivity of models described above, depending on the attributes of the molecules being evaluated. For example, when developing SAR for CYP TDI or for selecting among a number of compounds in early drug discovery, application of rank order of k_{inact}/K_i or preincubation IC_{50} may be appropriate (Figure 17). However, at candidate selection stage, more quantitative estimates of DDI potential will be needed for CYP MBI positives. For late stage candidates, a number of scenarios are possible (Figure 18). For example, for compounds that have measurable CYP3A4 TDI in

Considerations for CYP TDI prediction in drug discovery

- For early stage drug discovery – SAR against CYP TDI, with qualitative rank ordering of compounds based on preincubation IC_{50} or k_{inact}/K_i
- For late stage discovery/development, more quantitative methods are needed, e.g., static or dynamic (PBPK) models
 - Time-dependent inhibition only: Equation 1 or dynamic model
 - Presence of additional CYP interactions, e.g., reversible inhibition and/or induction: Equation 5 or dynamic models
 - Consider whether gut interaction term should be included (especially for CYP3A4 inactivators)
- If compound of interest has structural similarity to compounds with known clinical DDI, the known compounds can be used to validate the prediction approach utilized

Figure 18. Suggested strategies for dealing with time-dependent CYP inactivation in drug discovery.

in vitro but do not show relevant reversible CYP3A4 inhibition or induction, the simpler prediction model described in eqs 1 or 2 might be as accurate as or more accurate than the models incorporating additional variables (eq 5 or PBPK models). The ketolide example described above is a good illustration of this phenomenon. Since most marketed macrolides and ketolides display CYP TDI but are not potent competitive inhibitors or inducers, the marketed agents can be used as reference compounds using eq 1. As such, this was utilized as a tactic for predicting DDI for a series of second generation ketolides.¹³⁷ For compounds and/or chemical series that exhibit CYP TDI in addition to competitive CYP inhibition and/or induction, the more complicated models will be needed. The performance of the net effect model (eq 5) was compared to that of Simcyp for prediction of DDI with midazolam for 30 compounds with varying degrees of competitive and time-dependent CYP inhibition and/or CYP induction.¹⁷⁹ For the overall data set, both approaches performed about equally well, with average geometric mean fold errors of 1.74 and 1.55 for net effect model and Simcyp, respectively. However, both models yielded several significant over- or underpredictions for some compounds. This latter fact highlights the important point that currently no single model works for all compounds. Therefore, drug development teams need to make thoughtful decisions regarding which models they will apply to their DDI risk assessment strategies, and their choice may vary depending on the chemical series in question. Another important consideration is the amount of data available at various stages in the drug development process. Most TDI prediction methods, including the methods described above, were evaluated using a set of marketed compounds, which are relatively well-understood in terms of TDI, DDI, physicochemical, and PK parameters that need to be incorporated into the models. However, for early stage compounds, many of these aspects may be unknown, and drug discovery scientists need to rely on predicted values, particularly with respect to PK parameters. In these cases, PBPK models may not be as powerful, since there is generally a higher degree of uncertainty for many of the input variables. In such scenarios, it might be more prudent to use a simpler model such as eq 5, using an estimate of average unbound efficacious concentration as $[I]$.

7. CONCLUDING REMARKS

Increasing use of drugs in polypharmacy settings calls for more in-depth understanding of the biochemical interactions that can lead to increased toxicity or loss of pharmacological effect.

Factors such as patient population, medications that are likely to be coadministered in that population, and the elimination mechanisms of concomitantly administered medications have to be taken into account to determine the potential for a DDI. Polypharmacy especially in the aging population significantly increases the risk of CYP DDIs, leading to decreased therapeutic efficacy via enzyme induction or increased incidence of toxicity via enzyme inhibition/inactivation. With respect to time-dependent CYP inhibition caused by the formation of CYP-reactive intermediates, most drug discovery efforts exercise the appropriate caution with regard to incorporating structural alerts in drug design. However, it is likely that unanticipated oxidative metabolism yielding reactive species will emerge, as increasingly novel and proprietary functional groups are continuously sought in drug design. A pragmatic starting point to deal with CYP TDI in early discovery should involve mechanistic studies to elucidate the biochemical/molecular basis for enzyme inactivation, followed by rational structural manipulations and iterative SAR analysis for CYP TDI. Hopefully, this will result in the identification of structural types wherein the TDI liability has been eliminated or drastically reduced, relative to the prototype(s). In cases where the functional group(s) responsible for CYP inactivation is required for primary pharmacology, project teams could choose to go forward with a compound that has some degree of CYP TDI liability, especially if there is reason to believe that the combination of in vivo systemic exposure needed for efficacy relative to potency of CYP inactivation will not result in a clinically relevant DDI. In the latter case, confidence in the ability to predict clinical DDI from in vitro DDI data becomes a critical component in the decision to advance an in vitro CYP TDI positive compound into the clinic. Although much progress has been made in DDI prediction capabilities, there exists uncertainty in several of the input parameters that are used to generate the prediction, and hence, over- or underprediction of DDI is not uncommon. In order to decrease the prediction uncertainty, more work is needed to understand prediction parameters and to know which parameters are most important for a given compound or series of compounds. The combination of mechanistic understanding of TDI and confidence in a predicted lack of clinically relevant DDI will enable drug discovery and development teams to progress more safe and effective therapies to patients.

AUTHOR INFORMATION

Corresponding Author

*Phone: (617) 551-3336. E-mail: amit.kalgutkar@pfizer.com.

Notes

The authors declare no competing financial interest.

Biographies

Suvi T. M. Orr (née Simila) is Principal Scientist and Laboratory Manager in the Worldwide Medicinal Chemistry Group at Pfizer. Before joining Pfizer in 2008, she worked in the Drug Discovery Team at Transtech Pharma (2001–2003) and earned her Ph.D. in Organic Chemistry from the University of Texas at Austin under the supervision of Prof. Stephen F. Martin. Her research at Pfizer focuses on the discovery (design and synthesis) of small molecule agents for treatment of cardiovascular and metabolic diseases. She has coauthored a number of publications in organic synthesis and is a co-inventor on several patents in the area of type-2-diabetes treatments.

Sharon L. Ripp is a Senior Principal Scientist in the Drug Metabolism Group at Pfizer. Since joining Pfizer in 2002, Sharon has contributed to numerous small molecule research and development programs and most recently is focused on support of Pfizer's late stage portfolio and marketed products. Sharon's training included a Ph.D. in Environmental Toxicology from the University of Wisconsin—Madison and postdoctoral work in the laboratory of Professor Russell Prough at the University of Louisville, KY. Sharon has a broad range of ADME interests and expertise and has published in the area of CYP induction and methods for in vitro to in vivo extrapolation.

T. Eric Ballard is a Postdoctoral Fellow in the Worldwide Medicinal Chemistry Group at Pfizer. He earned his Ph.D. in Organic Chemistry from North Carolina State University under Prof. Christian Melander in 2008. His research interests at Pfizer focus on the design and synthesis of clickable photoaffinity-based small molecule probes and their application to mechanism-of-action studies in neurologic and psychiatric disorders. He has coauthored numerous publications on organic synthesis, bioorganic chemistry, and chemical biology.

Jaclyn L. Henderson is a Senior Scientist in the Worldwide Medicinal Chemistry Group at Pfizer. She earned her Ph.D. in Organic Synthesis under the supervision of Prof. Michael F. Greaney at the University of Edinburgh, U.K., and carried out postdoctoral research in the group of Prof. Stephen Buchwald at Massachusetts Institute of Technology, MA. Before joining Pfizer she worked in Drug Discovery at Organon (2001–2004) and Vertex (2007–2008). Her research interests at Pfizer are focused on the design and synthesis of small molecule drugs for neuroscience indications.

Dennis O. Scott is a Senior Director in the Drug Metabolism Group at Pfizer. He received his Ph.D. (1991) in Chemistry from the University of Kansas and conducted postdoctoral research at the University of Kansas studying the in vivo disposition of camptothecin prodrugs. In 1992 he joined Marion Merrell Dow, and in 1998 he joined Pfizer in the Cardiovascular, Endocrinology and Metabolic Diseases Group, where he is currently a Senior Director, leading drug metabolism efforts at Cambridge, MA. He has coauthored more than 40 publications. Specific areas of scientific interest include semi-mechanistic PK/PD modeling, in silico ADME, in vivo microdialysis sampling, and active drug transport.

R. Scott Obach is a Senior Research Fellow in the Drug Metabolism Group at Pfizer. He earned his Ph.D. in Biochemistry from Brandeis University (1990), MA, and carried out postdoctoral research on cytochrome P450 enzymes at the New York State Department of Health Research Laboratories before joining Pfizer in 1992. His research interests include application of in vitro approaches to study drug metabolism, prediction of human pharmacokinetics and drug interactions, mechanisms of cytochrome P450 catalysis, and other biotransformation reactions, including generation of chemically reactive metabolites. He is currently on the editorial board of *Chemical Research in Toxicology*, *Drug Metabolism and Disposition* and *Xenobiotica*. He has coauthored more than 130 peer-reviewed publications, reviews, and book chapters.

Hao Sun is a Principal Scientist in the Drug Metabolism Group at Pfizer. He earned his Ph.D. in Pharmacology from the University of Utah in 2007 under the supervision of Prof. Garold S. Yost. His research interests include application of cytochrome P450 crystal structures and various molecular and quantum mechanics-based modeling tools to study catalytic mechanisms for structure-based drug design. He is currently on the editorial board of *Chemico-Biological Interactions*.

Amit S. Kalgutkar is a Research Fellow in the Drug Metabolism Group at Pfizer. He earned his Ph.D. in Organic Chemistry from

Virginia Tech, VA, and carried out postdoctoral research at Vanderbilt University, TN, before joining Pfizer. His research interest primarily focuses on medicinal chemistry and mechanistic drug metabolism. He has been a member of the editorial board of *Chemical Research in Toxicology* and is currently on the editorial board of *Xenobiotica* and *Drug Metabolism and Disposition*. Besides his current position at Pfizer, he is also an Adjunct Professor at the Department of Biomedical and Pharmaceutical Sciences, School of Pharmacy, University of Rhode Island. He has coauthored over 100 peer-reviewed papers, reviews, and book chapters and holds several patents in the area of selective COX-2 inhibition.

■ ABBREVIATIONS USED

CYP, cytochrome P450; DDI, drug–drug interaction; PK, pharmacokinetic; RM, reactive metabolite; PD, pharmacodynamic; TDI, time-dependent inhibition; MBI, mechanism-based inactivation; SAR, structure–activity relationship; PBPK, physiologically based pharmacokinetic; k_{inact} , maximal inactivation rate constant; K_I , inactivator concentration required to achieve 50% k_{inact} ; K_M , substrate concentration that yields half of the maximum rate of catalysis; IC_{50} , concentration of substrate required to achieve 50% inhibition; NADPH, nicotinamide adenine dinucleotide phosphate; UV, ultraviolet; MI, metabolite intermediate; LC–MS/MS, liquid chromatography–tandem mass spectrometry; ABT, 1-aminobenzotriazole; GSH, reduced glutathione; AUC, area under the plasma concentration versus time curve; COMT, catechol-*O*-methyltransferase; HLM, human liver microsome; HIV, human immunodeficiency virus; C_{max} , maximal plasma concentration; BBW, black box warning; TK, tyrosine kinase; UGT, uridine glucuronosyl transferase; GlyT1, glycine transporter 1; BPA, 4-*tert*-butylphenylacetylene; QD, once-a-day; NAPQI, *N*-acetyl-*p*-benzoquinoneimine; BPA, 4-*tert*-butylphenylacetylene; $[I]$, unbound plasma concentration of a CYP inactivator in vivo; k_{deg} , degradation rate constant for the CYP isoform; $f_{m,CYP}$, fraction of the drug that is metabolized by CYP; F_g , fraction of object drug that escapes gut extraction; E_{max} , maximum fold induction determined in an in vitro induction assay; EC_{50} , concentration of inducer producing half-maximal induction in vitro; ADME, absorption, distribution, metabolism, and excretion; K_i , inhibition constant for reversible CYP inhibition

■ REFERENCES

- (1) Guengerich, F. P. Common and uncommon cytochrome P450 reactions related to metabolism and chemical toxicity. *Chem. Res. Toxicol.* **2001**, *14*, 611–650.
- (2) Grimm, S. W.; Einolf, H. J.; Hall, S. D.; He, K.; Lim, H. K.; Ling, K. H.; Lu, C.; Nomeir, A. A.; Seibert, E.; Skordos, K. W.; Tonn, G. R.; Van Horn, R.; Wang, R. W.; Wong, Y. N.; Yang, T. J.; Obach, R. S. The conduct of in vitro studies to address time-dependent inhibition of drug metabolizing enzymes: a perspective of the pharmaceutical research and manufacturers of America. *Drug Metab. Dispos.* **2009**, *37*, 1355–1370.
- (3) Parkinson, A.; Kazmi, F.; Buckley, D. B.; Yerino, P.; Paris, B. L.; Holsapple, J.; Toren, P.; Otradovec, S. M.; Ogilvie, B. W. An evaluation of the dilution method for identifying metabolism-dependent inhibitors of cytochrome P450 enzymes. *Drug Metab. Dispos.* **2011**, *39*, 1370–1387.
- (4) Hollenberg, P. F.; Kent, U. M.; Bumpus, N. N. Mechanism-based inactivation of human cytochromes P450s: experimental characterization, reactive intermediates, and clinical implications. *Chem. Res. Toxicol.* **2008**, *21*, 189–205.
- (5) Berry, L. M.; Zhao, Z. An examination of IC_{50} and IC_{50} -shift experiments in assessing time-dependent inhibition of CYP3A4, CYP2D6 and CYP2C9 in human liver microsomes. *Drug Metab. Lett.* **2008**, *21*, 51–59.
- (6) Venkatakrishnan, K.; Obach, R. S. Drug–drug interactions via mechanism-based cytochrome P450 inactivation: points to consider for risk assessment from in vitro data and clinical pharmacologic evaluation. *Curr. Drug Metab.* **2007**, *8*, 449–462.
- (7) Mao, J.; Mohutsky, M. A.; Harrelson, J. P.; Wrighton, S. A.; Hall, S. D. Prediction of CYP-mediated drug–drug interactions using cryopreserved human hepatocytes suspended in human plasma. *Drug Metab. Dispos.* **2011**, *39*, 591–602.
- (8) Grime, K. H.; Bird, J.; Ferguson, D.; Riley, R. J. Mechanism-based inhibition of cytochrome P450 enzymes: an evaluation of early decision making in vitro approaches and drug–drug interaction prediction methods. *Eur. J. Pharm. Sci.* **2009**, *36*, 175–191.
- (9) Mayhew, B. S.; Jones, D. R.; Hall, S. D. An in vitro model for predicting in vivo inhibition of cytochrome P450 3A4 by metabolic intermediate complex formation. *Drug Metab. Dispos.* **2000**, *28*, 1031–1037.
- (10) Li, P.; Lu, C.; Balani, S. K.; Gan, L. S. A refined cytochrome P450 IC_{50} shift assay for reliably identifying CYP3A time-dependent inhibitors. *Drug Metab. Dispos.* **2011**, *39*, 1054–1057.
- (11) Sekiguchi, N.; Higashida, A.; Kato, M.; Nabuchi, Y.; Mitsui, T.; Takanashi, K.; Aso, Y.; Ishigai, M. Prediction of drug–drug interactions based on time-dependent inhibition from high throughput screening of cytochrome P450 3A4 inhibition. *Drug Metab. Pharmacokinet.* **2009**, *24*, 500–510.
- (12) Bertelsen, K. M.; Venkatakrishnan, K.; Von Moltke, L. L.; Obach, R. S.; Greenblatt, D. J. Apparent mechanism-based inhibition of human CYP2D6 in vitro by paroxetine: comparison with fluoxetine and quinidine. *Drug Metab. Dispos.* **2003**, *31*, 289–293.
- (13) Kalgutkar, A. S.; Obach, R. S.; Maurer, T. S. Mechanism-based inactivation of cytochrome P450 enzymes: chemical mechanisms, structure–activity relationships and relationship to clinical drug–drug interactions and idiosyncratic adverse drug reactions. *Curr. Drug Metab.* **2007**, *8*, 407–447.
- (14) Lin, J. H.; Lu, A. Y. Inhibition and induction of cytochrome P450 and the clinical implications. *Clin. Pharmacokinet.* **1998**, *35*, 361–390.
- (15) Franklin, M. R. Cytochrome P450 metabolic intermediate complexes from macrolide antibiotics and related compounds. *Methods Enzymol.* **1991**, *206*, 559–573.
- (16) Pessayre, D.; Konstantinova-Mitcheva, M.; Descatoire, V.; Cobert, B.; Wandscheer, J.-C.; Level, R.; Feldmann, G.; Mansuy, D.; Benhamou, J.-P. Hypo activity of cytochrome P-450 after triacetyloleandomycin administration. *Biochem. Pharmacol.* **1981**, *30*, 559.
- (17) Murray, M. Mechanisms of inhibitory and regulatory effects of methylenedioxyphenyl compounds on cytochrome P450-dependent drug oxidation. *Curr. Drug Metab.* **2000**, *1*, 67–84.
- (18) Wu, D.; Otton, S. V.; Inaba, T.; Kalow, W.; Sellers, E. M. Interactions of amphetamine analogs with human liver CYP2D6. *Biochem. Pharmacol.* **1997**, *53*, 1605–1612.
- (19) Murray, M.; Hetnarski, K.; Wilkinson, C. F. Selective inhibitory interactions of alkoxyethylenedioxybenzenes towards mono-oxygenase activity in rat-hepatic microsomes. *Xenobiotica* **1985**, *15*, 369–379.
- (20) Grab, L. A.; Swanson, B. A.; Ortiz de Montellano, P. R. Cytochrome P-450 inactivation by 3-alkylsydnones. Mechanistic implications of *n*-alkyl and *n*-alkenyl heme adduct formation. *Biochemistry* **1988**, *27*, 4805–4814.
- (21) He, K.; He, Y. A.; Szklarz, G. D.; Halpert, J. R.; Correia, M. A. Secobarbital-mediated inactivation of cytochrome P450 2B1 and its active site mutants. Partitioning between heme and protein alkylation and epoxidation. *J. Biol. Chem.* **1996**, *271*, 25864–25872.
- (22) Brown, L. M.; Ford-Hutchinson, A. W. The destruction of cytochrome P-450 by alclofenac: possible involvement of an epoxide metabolite. *Biochem. Pharmacol.* **1982**, *31*, 195–199.
- (23) Ortiz de Montellano, P. R.; Watanabe, M. D. Free radical pathways in the in vitro hepatic metabolism of phenelzine. *Mol. Pharmacol.* **1987**, *31*, 213–219.

- (24) Ortiz de Montellano, P. R.; Mathews, J. M. Autocatalytic alkylation of the cytochrome P-450 prosthetic haem group by 1-aminobenzotriazole. Isolation of an NN-bridged benzyne–protoporphyrin IX adduct. *Biochem. J.* **1981**, *195*, 761–764.
- (25) Lightning, L. K.; Trager, W. F. Characterization of covalent adducts to intact cytochrome P450s by mass spectrometry. *Methods Enzymol.* **2002**, *357*, 296–300.
- (26) Halpert, J. Further studies of the suicide inactivation of purified rat liver cytochrome P-450 by chloramphenicol. *Mol. Pharmacol.* **1982**, *21*, 166–172.
- (27) Halpert, J. Covalent modification of lysine during the suicide inactivation of rat liver cytochrome P-450 by chloramphenicol. *Biochem. Pharmacol.* **1981**, *30*, 875–881.
- (28) Boitier, E.; Beaune, P. Cytochrome P450 as targets to autoantibodies in immune mediated diseases. *Mol. Aspects Med.* **1999**, *20*, 84–137.
- (29) Belloc, C.; Gauffre, A.; Andre, C.; Beaune, P. H. Epitope mapping of human CYP1A2 in dihydralazine-induced autoimmune hepatitis. *Pharmacogenetics* **1997**, *7*, 181–186.
- (30) Masubuchi, Y.; Horie, T. Mechanism-based inactivation of cytochrome P450s 1A2 and 3A4 by dihydralazine in human liver microsomes. *Chem. Res. Toxicol.* **1999**, *12*, 1028–1032.
- (31) Bourdi, M.; Chen, W.; Peter, R. M.; Martin, J. L.; Buters, J. T.; Nelson, S. D.; Pohl, L. R. Human cytochrome P450 2E1 is a major autoantigen associated with halothane hepatitis. *Chem. Res. Toxicol.* **1996**, *9*, 1159–1166.
- (32) Spracklin, D. K.; Hankins, D. C.; Fisher, J. M.; Thummel, K. E.; Kharasch, E. D. Cytochrome P450 2E1 is the principal catalyst of human oxidative halothane metabolism in vitro. *J. Pharmacol. Exp. Ther.* **1997**, *281*, 400–411.
- (33) Osawa, Y.; Pohl, L. R. Covalent binding of the prosthetic heme to protein: a potential mechanism for the suicide inactivation of hemoproteins. *Chem. Res. Toxicol.* **1989**, *2*, 131–141.
- (34) Guzelian, P. S.; Swisher, R. W. Degradation of cytochrome P-450 haem by carbon tetrachloride and 2-allyl-2-isopropylacetamide in rat liver in vivo and in vitro: involvement of non-carbon monoxide-forming mechanisms. *Biochem. J.* **1979**, *184*, 481–489.
- (35) Ring, B. J.; Patterson, B. E.; Mitchell, M. I.; Vandenbranden, M.; Gillespie, J.; Bedding, A. W.; Jewell, H.; Payne, C. D.; Fogue, S. T.; Eckstein, J.; Wrighton, S. A.; Phillips, D. L. Effect of tadalafil on cytochrome P403A4-mediated clearance: studies in vitro and in vivo. *Clin. Pharmacol. Ther.* **2005**, *77*, 63–75.
- (36) Zhao, S. X.; Dalvie, D. K.; Kelly, J. M.; Soglia, J. R.; Frederick, K. S.; Smith, E. B.; Obach, R. S.; Kalgutkar, A. S. NADPH-dependent covalent binding of [³H]paroxetine to human liver microsomes and S-9 fractions: identification of an electrophilic quinone metabolite of paroxetine. *Chem. Res. Toxicol.* **2007**, *20*, 1649–1657.
- (37) Kaye, C. M.; Haddock, R. E.; Langley, P. F.; Mellows, G.; Tasker, T. C.; Zussman, B. D.; Greb, W. H. A review of the metabolism and pharmacokinetics of paroxetine in man. *Acta Psychiatr. Scand., Suppl.* **1989**, *350*, 60–75.
- (38) Alderman, J.; Preskorn, S. H.; Greenblatt, D. J.; Harrison, W.; Penenberg, D.; Allison, J.; Chung, M. Desipramine pharmacokinetics when coadministered with paroxetine or sertraline in extensive metabolizers. *J. Clin. Psychopharmacol.* **1997**, *17*, 284–291.
- (39) Hemeryck, A.; Lefebvre, R. A.; De Vriendt, C.; Belpaire, F. M. Paroxetine affects metoprolol pharmacokinetics and pharmacodynamics in healthy volunteers. *Clin. Pharmacol. Ther.* **2000**, *67*, 283–291.
- (40) Spina, E.; Avenoso, A.; Facciola, G.; Scordo, M. G.; Ancione, M.; Madia, A. Plasma concentrations of risperidone and 9-hydroxyrisperidone during combined treatment with paroxetine. *Ther. Drug Monit.* **2001**, *23*, 223–227.
- (41) Belle, D. J.; Ernest, C. S.; Sauer, J. M.; Smith, B. P.; Thomasson, H. R.; Witcher, J. W. Effect of potent CYP2D6 inhibition by paroxetine on atomoxetine pharmacokinetics. *J. Clin. Pharmacol.* **2002**, *42*, 1219–1227.
- (42) Venkatakrishnan, K.; Obach, R. S. In vitro–in vivo extrapolation of CYP2D6 inactivation by paroxetine: prediction of nonstationary pharmacokinetics and drug interaction magnitude. *Drug Metab. Dispos.* **2005**, *33*, 845–852.
- (43) Wang, Y. H.; Jones, D. R.; Hall, S. D. Prediction of cytochrome P4503A inhibition by verapamil enantiomers and their metabolites. *Drug Metab. Dispos.* **2004**, *32*, 259–266.
- (44) Lemma, G. L.; Wang, Z.; Hamman, M. A.; Zaheer, N. A.; Gorski, J. C.; Hall, S. D. The effect of short and long-term administration of verapamil on the disposition of cytochrome P450 3A and P-glycoprotein substrates. *Clin. Pharmacol. Ther.* **2006**, *79*, 218–230.
- (45) Jerling, M.; Huan, B. L.; Leung, K.; Chu, N.; Abdallah, H.; Hussein, Z. Studies to investigate the pharmacokinetic interactions between ranolazine and ketoconazole, diltiazem, or simvastatin during combined administration in healthy subjects. *J. Clin. Pharmacol.* **2005**, *45*, 422–433.
- (46) Sutton, D.; Butler, A. M.; Nadin, L.; Murray, M. Role of CYP3A4 in human hepatic diltiazem N-demethylation: inhibition of CYP3A4 activity by oxidized diltiazem metabolites. *J. Pharmacol. Exp. Ther.* **1997**, *282*, 294–300.
- (47) Jones, D. R.; Gorski, J. C.; Hamman, M. A.; Mayhew, B. S.; Rider, S.; Hall, S. D. Diltiazem inhibition of cytochrome P-450 3A activity is due to metabolite intermediate complex formation. *J. Pharmacol. Exp. Ther.* **1999**, *290*, 1116–1125.
- (48) Zhao, P.; Lee, C. A.; Kunze, K. L. Sequential metabolism is responsible for diltiazem-induced time-dependent loss of CYP3A. *Drug Metab. Dispos.* **2007**, *35*, 704–712.
- (49) Lesko, L. J. Pharmacokinetic drug interactions with amiodarone. *Clin. Pharmacokinet.* **1989**, *17*, 130–140.
- (50) Larrey, D.; Tinel, M.; Letteron, P.; Geneve, J.; Descatoire, V.; Pessayre, D. Formation of an inactive cytochrome P-450Fe(II)-metabolite complex after administration of amiodarone in rats, mice and hamsters. *Biochem. Pharmacol.* **1986**, *35*, 2213–2220.
- (51) Ohyama, K.; Nakajima, M.; Suzuki, M.; Shimada, N.; Yamazaki, H.; Yokoi, T. Inhibitory effects of amiodarone and its N-deethylated metabolite on human cytochrome P450 activities: prediction of in vivo drug interactions. *Br. J. Clin. Pharmacol.* **2000**, *49*, 244–253.
- (52) Mori, K.; Hashimoto, H.; Takatsu, H.; Tsuda-Tsukimoto, M.; Kume, T. Cocktail-substrate assay system for mechanism-based inhibition of CYP2C9, CYP2D6, and CYP3A using human liver microsomes at an early stage of drug development. *Xenobiotica* **2009**, *39*, 415–422.
- (53) Polasek, T. M.; Elliot, D. J.; Lewis, B. C.; Minors, J. O. Mechanism-based inactivation of human cytochrome P4502C8 by drugs in vitro. *J. Pharmacol. Exp. Ther.* **2004**, *311*, 996–1007.
- (54) Nagauma, M.; Shiga, T.; Nishikata, K.; Tsuchiya, T.; Kasanuki, H.; Fujii, E. Role of desethylamiodarone in the anticoagulant effect of concurrent amiodarone and warfarin therapy. *J. Cardiovasc. Pharmacol. Ther.* **2001**, *6*, 363–367.
- (55) Mandrioli, R.; Forti, G. C.; Raggi, M. A. Fluoxetine metabolism and pharmacological interactions: the role of cytochrome P450. *Curr. Drug Metab.* **2006**, *7*, 127–133.
- (56) Stevens, J. C.; Wrighton, S. A. Interaction of the enantiomers of fluoxetine and norfluoxetine with human liver cytochromes P450. *J. Pharmacol. Exp. Ther.* **1993**, *266*, 964–971.
- (57) Stresser, D. M.; Mason, A. K.; Perloff, E. S.; Ho, T.; Crespi, C. L.; Dandeneau, A. A.; Morgan, L.; Dehal, S. S. Differential time- and NADPH-dependent inhibition of CYP2C19 by enantiomers of fluoxetine. *Drug Metab. Dispos.* **2009**, *37*, 695–698.
- (58) Bensoussan, C.; Delaforge, M.; Mansuy, D. Particular ability of cytochrome P450 3A to form inhibitory P450-iron-metabolite complexes upon metabolic oxidation of aminodrugs. *Biochem. Pharmacol.* **1995**, *49*, 591–602.
- (59) Mansuy, D. Formation of reactive intermediates and metabolites: effects of macrolide antibiotics on cytochrome P-450. *Pharmacol. Ther.* **1987**, *33*, 41–45.
- (60) Piacentini, N.; Trifiro, G.; Tari, M.; Moretti, S.; Arcoraci, V. UVEC group. Statin–macrolide interaction risk: a population-based study throughout a general practice database. *Eur. J. Clin. Pharmacol.* **2005**, *61*, 615–620.

- (61) Larrey, D.; Funck-Bretano, C.; Breil, P.; Vitau, J.; Theodore, C.; Babany, G.; Pessayre, D. Effects of erythromycin on hepatic drug-metabolizing enzymes in humans. *Biochem. Pharmacol.* **1983**, *32*, 1063–1068.
- (62) Larrey, D.; Tinel, M.; Pessayre, D. Formation of inactive cytochrome P-450 Fe(II)-metabolite complexes with several erythromycin derivatives but not with josamycin and midecamycin in rats. *Biochem. Pharmacol.* **1983**, *32*, 1487–1493.
- (63) Yamazaki, H.; Shimada, T. Comparative studies of in vitro inhibition of cytochrome P450 3A4-dependent testosterone 6 β -hydroxylation by roxithromycin and its metabolites, troleandomycin, and erythromycin. *Drug Metab. Dispos.* **1998**, *26*, 1053–1057.
- (64) Amacher, D. E.; Schomaker, S. J.; Retsema, J. A. Comparison of the effects of the new azalide antibiotic, azithromycin, and erythromycin estolate on rat liver cytochrome P-450. *Antimicrob. Agents Chemother.* **1991**, *35*, 1186–1190.
- (65) Sartori, E.; Delaforge, M.; Mansuy, D. In vivo interaction of rat liver cytochrome P-450 with erythromycin, oleandomycin and erythralosamine derivatives. Importance of structural factor. *Biochem. Pharmacol.* **1989**, *38*, 2061–2068.
- (66) Ekroos, M.; Sjogren, T. Structural basis for ligand promiscuity in cytochrome P450 3A4. *Proc. Natl. Acad. Sci. U.S.A.* **2006**, *103*, 13682–13687.
- (67) Paris, B. L.; Ogilvie, B. W.; Scheinkoenig, J. A.; Ndikum-Moffor, F.; Gibson, R.; Parkinson, A. In vitro inhibition and induction of human liver cytochrome P450 enzymes by milnacipran. *Drug Metab. Dispos.* **2009**, *37*, 2045–2054.
- (68) Chan, C. Y.; New, L. S.; Ho, H. K.; Chan, E. C. Reversible time-dependent inhibition of cytochrome P450 enzymes by duloxetine and inertness of its thiophene ring towards bioactivation. *Toxicol. Lett.* **2011**, *206*, 314–324.
- (69) Knadler, M. P.; Lobo, E.; Chappell, J.; Bergstrom, R. Duloxetine: clinical pharmacokinetics and drug interactions. *Clin. Pharmacokinet.* **2011**, *50*, 281–294.
- (70) Wu, G.; Vashishtha, S. C.; Erve, J. C. Characterization of glutathione conjugates of duloxetine by mass spectrometry and evaluation of in silico approaches to rationalize the site of conjugation for thiophene containing rings. *Chem. Res. Toxicol.* **2010**, *23*, 1393–1404.
- (71) Winston, A.; Boffito, M. The management of HIV-1 protease inhibitor pharmacokinetic interactions. *J. Antimicrob. Chemother.* **2005**, *56*, 1–5.
- (72) Ernest, C. S. 2nd; Hall, S. D.; Jones, D. R. Mechanism-based inactivation of CYP3A by HIV protease inhibitors. *J. Pharmacol. Exp. Ther.* **2005**, *312*, 583–591.
- (73) Lillibridge, J. H.; Liang, B. H.; Kerr, B. M.; Webber, S.; Quart, B.; Shetty, B. V.; Lee, C. A. Characterization of the selectivity and mechanism of human cytochrome P450 inhibition by the human immunodeficiency virus protease inhibitor nelfinavir mesylate. *Drug Metab. Dispos.* **1998**, *26*, 609–616.
- (74) Kempf, D. J.; Marsh, K. C.; Kumar, G.; Rodrigues, A. D.; Denissen, J. F.; McDonald, E.; Kukulka, M. J.; Hsu, A.; Granneman, G. R.; Baroldi, P. A.; Sun, E.; Pizzuti, D.; Plattner, J. J.; Norbeck, D. W.; Leonard, J. M. Pharmacokinetic enhancement of inhibitors of the human immunodeficiency virus protease by coadministration with ritonavir. *Antimicrob. Agents Chemother.* **1997**, *41*, 654–660.
- (75) Ma, X.; Li, F.; Lu, J. Metabolomic screening and identification of bioactivation pathways of ritonavir. *Chem. Res. Toxicol.* **2011**, *24*, 2109–2114.
- (76) Mathias, A. A.; German, P.; Murray, B. P.; Wei, L.; Jain, A.; West, S.; Warren, D.; Hui, J.; Kearney, B. P. Pharmacokinetics and pharmacodynamics of GS-9350: a novel pharmacokinetic enhancer without anti-HIV activity. *Clin. Pharmacol. Ther.* **2010**, *87*, 322–329.
- (77) Kalgutkar, A. S.; Vaz, A. D.; Lame, M. E.; Henne, K. R.; Soglia, J.; Zhao, S. X.; Abramov, Y. A.; Lombardo, F.; Collin, C.; Hendsch, Z. S.; Hop, C. E. Bioactivation of the nontricyclic antidepressant nefazodone to a reactive quinone-imine species in human liver microsomes and recombinant cytochrome P4503A4. *Drug Metab. Dispos.* **2005**, *33*, 243–253.
- (78) Bauman, J. N.; Frederick, K. S.; Sawant, A.; Walsky, R. L.; Cox, L. M.; Obach, R. S.; Kalgutkar, A. S. Comparison of the bioactivation potential of the antidepressant and hepatotoxin nefazodone with aripiprazole, a structural analog and marketed drug. *Drug Metab. Dispos.* **2008**, *36*, 1016–1029.
- (79) Greene, D. S.; Barbhayia, R. H. Clinical pharmacokinetics of nefazodone. *Clin. Pharmacokinet.* **1997**, *33*, 260–275.
- (80) DeVane, C. L.; Donovan, J. L.; Liston, H. L.; Markowitz, J. S.; Cheng, K. T.; Risch, S. C.; Willard, L. Comparative CYP3A4 inhibitory effects of venlafaxine, fluoxetine, sertraline, and nefazodone in healthy volunteers. *J. Clin. Psychopharmacol.* **2004**, *24*, 4–10.
- (81) Thompson, M.; Samuels, S. Rhabdomyolysis with simvastatin and nefazodone. *Am. J. Psychiatry* **2002**, *159*, 1607.
- (82) Choi, S. Nefazodone (Serzone) withdrawn because of hepatotoxicity. *Can. Med. Assoc. J.* **2003**, *169*, 1187.
- (83) Obach, R. S.; Kalgutkar, A. S.; Soglia, J. R.; Zhao, S. X. Can in vitro metabolism-dependent covalent binding data in liver microsomes distinguish hepatotoxic from nonhepatotoxic drugs? An analysis of 18 drugs with consideration of intrinsic clearance and daily dose. *Chem. Res. Toxicol.* **2008**, *21*, 1814–1822.
- (84) Zimmerlin, A.; Trunzer, M.; Faller, B. CYP3A time-dependent inhibition risk assessment validated with 400 reference drugs. *Drug Metab. Dispos.* **2011**, *39*, 1039–1046.
- (85) Kalgutkar, A. S.; Henne, K. R.; Lame, M. E.; Vaz, A. D.; Collin, C.; Soglia, J. R.; Zhao, S. X.; Hop, C. E. Metabolic activation of the nontricyclic antidepressant trazodone to electrophilic quinone-imine and epoxide intermediates in human liver microsomes and recombinant P4503A4. *Chem.-Biol. Interact.* **2005**, *155*, 10–20.
- (86) Di Gion, P.; Kanefendt, F.; Lindauer, A.; Scheffler, M.; Doroshenko, O.; Fuhr, U.; Wolf, J.; Jaehde, U. Clinical pharmacokinetics of tyrosine kinase inhibitors. *Clin. Pharmacokinet.* **2011**, *50*, 551–603.
- (87) O'Brien, S. G.; Meinhardt, P.; Bond, E.; Beck, J.; Peng, B.; Dutreix, C.; Mehring, G.; Milosavljev, S.; Huber, C.; Capdeville, R.; Fischer, T. Effects of imatinib mesylate (STI571, Glivec) on the pharmacokinetics of simvastatin, a cytochrome P450 3A4 substrate, in patients with chronic myeloid leukaemia. *Br. J. Cancer* **2003**, *89*, 1855–1859.
- (88) Connolly, R. M.; Rudek, M. A.; Garrett-Mayer, E.; Jeter, S. C.; Donehower, M. G.; Wright, L. A.; Zhao, M.; Fetting, J. H.; Emens, L. A.; Stearns, V.; Davidson, N. E.; Baker, S. D.; Wolff, A. C. Docetaxel metabolism is not altered by imatinib: findings from an early phase study in metastatic breast cancer. *Breast Cancer Res. Treat.* **2011**, *127*, 153–162.
- (89) Filppula, A. M.; Laitila, J.; Neuvonen, P. J.; Backman, J. T. Potent mechanism-based inhibition of CYP3A4 by imatinib explains its interaction liability with CYP3A4 substrates. *Br. J. Pharmacol.* [Online early access]. DOI: 10.1111/j.1476-5381.2011.01732.x. Published Online: Oct 20, **2011**.
- (90) Haouala, A.; Widmer, N.; Duchosal, M. A.; Montemurro, M.; Buclin, T.; Decosterd, L. A. Drug interactions with the tyrosine kinase inhibitors imatinib, dasatinib, and nilotinib. *Blood* **2011**, *117*, e75–87.
- (91) Li, X.; He, Y.; Ruiz, C. H.; Koenig, M.; Cameron, M. D. Characterization of dasatinib and its structural analogs as CYP3A4 mechanism-based inactivators and the proposed bioactivation pathways. *Drug Metab. Dispos.* **2009**, *37*, 1242–1250.
- (92) Teng, W. C.; Oh, J. W.; New, L. S.; Wahlin, M. D.; Nelson, S. D.; Ho, H. K.; Chan, E. C. Mechanism-based inactivation of cytochrome P4503A4 by lapatinib. *Mol. Pharmacol.* **2010**, *78*, 693–703.
- (93) Takakusa, H.; Wahlin, M. D.; Zhao, C.; Hanson, K. L.; New, L. S.; Chan, E. C.; Nelson, S. D. Metabolic intermediate complex formation of human cytochrome P4503A4 by lapatinib. *Drug Metab. Dispos.* **2011**, *39*, 1022–1030.
- (94) Li, X.; Kamenecka, T. M.; Cameron, M. D. Bioactivation of the epidermal growth factor receptor inhibitor gefitinib: implications for pulmonary and hepatic toxicities. *Chem. Res. Toxicol.* **2009**, *22*, 1736–1742.

- (95) Li, X.; Kamenecka, T. M.; Cameron, M. D. Cytochrome P450-mediated bioactivation of the epidermal growth factor receptor inhibitor erlotinib to a reactive electrophile. *Drug Metab. Dispos.* **2010**, *38*, 1238–1245.
- (96) Veeraputhiran, M.; Sundermeyer, M. Rhabdomyolysis resulting from pharmacologic interaction between erlotinib and simvastatin. *Clin. Lung Cancer* **2008**, *9*, 232–234.
- (97) Flaherty, K. T.; Lathia, C.; Frye, R. F.; Schuchter, L.; Redlinger, M.; Rosen, M.; O'Dwyer, P. J. Interaction of sorafenib and cytochrome P450 isoenzymes in patients with advanced melanoma: a phase I/II pharmacokinetic interaction study. *Cancer Chemother. Pharmacol.* **2011**, *68*, 1111–1118.
- (98) Lathia, C.; Lettieri, J.; Cihon, F.; Gallentine, M.; Radtke, M.; Sundaresan, P. Lack of effect of ketoconazole-mediated CYP3A inhibition on sorafenib clinical pharmacokinetics. *Cancer Chemother. Pharmacol.* **2006**, *57*, 685–692.
- (99) Li, L.; Zhao, M.; Navid, F.; Pratz, K.; Smith, B. D.; Rudek, M. A.; Baker, S. D. Quantitation of sorafenib and its active metabolite sorafenib *N*-oxide in human plasma by liquid chromatography–tandem mass spectrometry. *J. Chromatogr., B: Anal. Technol. Biomed. Life Sci.* **2010**, *878*, 3033–3038.
- (100) Pereillo, J. M.; Maftouh, M.; Andrieu, A.; Uzabiaga, M. F.; Fedili, O.; Savi, P.; Pascal, M.; Herbert, J. M.; Maffrand, J. P.; Picard, C. Structure and stereochemistry of the active metabolite of clopidogrel. *Drug Metab. Dispos.* **2002**, *30*, 1288–1295.
- (101) Dansette, P. M.; Libraire, J.; Bertho, G.; Mansuy, D. Metabolic oxidative cleavage of thioesters: evidence for the formation of sulfenic acid intermediates in the bioactivation of the antithrombotic prodrugs ticlopidine and clopidogrel. *Chem. Res. Toxicol.* **2009**, *22*, 369–373.
- (102) Ha-Duong, N. T.; Dijols, S.; Macherey, A. C.; Goldstein, J. A.; Dansette, P. M.; Mansuy, D. Ticlopidine as a selective mechanism-based inhibitor of human cytochrome P450C19. *Biochemistry* **2001**, *40*, 12112–12122.
- (103) Nishiya, Y.; Hagihara, K.; Kurihara, A.; Okudaira, N.; Farid, N. A.; Okazaki, O.; Ikeda, T. Comparison of mechanism-based inhibition of human cytochrome P450 2C19 by ticlopidine, clopidogrel, and prasugrel. *Xenobiotica* **2009**, *39*, 836–843.
- (104) Mega, J. L.; Close, S. L.; Wiviott, S. D.; Shen, L.; Hockett, R. D.; Brandt, J. T.; Walker, J. R.; Antman, E. M.; Macias, W.; Braunwald, E.; Sabatine, M. S. Cytochrome P-450 polymorphisms and response to clopidogrel. *N. Engl. J. Med.* **2009**, *360*, 354–362.
- (105) Kurihara, A.; Hagihara, K.; Kazui, M.; Ozeki, T.; Farid, N. A.; Ikeda, T. In vitro metabolism of antiplatelet agent clopidogrel: cytochrome P450 isoforms responsible for two oxidation steps involved in the active metabolite formation. *Drug Metab. Rev., Suppl.* **2005**, *2*, 99.
- (106) Hagihara, K.; Nishiya, Y.; Kurihara, A.; Kazui, M.; Farid, N. A.; Ikeda, T. Comparison of human cytochrome P450 inhibition by the thienopyridines prasugrel, clopidogrel and ticlopidine. *Drug Metab. Pharmacokin.* **2008**, *23*, 412–420.
- (107) Rehm, J. L. F.; Eckstein, J. A.; Farid, N. A.; Heim, J. B.; Kasper, S. C.; Kurihara, A.; Wrighton, S. A.; Ring, B. J. Interactions of two major metabolites of prasugrel, a thienopyridine antiplatelet agent, with the cytochromes P450. *Drug Metab. Dispos.* **2006**, *34*, 600–607.
- (108) Nishiya, Y.; Hagihara, K.; Ito, T.; Tajima, M.; Miura, S.; Kurihara, A.; Farid, N. A.; Ikeda, T. Mechanism-based inhibition of human cytochrome P450 2B6 by ticlopidine, clopidogrel, and the thiolactone metabolite of prasugrel. *Drug Metab. Dispos.* **2009**, *37*, 589–593.
- (109) Richter, T.; Murdter, T. E.; Heinkele, G.; Pleiss, J.; Tatzel, S.; Schwab, M.; Eichelbaum, M.; Zanger, U. M. Potent mechanism-based inhibition of human CYP2B6 by clopidogrel and ticlopidine. *J. Pharmacol. Exp. Ther.* **2004**, *308*, 189–197.
- (110) Zhang, H.; Amunugama, H.; Ney, S.; Cooper, N.; Hollenberg, P. F. Mechanism-based inactivation of human cytochrome P450 2B6 by clopidogrel: involvement of both covalent modification of cysteinyl residue 475 and loss of heme. *Mol. Pharmacol.* **2011**, *80*, 839–847.
- (111) Turpeinen, M.; Tolonen, A.; Uusitalo, J.; Jalonen, J.; Pelkonen, O.; Laine, K. Effect of clopidogrel and ticlopidine on cytochrome P450 2B6 activity as measured by bupropion hydroxylation. *Clin. Pharmacol. Ther.* **2005**, *77*, 553–559.
- (112) Farid, N. A.; Payne, C. D.; Ernest, C. S. 2nd.; Li, Y. G.; Winters, K. J.; Salazar, D. E.; Small, D. S. Prasugrel, a new thienopyridine antiplatelet drug, weakly inhibits cytochrome P450 2B6 in humans. *J. Clin. Pharmacol.* **2008**, *48*, 53–59.
- (113) Wen, X.; Wang, J. S.; Backman, J. T.; Kivisto, K. T.; Neuvonen, P. J. Gemfibrozil is a potent inhibitor of human cytochrome P450C9. *Drug Metab. Dispos.* **2001**, *29*, 1359–1361.
- (114) Wang, J. S.; Neuvonen, M.; Wen, X.; Backman, J. T.; Neuvonen, P. J. Gemfibrozil inhibits CYP2C8-mediated cerivastatin metabolism in human liver microsomes. *Drug Metab. Dispos.* **2002**, *30*, 1352–1356.
- (115) Backman, J. T.; Kyrklund, C.; Neuvonen, M.; Neuvonen, P. J. Gemfibrozil greatly increases plasma concentrations of cerivastatin. *Clin. Pharmacol. Ther.* **2002**, *72*, 685–691.
- (116) Jaakkola, T.; Backman, J. T.; Neuvonen, M.; Neuvonen, P. J. Effects of gemfibrozil, itraconazole, and their combination on the pharmacokinetics of pioglitazone. *Clin. Pharmacol. Ther.* **2005**, *77*, 404–414.
- (117) Lilja, J. J.; Backman, J. T.; Neuvonen, P. J. Effect of gemfibrozil on the pharmacokinetics and pharmacodynamics of racemic warfarin in healthy subjects. *Br. J. Clin. Pharmacol.* **2005**, *59*, 433–439.
- (118) Shitara, Y.; Hirano, M.; Sato, H.; Sugiyama, Y. Gemfibrozil and its glucuronide inhibit the organic anion transporting polypeptide 2 (OATP2/OATP1B1:SLC21A6)-mediated hepatic uptake and CYP2C8-mediated metabolism of cerivastatin: analysis of the mechanism of the clinically relevant drug–drug interaction between cerivastatin and gemfibrozil. *J. Pharmacol. Exp. Ther.* **2004**, *311*, 228–236.
- (119) Ogilvie, B. W.; Zhang, D.; Li, W.; Rodrigues, A. D.; Gipson, A. E.; Holsapple, J.; Toren, P.; Parkinson, A. Glucuronidation converts gemfibrozil to a potent, metabolism-dependent inhibitor of CYP2C8: implications for drug–drug interactions. *Drug Metab. Dispos.* **2006**, *34*, 191–197.
- (120) Tornio, A.; Niemi, M.; Neuvonen, M.; Laitila, J.; Kalliokoski, A.; Neuvonen, P. J.; Backman, J. T. The effect of gemfibrozil on repaglinide pharmacokinetics persists for at least 12 h after the dose: evidence for mechanism-based inhibition of CYP2C8 in vivo. *Clin. Pharmacol. Ther.* **2008**, *84*, 403–411.
- (121) Honkalammi, J.; Niemi, M.; Neuvonen, P. J.; Backman, J. T. Mechanism-based inactivation of CYP2C8 by gemfibrozil occurs rapidly in humans. *Clin. Pharmacol. Ther.* **2011**, *89*, 579–586.
- (122) Baer, B. R.; DeLisle, R. K.; Allen, A. Benzyl oxidation of gemfibrozil-1-*O*-beta-glucuronide by P450 2C8 leads to heme alkylation and irreversible inhibition. *Chem. Res. Toxicol.* **2009**, *22*, 1298–1309.
- (123) Jenkins, S. M.; Zvyaga, T.; Johnson, S. R.; Hurley, J.; Wagner, A.; Burrell, R.; Turley, W.; Leet, J. E.; Philip, T.; Rodrigues, A. D. Studies to further investigate the inhibition of human liver microsomal cytochrome P450C8 (CYP2C8) by the acyl- β -glucuronide of gemfibrozil. *Drug Metab. Dispos.* **2011**, *39*, 2421–2430.
- (124) Prueksaritanont, T.; Zhao, J. J.; Ma, B.; Roadcap, B. A.; Tang, C.; Qiu, Y.; Liu, L.; Lin, J. H.; Pearson, P. G.; Baillie, T. A. Mechanistic studies on metabolic interactions between gemfibrozil and statins. *J. Pharmacol. Exp. Ther.* **2002**, *301*, 1042–1051.
- (125) Prueksaritanont, T.; Richards, K. M.; Qiu, Y.; Strong-Basalys, K.; Miller, A.; Li, C.; Eisenhandler, R.; Carlini, E. J. Comparative effects of fibrates on drug metabolizing enzymes in human hepatocytes. *Pharm. Res.* **2005**, *22*, 71–78.
- (126) Chen, P.; Ngui, J. S.; Doss, G. A.; Wang, R. W.; Cai, X.; DiNinno, F. P.; Blizzard, T. A.; Hammond, M. L.; Stearns, R. A.; Evans, D. C.; Baillie, T. A. Cytochrome P450 3A4-mediated bioactivation of raloxifene: irreversible enzyme inhibition and thiol adduct formation. *Chem. Res. Toxicol.* **2002**, *15*, 907–914.
- (127) Baer, B. R.; Wienkers, L. C.; Rock, D. A. Time-dependent inactivation of P4503A4 by raloxifene: identification of Cys239 as the site of apoprotein alkylation. *Chem. Res. Toxicol.* **2007**, *20*, 954–964.

- (128) Pearson, J. T.; Wahlstrom, J. L.; Dickman, L. J.; Kumar, S.; Halpert, J. R.; Wienkers, L. C.; Foti, R. S.; Rock, D. A. Differential time-dependent inactivation of P450 3A4 and P450 3A5 by raloxifene: a key role for C239 in quenching reactive intermediates. *Chem. Res. Toxicol.* **2007**, *20*, 1778–1786.
- (129) Yukinaga, H.; Takami, T.; Shioyama, S. H.; Tozuka, Z.; Masumoto, H.; Okazaki, O.; Sudo, K. Identification of cytochrome P450 3A4 modification site with reactive metabolite using linear ion trap-Fourier transform mass spectrometry. *Chem. Res. Toxicol.* **2007**, *20*, 1373–1378.
- (130) Mizuma, T. Intestinal glucuronidation metabolism may have a greater impact on oral bioavailability than hepatic glucuronidation metabolism in humans: a study with raloxifene, substrate for UGT1A1, 1A8, 1A9, and 1A10. *Int. J. Pharm.* **2009**, *378*, 140–141.
- (131) Mullins, M. E.; Horowitz, B. Z.; Linden, D. H.; Smith, G. W.; Norton, R. L.; Stump, J. Life-threatening interaction between mibefradil and beta-blockers with dihydropyridine calcium channel blockers. *JAMA, J. Am. Med. Assoc.* **1998**, *280*, 157–158.
- (132) Schmassmann-Suhijar, D.; Bullingham, R.; Gasser, R.; Schmutz, J.; Haefeli, W. E. Rhabdomyolysis due to interaction of simvastatin with mibefradil. *Lancet* **1998**, *351*, 1929–1930.
- (133) Billups, S. J.; Carter, B. L. Mibefradil withdrawn from the market. *Ann. Pharmacother.* **1998**, *32*, 841.
- (134) Prueksaritanont, T.; Ma, B.; Tang, C.; Meng, Y.; Assang, C.; Lu, P.; Reider, P. J.; Lin, J. H.; Baillie, T. A. Metabolic interactions between mibefradil and HMG-CoA reductase inhibitors: an in vitro investigation with human liver microsomes. *Br. J. Clin. Pharmacol.* **1999**, *47*, 291–298.
- (135) Wiltshire, H. R.; Sutton, B. M.; Heeps, G.; Betty, A. M.; Angus, D. W.; Madigan, M. J.; Sharp, S. R. Metabolism of the calcium antagonist, mibefradil (POSICOR, Ro 40-5967). Part II. Metabolism in hepatic microsomes from rat, marmoset, cynomolgus monkey, rabbit and man. *Xenobiotica* **1997**, *27*, 539–556.
- (136) Foti, R. S.; Rock, D. A.; Pearson, J. T.; Wahlstrom, J. L.; Wienkers, L. C. Mechanism-based inactivation of cytochrome P4503A4 by mibefradil through heme destruction. *Drug Metab. Dispos.* **2011**, *39*, 1188–1195.
- (137) Magee, T. V.; Ripp, S. L.; Li, B.; Buzon, R. A.; Chupak, L.; Dougherty, T. J.; Finegan, S. M.; Girard, D.; Hagen, A. E.; Falcone, M. J.; Farley, K. A.; Granskog, K.; Hardnik, J. R.; Huband, M. D.; Kamicker, B. J.; Kaneko, T.; Knickerbocker, M. J.; Liras, J. L.; Marra, A.; Medina, I.; Nguyen, T.-T.; Noe, M. C.; Obach, R. S.; O'Donnell, J. P.; Penzien, J. B.; Reilly, U. D.; Schafer, J. R.; Shen, Y.; Stone, G. G.; Strelevitz, T. J.; Sun, J.; Tait-Kamradt, A.; Vaz, A. D. N.; Whipple, D. A.; Widlicka, D. W.; Wishka, D. G.; Wolkowski, J. P.; Flanagan, M. E. Discovery of azetidiny ketolides for the treatment of susceptible and multidrug resistant community-acquired respiratory tract infections. *J. Med. Chem.* **2009**, *52*, 7446–7457.
- (138) Linus, L. S.; Lanza, T. Jr.; Jewell, J. P.; Liu, P.; Jones, C.; Kieczkowski, G. R.; Treonze, K.; Si, Q.; Manior, S.; Koo, G.; Tong, X.; Wang, J.; Schuelke, A.; Pivnichny, J.; Wang, R.; Raab, C.; Vincent, S.; Davies, P.; MacCoss, M.; Mumford, R. A.; Hagmann, W. K. Discovery of *N*-[*N*-[(3-cyanophenyl)sulfonyl]-4(*R*)-cyclobutylamino-(*L*)-prolyl]-4-[(3',5'-dichloroisonicotinoyl)amino]-(*L*)-phenylalanine (MK-0668), an extremely potent and orally active antagonist of very late antigen-4. *J. Med. Chem.* **2009**, *52*, 3449–3452.
- (139) Westaway, S. M.; Brown, S. L.; Fell, S. C. M.; Johnson, C. N.; MacPherson, D. T.; Mitchell, D. J.; Myatt, J. W.; Stanway, S. J.; Seal, J. T.; Stemp, G.; Thompson, M.; Lawless, K.; McKay, F.; Muir, A. I.; Barford, J. M.; Cluff, C.; Mahmood, S. R.; Matthews, K. L.; Mohamed, S.; Smith, B.; Stevens, A. J.; Bolton, V. J.; Jarvie, E. M.; Sanger, G. J. Discovery of *N*-(3-fluorophenyl)-1-[4-((3*S*)-3-methyl-1-piperazinyl)methyl]phenyl)acetyl]-4-piperidinamine (GSK962040), the first small molecule motilin receptor agonist clinical candidate. *J. Med. Chem.* **2009**, *52*, 1180–1189.
- (140) Zhao, Z.; Leister, W. H.; O'Brien, J. A.; Lemaire, W.; Williams, D. L. Jr.; Jacobson, M. A.; Sur, C.; Kinney, G. G.; Pettibone, D. J.; Tiller, P.; R.; Smith, S.; Hartman, G. D.; Lindsley, C. W.; Wolkenberg, S. C. Discovery of *N*-[[1-(propylsulfonyl)-4-pyridin-2-yl]piperidin-4-yl]methyl]benzamides as novel, selective and potent GlyT1 inhibitors. *Bioorg. Med. Chem. Lett.* **2009**, *19*, 1488–1491.
- (141) Wu, Y.-J.; Davis, C. D.; Dworetzky, S.; Fitzpatrick, W. C.; Harden, D.; He, H.; Knox, R. J.; Newton, A. E.; Philip, T.; Polson, C.; Sivarao, D. V.; Sun, L.-Q.; Tertyshnikova, S.; Weaver, D.; Yeola, S.; Zoeckler, M.; Sinz, M. W. Fluorine substitution can block CYP3A4 metabolism-dependent inhibition: identification of (*S*)-*N*-[1-(4-fluoro-3-morpholin-4-ylphenyl)ethyl]-3-(4-fluorophenyl)acrylamide as an orally bioavailable KCNQ2 opener devoid of CYP3A4 metabolism-dependent inhibition. *J. Med. Chem.* **2003**, *46*, 3778–3781.
- (142) Velaparthi, U.; Wittman, M.; Liu, P.; Carboni, J. M.; Lee, F. Y.; Attar, R.; Balimane, P.; Clarke, W.; Sinz, M. W.; Hurlburt, W.; Patel, K.; Discenza, L.; Kim, S.; Gottardis, M.; Greer, A.; Li, A.; Saulnier, M.; Yang, Z.; Zimmermann, K.; Trainor, G.; Vyas, D. Discovery and evaluation of 4-(2-(4-chloro-1*H*-pyrazol-1-yl)ethylamino)-3-(6-(1-(3-fluoropropyl)piperidin-4-yl)-4-methyl-1*H*-benzo[*d*]imidazol-2-yl)-pyridin-2(1*H*)-one (BMS-695735), an orally efficacious inhibitor of insulin-like growth factor-1 receptor kinase with broad spectrum in vivo antitumor activity. *J. Med. Chem.* **2008**, *51*, 5897–5900.
- (143) Tang, W.; Stearns, R. A.; Wang, R. W.; Miller, R. R.; Chen, Q.; Ngui, J.; Bakshi, R. K.; Nargund, R. P.; Dean, D. C.; Baillie, T. A. Assessing and minimizing time-dependent inhibition of cytochrome P450 3A in drug discovery: a case study with melanocortin-4 receptor agonists. *Xenobiotica* **2008**, *38*, 1437–1451.
- (144) Roberts, W. G.; Ung, E.; Whalen, P.; Cooper, B.; Hulford, C.; Autry, C.; Richter, D.; Emerson, E.; Lin, J.; Kath, J.; Coleman, K.; Yao, L.; Martinez-Alsina, L.; Lorenzen, M.; Berliner, M.; Luzzio, M.; Patel, N.; Schmitt, E.; LaGreca, S.; Jani, J.; Wessel, M.; Marr, E.; Griffor, M.; Vajdos, F. Antitumor activity and pharmacology of a selective focal adhesion kinase inhibitor, PF-562,271. *Cancer Res.* **2008**, *68*, 1935–1944.
- (145) Walker, D. P.; Bi, F. C.; Kalgutkar, A. S.; Bauman, J. N.; Zhao, S. X.; Soglia, J. R.; Aspnes, G. E.; Kung, D. W.; Klug-McLeod, J.; Zawistoski, M. P.; McGlynn, M. A.; Oliver, R.; Dunn, M.; Li, J. C.; Richter, D. T.; Cooper, B. A.; Kath, J. C.; Hulford, C. A.; Autry, C. L.; Luzzio, M. J.; Ung, E. J.; Roberts, W. G.; Bonnette, P. C.; Buckbinder, L.; Mistry, A.; Griffor, M. C.; Han, S.; Guzman-Perez, A. Trifluoromethylpyrimidine-based inhibitors of proline-rich tyrosine kinase 2 (PYK2): structure–activity relationships and strategies for the elimination of reactive metabolite formation. *Bioorg. Med. Chem. Lett.* **2008**, *18*, 6071–6077.
- (146) Wong, S. G.; Fan, P. W.; Subramanian, R.; Tonn, G. R.; Henne, K. R.; Johnson, M. G.; Tadano Lohr, M.; Wong, B. K. Bioactivation of a novel 2-methylindole-containing dual chemoattractant receptor-homologous molecule expressed on T-helper type-2 cells/D-prostanoid receptor antagonist leads to mechanism-based CYP3A inactivation: glutathione adduct characterization and prediction of in vivo drug–drug interaction. *Drug Metab. Dispos.* **2010**, *38*, 841–850.
- (147) Chen, A.; Dube, D.; Dube, L.; Gagne, S.; Gallant, M.; Gaudreault, M.; Grimm, E.; Houle, R.; Lacombe, P.; Laliberte, S.; Liu, S.; MacDonald, D.; Mackay, B.; Martin, D.; McKay, D.; Powell, D.; Levesque, J.-F. Addressing time-dependent CYP3A4 inhibition in a novel series substituted amino propanamide renin inhibitors, a case study. *Bioorg. Med. Chem. Lett.* **2010**, *20*, 5074–5079.
- (148) Chen, A.; Aspiotis, R.; Campeau, L.-C.; Cauchon, E.; Chefson, A.; Ducharme, Y.; Falgueyret, J.-P.; Gagné, S.; Han, Y.; Houle, R.; Laliberté, S.; Larouche, G.; Lévesque, J.-F.; McKay, D.; Percival, D. Renin inhibitors for treatment of hypertension: design and optimization of a novel series of spirocyclic piperidines. *Bioorg. Med. Chem. Lett.* **2011**, *21*, 7399–7404.
- (149) Yarnell, A. T. Heavy-hydrogen drugs turn heads, again. *Chem. Eng. News* **2009**, *87*, 36–39; <http://pubs.acs.org/cen/science/87/8725sci1.html>.
- (150) Kalgutkar, A. S.; Choo, E.; Taylor, T. J.; Marfat, A. Disposition of CP-671,305, a selective phosphodiesterase 4 inhibitor in preclinical species. *Xenobiotica* **2004**, *34*, 755–770.
- (151) Ishiguro, N.; Saito, A.; Yokoyama, K.; Morikawa, M.; Igarashi, T.; Tamai, I. Transport of the dopamine D2 agonist pramipexole by

rat organic cation transporters OCT1 and OCT2 in kidney. *Drug Metab. Dispos.* **2005**, *33*, 495–499.

(152) James, L. P.; Mayeux, P. R.; Hinson, J. A. Acetaminophen-induced hepatotoxicity. *Drug Metab. Dispos.* **2003**, *31*, 1499–1506.

(153) Halmes, N. C.; Samokyszyn, V. M.; Hinton, T. W.; Hinson, J. A.; Pumford, N. R. The acetaminophen regioisomer 3'-hydroxyacetanilide inhibits and covalently binds to cytochrome P4502E1. *Toxicol. Lett.* **1998**, *94*, 65–71.

(154) Zientek, M.; Stoner, C.; Ayscue, R.; Klug-McLeod, J.; Jiang, Y.; West, M.; Collins, C.; Ekins, S. Integrated in silico–in vitro strategy for addressing cytochrome P450 3A4 time-dependent inhibition. *Chem. Res. Toxicol.* **2010**, *23*, 664–676.

(155) Kassahun, K.; Skordos, K.; McIntosh, I.; Slaughter, D.; Doss, G. A.; Baillie, T. A.; Yost, G. S. Zafirlukast metabolism by cytochrome P450 3A4 produces an electrophilic alpha,beta-unsaturated iminium species that results in the selective mechanism-based inactivation of the enzyme. *Chem. Res. Toxicol.* **2005**, *18*, 1427–1437.

(156) Sun, H.; Yost, G. S. Metabolic activation of a novel 3-substituted indole-containing TNF-alpha inhibitor: dehydrogenation and inactivation of CYP3A4. *Chem. Res. Toxicol.* **2008**, *21*, 374–385.

(157) Gay, S. C.; Zhang, H.; Wilderman, P. R.; Roberts, A. G.; Liu, T.; Li, S.; Lin, H. L.; Zhang, Q.; Woods, V. L. Jr.; Stout, C. D.; Hollenberg, P. F.; Halpert, J. R. Structural analysis of mammalian cytochrome P450 2B4 covalently bound to the mechanism-based inactivator *tert*-butylphenylacetylene: insight into partial enzymatic activity. *Biochemistry* **2011**, *50*, 4903–4911.

(158) Lin, H. L.; Zhang, H.; Pratt-Hyatt, M.; Hollenberg, P. F. Thr302 is the site for the covalent modification of human cytochrome P450 2B6 leading to mechanism-based inactivation by *tert*-butylphenylacetylene. *Drug Metab. Dispos.* **2011**, *39*, 2431–2439.

(159) Lightning, L. K.; Jones, J. P.; Friedberg, T.; Pritchard, M. P.; Shou, M.; Rushmore, T. H.; Trager, W. F. Mechanism-based inactivation of cytochrome P450 3A4 by L-754,394. *Biochemistry* **2000**, *39*, 4276–4287.

(160) He, K.; Iyer, K. R.; Hayes, R. N.; Sinz, M. W.; Woolf, T. F.; Hollenberg, P. F. Inactivation of cytochrome P450 3A4 by bergamottin, a component of grapefruit juice. *Chem. Res. Toxicol.* **1998**, *11*, 252–259.

(161) Chang, S. Y.; Fancher, R. M.; Zhang, H.; Gan, J. Mechanism-based inhibition of human cytochrome P4503A4 by domperidone. *Xenobiotica* **2010**, *40*, 138–145.

(162) Kajbaf, M.; Longhi, R.; Fontana, S. Evaluation of different approaches to identifying a higher throughput assay for time-dependent inhibition (TDI). *Drug Metab. Lett.* **2011**, *5*, 104–113.

(163) Ortiz de Montellano, P. R.; Kunze, K. L.; Yost, G. S.; Mico, B. A. Self-catalyzed destruction of cytochrome P450: covalent binding of ethynyl sterols to prosthetic heme. *Proc. Natl. Acad. Sci. U.S.A.* **1979**, *76*, 746–749.

(164) Guengerich, F. P. Metabolism of 17 α -ethynylestradiol in humans. *Life Sci.* **1990**, *47*, 1981–1988.

(165) Lin, H.-L.; Kent, U. M.; Hollenberg, P. F. Mechanism-based inactivation of cytochrome P4503A4 by 17 α -ethynylestradiol: evidence for heme destruction and covalent binding to protein. *J. Pharmacol. Exp. Ther.* **2002**, *301*, 160–167.

(166) Purba, H. S.; Maggs, J. L.; Orme, M. L.; Back, D. J.; Park, B. K. The metabolism of 17 α -ethynylestradiol by human liver microsomes: formation of catechol and chemically reactive metabolites. *Br. J. Clin. Pharmacol.* **1987**, *23*, 447–453.

(167) Nakayama, S.; Atsumi, R.; Takakusa, H.; Kobayashi, Y.; Kurihara, A.; Nagai, Y.; Nakai, D.; Okazaki, O. A zone classification system for risk assessment of idiosyncratic drug toxicity using daily dose and covalent binding. *Drug Metab. Dispos.* **2009**, *37*, 1970–1977.

(168) Park, B. K.; Boobis, A.; Clarke, S.; Goldring, C. E.; Jones, D.; Kenna, J. G.; Lambert, C.; Laverty, H. G.; Naisbitt, D. J.; Nelson, S.; Nicoll-Griffith, D. A.; Obach, R. S.; Routledge, P.; Smith, D. A.; Tweedie, D. J.; Vermeulen, N.; Williams, D. P.; Wilson, I. D.; Baillie, T. A. Managing the challenge of chemically reactive metabolites in drug development. *Nat. Rev. Drug Discovery* **2011**, *10*, 292–306.

(169) Stepan, A. F.; Walker, D. P.; Bauman, J.; Price, D. A.; Baillie, T. A.; Kalgutkar, A. S.; Aleo, M. D. Structural alert/reactive metabolite concept as applied in medicinal chemistry to mitigate the risk of idiosyncratic drug toxicity: a perspective based on the critical examination of trends in the top 200 drugs marketed in the United States. *Chem. Res. Toxicol.* **2011**, *24*, 1345–1410.

(170) Brown, H. S.; Ito, K.; Galetin, A.; Houston, J. B. Prediction of in vivo drug–drug interactions from in vitro data: impact of incorporating parallel pathways of drug elimination and inhibitor absorption rate constant. *Br. J. Clin. Pharmacol.* **2005**, *60*, 508–518.

(171) Rong, H.; Maclin, D.; Yao, L.; Lin, J.; Yin, D.; Xu, H. Mechanism-based inhibition of human liver microsomal cytochrome P450 3A by a focal adhesion kinase (FAK) inhibitor PF-562,271. *Drug Metab. Rev.* **2008**, *40* (Suppl. 2), 86.

(172) Tucker, G. T.; Houston, J. B.; Huang, S. M. Optimizing drug development: strategies to assess drug metabolism/transporter interaction potential—towards a consensus. *Br. J. Clin. Pharmacol.* **2001**, *52*, 107–117.

(173) Fahmi, O. A.; Ripp, S. L. Evaluation of models for predicting drug–drug interactions due to induction. *Expert Opin. Drug Metab. Toxicol.* **2010**, *6*, 1399–1416.

(174) Fahmi, O. A.; Maurer, T. S.; Kish, M.; Cardenas, E.; Boldt, S.; Nettleton, D. A combined model for predicting CYP3A4 clinical net drug–drug interaction based on CYP3A4 inhibition, inactivation, and induction determined in vitro. *Drug Metab. Dispos.* **2008**, *36*, 1698–1708.

(175) Jones, H. M.; Dickins, M.; Youdim, K.; Gosset, J. R.; Attkins, N. J.; Hay, T. L.; Gurrell, I. K.; Logan, Y. R.; Bungay, P. J.; Jones, B. C.; Gardner, I. B. Application of PBPK modelling in drug discovery and development at Pfizer. *Xenobiotica* **2011**, *42*, 94–106.

(176) de LT Vieira, M.; Zhao, P.; Huang, S.-M. Predicting Drug Interaction Potential of Telithromycin Using a Physiologically-Based Pharmacokinetic (PBPK) Model That Incorporates Time-Dependent Enzyme Inhibition Mechanism Derived from Nonlinear Pharmacokinetics. Presented at the AAPS Annual Meeting, Washington, DC, October 23–27, 2011; Poster.

(177) Rowland Yeo, K.; Walsky, R. L.; Jamei, M.; Rostami-Hodjegan, A.; Tucker, G. T. Prediction of time-dependent CYP3A4 drug–drug interactions by physiologically based pharmacokinetic modelling: impact of inactivation parameters and enzyme turnover. *Eur. J. Pharm. Sci.* **2011**, *43*, 160–173.

(178) Zientek, M.; Dalvie, D. Utilization of a multi-staged time-dependent inhibition assay to assess the impact of intestinal metabolism on drug–drug interaction potential. *Drug Metab. Dispos.* **2012**, *40*, 467–473.

(179) Fahmi, O. A.; Hurst, S.; Plowchalk, D.; Cook, J.; Guo, F.; Youdim, K.; Dickins, M.; Phipps, A.; Darekar, A.; Hyland, R.; Obach, R. S. Comparison of different algorithms for predicting clinical drug–drug interactions, based on the use of CYP3A4 in vitro data: predictions of compounds as precipitants of interaction. *Drug Metab. Dispos.* **2009**, *37*, 1658–1666.